TECHNISCHE UNIVERSITÄT WIEN

Investigation of RF Characteristics of Propsim C2 Channel Emulator for the Wireless LAN Standard IEEE 802.11p

by

Mehdi Ashury BSc.

Advisors:

Univ. Prof. Dr. -Ing. Christoph Mecklenbräuker

Dr. techn. Alexander Paier

A thesis submitted in fulfillment of the
degree of Master in Telecommunications

at the
Faculty of Electrical Engineering and Information Technology
Institute of Telecommunications

March 2016

تقدیم به مادر عزیزم

Declaration of Authorship

I hereby certified that the work reported in this thesis is my own, and the work done by other authors is appropriately cited.

Mehdi Ashury Vienna, March 2016

Abstract

Industrial development of wireless systems demands benchmarking methods and testing. The real-time measurements and performance evaluation of a wireless communication system in different development stages, enable detection of system design errors at the earliest and less expensive stage of the development. The radio channel, as the medium, linking the transmitter to the receiver has an high impact on the wireless system performance. Thus the understanding of the radio channel behavior, is a key factor in developing wireless products. The radio channel characterizations are determined through a measurement campaign and mathematically formulated as a radio channel model.

A real-world performance measurement is costly, and due to the unpredictable variations in the interference and stochastic behaviour of the wireless propagation channel, specifically in a time-varying system, not reproducible. This motivates the need for a radio frequency platform which reproduces real-world conditions for the wireless system performance evaluation in the laboratory environment. The channel emulator, which replaces the real-world radio channel, is a major component of this testing platform. In this thesis the channel emulator Elektrobit (EB) Propsim C2, and the methodology of channel model implementation on it is investigated. Furthermore the vehicular channel models, such as the *Six Time- and Frequency-Selective Empirical Channel Models for Vehicular Wireless LANs* [1] and the *ETSI ITS* channel models [2], which were proposed in 2013 [2], are studied. The *ETSI ITS* channel models contain five Vehicle-to-Vehicle (VTV) scenarios, whereby two of them are without a Line Of Sight (LOS) path. The aim of this study is to understand the channel model parameters, presented in these models, for the further implementation on the EB Propsim C2. There are two options for the implementation of the channel models on the Propsim C2, namely through the Graphical User Interface (GUI), or through generating the Impulse Responses (IRs) on the computer, storing the IR-file on the Propsim C2 and running the emulation through this IR-file. Both methods are presented and the restrictions and advantages of each method are described.

The major part of this thesis, is about estimating the Packet Error Ratio (PER) of the Kapsch transceiver MTX-9450, which is based on the IEEE 802.11p Physical layer (PHY), for the ETSI ITS channel models. For this purpose a measurement plan is developed. The PER graphs are plotted in logarithmic scale over the average received power. The PER estimation is performed for three LOS scenarios and two Non Line Of Sight (NLOS) scenarios of the ETSI ITS channel models in data rates 3 Mbps, 6 Mbps, and 12 Mbps, which utilize the BPSK, QPSK and 16-QAM baseband modulation scheme. The PER measurement in channel models without a LOS path is carried out with the reduced relative speed of the vehicle to approx. 40 km/h, in order to be able to receive packets through the Propsim C2.

Kurzfassung

Eine erfolgreiche Entwicklung eines drahtlosen Kommunikationsssystems stellt bestimmte Anforderungen an Produktions- und Testmethoden. Die Echtzeitmessungen und Leistungsauswertungen eines drahtlosen Kommunikationssystems in unterschiedlichen Entwicklungsphasen ermöglichen die Entdeckung von Fehler in früheren und daher weniger kostenintensiven Phasen der Entwicklung. Der Funkkanal als Medium, welches den Sender mit dem Empfänger verbindet, hat einen sehr großen Einfluss auf die Leistung von drahtlosen Kommunikationssystemen. Daher ist das Verständnis vom Verhalten eines Funkkanals ein Schlüsselfaktor bei der Entwicklung von drahtlosen Systemen. Funkkanäle werden durch Messungen charakteriesiert und mathematisch als Funkkanalmodellen formuliert. Eine Leistungsmessung unter realen Bedingungen ist sehr kostenintensiv und auf Grund von unvorhersehbaren Änderungen in Interferenz und stochastischen Schwankungen der drahtlosen Ausbreitungswege -insbesondere in einem zeitvarianten System- nicht reproduzierbar. Daher besteht Nachfrage für eine Hochfrequenzplattform, welche die realen Bedingungen für eine Leistungsmessung von einem drahtlosen System unter Laborbedingungen ermöglicht. Der Kanalemulator, welcher der realen drahtlosen Kanal ersetzt, ist ein Hauptkomponent von einer Messplattform. Im ersten Teil dieser Arbeit werden der Kanalemulator Propsim C2 und die Methodologie der Implementierung von Kanalmodellen auf dem Propsim C2 untersucht. Darüber hinaus werden vehiculare Kanalmodelle, sowie *Six Time- and Frequency-Selective Empirical Channel Models for Vehicular Wireless LANs* [1] und die *ETSI ITS* Kanalmodelle [2] untersucht. Die *ETSI ITS* kanalmodelle beinhalten fünf Vehicle-to-Vehicle(VTV) Szenarien, von denen zwei keine Line Of Sight (LOS) Komponenten besitzen. Das Ziel dieser Analyse ist, das Verständnis der einzelnen Parameter der erwähnten Kanalmodelle und deren spätere Implementierung auf dem Propsim C2. Für das Implementieren der Kanalmodelle im Propsim C2 stehen zwei Methoden zur Verfügung: über die grafischen Benutzeroberfläche (GUI), oder durch die Generierung von Impulsantworten (IR) im PC, die Übertragung vom IR-File auf dem Propsim C2, und im letzten Schritt, die Ausführung der Emulation durch das bereits gespeicherte IR-File. Beide Methoden, samt deren Vor- und Nachteile, sind beschrieben. Der zweite Teil dieser Arbeit

widmet sich der Packet Error Ratio(PER)- Berechnung von einem Kapsch Transceiver MTX-9450 für die *ETSI ITS* Kanal Modelle. Die physikalische Schicht (physical layer (PHY)) des MTX-9450 basiert auf dem Standrad IEEE 802.11p. Hierfür wurde ein Messplan entwickelt. Im nächten Schritt wurden die PER-Werte mittels Kurven in logarithmischen Massstab über die Empfangsleistung dargestellt. Die Messungen von PER wurden für drei LOS Szenarien und zwei Non Line Of Sight (NLOS) Szenarien von den ETSI ITS Kanalmodelle durchgeführt. Die dafür verwendeten Datenraten sind 3 Mbps, 6Mbps, 12 Mbps, welche die Basisband Modulation BPSK, QPSK und 16-QAM benutzen. Bei den PER Messungen für die NLOS Modelle ist die relative Geschwindigkeit der Fahrzeuge auf 40 km/h reduziert, um das Empfangen der Pakete durch dem Propsim C2 zu ermöglichen.

Acknowledgements

Firstly I would like to express my sincere gratitude to my thesis advisor Prof. Christoph Mecklenbräuker of the Institute of Telecommunications at Vienna University of Technology for guiding my analysis in my research and for the valuable motivating and constructive comments. I have learned a lot from him and enjoyed the days during my thesis. I also want to thank my advisor at Kapsch TrafficCom Dr. Alexander Paier for his guidance, support and the useful discussions and comments.

I express my very profound gratitude to my mother and my sisters for providing me with continuous encouragement and unfailing support throughout my years of study and specially through the process of researching and writing this thesis. And also for tolerating and supporting me in my bad days! Thank you! I would also like to express my special thanks to my dear Alexy for her supports and her patience in the difficult times.

I would also like to thank the experts who were involved in CD Lab Modul 1, Dipl.-Ing. Josef Winkler, Dr. Thomas Zemen and Dr. Dieter Smely for their useful inputs. My special thanks are going to Mr. Juha Virtala and Mr. Niklas Lillsunde at Anite (former Elektrobit) for the very kind and great supports during this project. I appreciate highly your support. I want also to thank my colleagues and friends at the TU Vienna, Dr. Walter Ehrlich-Schupita, Dr. Golsa Ghiaasi, Dipl.-Ing. Thomas Blazek, Dr. Gregor Lasser, Dr. Robert Langwieser, M.Sc. Mona Shemshaki, Ing. Bernhard Wistawel and Ing. Walter Schüttengruber.

last but not least I want to thank all my friends for the interesting discussions, their support and all enjoyable moments, keep it up!

Thank you all!

This work has been supported by the Christian Doppler Laboratory for Wireless Technologies for Sustainable Mobility, and its industrial partner Kapsch TrafficCom. I want to express my gratitude to Kapsch TrafficCom and the the Christian Doppler Laboratory for the possibility of this project and for the provision of equipment.

Contents

List of Figures

List of Tables

List of Abbreviations

ABB Analog Base Band

ACF Auto Correlation Function

ADC Analog Digital Converter

ATE Automatic Test Equipment

BER Bit Error Ratio

BS Base Station

CAM Cooperative Awareness Message

CIR Channel Impulse Response

CL Carrier Leakage

CP Cyclic Prefix

CRC Cyclic Redundancy Check

CW Continues Wave

DAC Digital Analog converter

DBB Digital Base Band

DENM Decentralized Environmental Notification Messages

DSP Digital Signal Processing

ETSI European Telecommunications Standards Institute

FPGA Field Programmable Gate Array

GDP Gross Domestic Product

GI Guard Interval

GPIB General Purpose Interface Bus

GUI Graphical User Interface

I/Q In-phase / Quadrature

ICI Inter Carrier Interference

IDFT Inverse Discrete Fourier Transform

IF Intermediate Frequency

IFFT Inverse Fast Fourier Transform

IO Interacting Object

IR Impulse Response

ISI Intersymbol Interference

ITS Intelligent Transport System

LAN Local Area Network

LO Local Oscillator

LOS Line Of Sight

MAC Media Access Control

MIMO Multiple Input Multiple Output

MPC Multipath Components

MS Mobile Station

NLOS Non Line Of Sight

OFDM Orthogonal Frequency-Division Modulation

PDP Power Delay Profile

PER Packet Error Ratio

PHY Physical layer

RF Radio Frequency

RFU Radio Frequency Unit

RMS Root Mean Square

RSU Road Side Unit

RTV Roadside-to-Vehicle

RX Receiver

SDR Software Defined Radio

TDL Tapped Delay Line

TX Transmitter

UC Up Converter

US Uncorrelated Scatterer

V2I Vehicle-to-Infrastructure

VTV Vehicle-to-Vehicle

WAVE Wireless Access in Vehicular Environments

WSS Widesense Stationary

Chapter 1

Introduction

1.1 Motivation

Road crashes cause serious health problems and very high economical costs. "The World Health Organization (WHO) predicts that by 2020, road traffic injuries will increase in total number by 65 % and will be the third highest cause of disability adjusted life years. Worldwide, injuries due to road crashes result in an economic cost typically ranging between 1% and 2% of Gross Domestic Product (GDP), a global total that exceeds $145 billion per annum" [10]. According to [10], "Australian statistics for the state of New South Wales show that in terms of the total number of crashes (all recorded fatal, injury and noninjury crashes), 61% of crashes, involve collision of two moving vehicles. Furthermore, 46% of all crashes occur at some kind of intersection (Cross, T-junction, Y-junction, or roundabout)" [10]. Therefore one of the major fields in Intelligent Transport System (ITS) technology is the safety application, which will be able to reduce the number of road crashes notably.

The ITS related applications utilized the wireless technology for communication among vehicles, as well as among vehicles and base stations. One major task of the ITS wireless communication systems, besides the reduction of traffic congestion, is to identify unsafe conditions and to warn the driver, in order to prevent avoidable collisions, e.g. in situations where the vehicles are in danger of collision, but the drivers can not see the other vehicle.

It is stated in [10] that "Initial Organization for Economic Cooperation and development (OECD) estimates indicate that emerging road safety technologies could reduce fatalities and injuries by as much as 40%."

The major components of the ITS wireless systems are the transmitter, the receiver and the linking medium between them, namely the radio channel. The understanding of the radio channel characteristics is a very important factor for developing the transceivers and therefore the performance of the entire wireless communication system. The motion of the vehicles and the scatterers result in the vehicular channels to be time varying, i.e. the channel transfer function is dependent on the instantaneous time, which means that the radio channel is time-selective. The other characteristics is, that different signal paths (multipath components) arrive at the receiver at different times, i.e. the radio channel is delay dispersive, which is equivalent to the frequency-selectivity in the frequency domain. Thus the vehicular channels represented by the channel transfer function $H(t; f)$ are doubly-selective [11]. The radio channel models are constructed by mathematical formulation of measurement results of different radio channel propagation parameters through channel sounding.

A successful development of a wireless system, requires the evaluation of the transceivers performance, for a particular radio channel model, in different product development cycles. This enables the detection of design errors at the earliest and less expensive phase of the system development. The real-world measurements of wireless system performance can be performed by moving transceivers around their operational area and measuring the relevant performance parameters, such as PER, received power, SNR, etc. However, such results are dependent on the location and also on the time of the measurement, i.e. the measurement data can not be applied by other applications. Thus, real-world measurement is a highly complicated process and not reproducible. In order to avoid these drawbacks, the real-world measurements are replaced with laboratory controlled condition measurements. Whereby, the real radio channel is replaced with emulated channel models through the radio channel emulator, which reproduces real-world propagation phenomena, such as multipath, fast fading, path delays, path loss and Doppler shift in laboratory conditions.

In this thesis the implementation of vehicular channels on the channel emulator EB Propsim C2 is investigated. The implementation of particular channel models on a commercial radio channel emulator is not a straightforward process. The first aim of this thesis is, to study the vehicular channel models, namely *Six Time- and Frequency-Selective Empirical Channel Models for Vehicular Wireless LANs* and the proposed *ETSI ITS channel models*. Furthermore an approach, for implementation of these models on the EB Propsim C2 is proposed. In the next step a platform to measure the Packet Error Ratio of the *Kapsch* transceiver *MTX-9450* for the ETSI ITS channel models is developed. The 5.9 GHz transceiver MTX-9450 is a compact V2X Roadside ITS Station (R-ITS-S), utilizing wireless communications in the 5.9 GHz Dedicated Short Range Communication (DSRC) band [12]. Since 2013, there is a draft of the vehicular

channel model proposed by ETSI, reffered to as the ETSI ITS channel models [2]. Up to our knowledge there is no existing investigation of the Propsim C2, particularly related to ETSI ITS channel models, so it is very interesting to investigate, if and how these channel models on Propsim C2 will be implemented and also to carry out the PER measurements of the transceivers using ETSI ITS G5.

1.2 Contribution

The main question I adressed within this thesis is, to evaluate the performance of the Kapsch transceiver MTX-9450 for the ETSI ITS channel models. In order to do so, a PER measurement platform is developed. One major component of this measurement setup is, the channel emulator EB Propsim C2, on which the ETSI ITS channel models are implemented. First, it is necessary to investigate the RF characteristics of the Propsim C2. The methodology for implementation of the channel model on Propsim C2 is presented in [3]. A major problem occurring during the emulation on Propsim C2 is the carrier signal leakage at emulation center frequency, which causes un-wanted interference in the emulation, as discussed in EB Propsim C-series output spectrum [13]. To avoid this problem, I have used the solution presented in EB Propsim C2 DCTuner operation guide [14]. The essential statistical descriptions of wireless channels in vehicular communication, such as (quasi-) Widesense Stationary (WSS) and Uncorrelated Scatterer (US), are presented in [11], [15], [16], [17], [5].

The Cooperative ITS and the vehicular channel characterization for 5.9 GHz band, such as the characteristics of the doubly-selective fading channel, the delay spread, the Doppler spread and the Tapped Delay Line (TDL) model and its impact on the wireless systems, whose PHY is based on the standard IEEE 802.11p [8] are described by Paul Alexander et al. [10] and by Christoph F. Mecklenbraüker et al. [18]. A delay spread longer than the Guard Interval (GI) of the OFDM system, namely the Cyclic Prefix (CP) causes an Intersymbol Interference (ISI) at the equalizer, and therefore has an impact on the wireless system performance.

Furthermore the *Six Time and Frequency Selective Empirical Channel Models for Vehicular Wireless LANs* by Acosta and Ingram [1], as a basis for the vehicular channel models, and the ETSI ITS channel models [2], [4], both for 5.9 GHz frequency band are studied in this thesis. Particularly in ETSI ITS channel models, there are three scenarios with LOS path, viz. the Rural LOS, Urban Approaching LOS and the Highway LOS, and two scenarios without availability of LOS path, namely cross NLOS and Highway NLOS. Moreover the Doppler spread and the delay spread of the ETSI ITS scenarios are calculated, which describe the channel model behaviors. Some necessary measurement

values for the PER measurement are presented in the ETSI ITS plugtest [4], which will be utilized for the PER measurement in Chapter 6. MTX-9450 is based on the standards IEEE 802.11p and the ETSI ITS-G5 [6]. For the performance evaluation of this transmitter, the PER over the received average power for all five scenarios of ETSI ITS channel models are measured and the PER over varying received power are calculated and presented. According to the ETSI ITS Plugtest [4] the sensitivity power level is presented as the point of the PER curve, where the PER is equal to 10%.

1.3 Thesis outline

The rest of this thesis is structured as follows:

Chapter 2 presents a description of the wireless channels including the definition of line of sight path, non-line of sight path, Doppler spectrum, delay spread, Doppler spread, (quasi-)WSSUS assumption and the TDL models. Also the coherence time and the coherence bandwidth are described.

Chapter 3 is dedicated to studying the vehicular channel models such as, the *Six Time and Frequency Selective Empirical Channel Models for Vehicular Wireless LANs* and the ETSI ITS channel models. It includes a description of the channel model parameters. The five different scenarios and the parameters of the ETSI ITS channel models are presented more clearly. Furthermore the RMS Delay spread and the RMS Doppler spread of the ETSI ITS channel models are calculated.

Chapter 4 consists of a description of the system architecture of the radio channel emulator EB Propsim C2, including the hardware and software interfaces. The carrier leakage at emulation center frequency and a tuning mechanism for this problem are explained. The channel model implementation methods on the EB Propsim C2 are presented.

The characteristics of the wideband communication system and the requirements are presented in details in chapter 5. Moreover, the OFDM is described as a suitable modulation technique for the time-varying wideband communication systems. This chapter provides a description of the standards IEEE 802.11p and the ETSI ITS G5, and how these two standards are linked together.

The Packet Error Ratio measurement setup is presented in chapter 6. The components and the measurement values are described explicitly. The Measurement evaluation and the conclusions from this thesis are reported in this chapter. The summary and conclusion are presented in Chapter 7.

Chapter 2

Statistical Description of the Wireless Channel

In a wireless communication system a radio channel is the medium linking the transmitter and the receiver. Properties of a radio channel determine the performance limit of a wireless communication system and also its behaviour. Therefore, it is very important to understand and model the suitable radio channel [11]. In this chapter, I will describe the way to characterize the radio channel properties as mathematical models and how to parameterize these models.

2.1 Multipath Propagation

The major difference between radio channels and wired channels is the multhipath propagation in radio channel, i.e. that the existence of a multitude propagation paths from transmitter to receiver. On its way, the transmitted signal can be reflected, diffracted or scattered concerning different objects called scatterers and in the environment named mountains, houses, vehicles, etc. In a multipath propagation, the signal from different paths will be superimposed at the receiver. If a single pulse is transmitted over a multipath channel, then the received signal will be a pulse train. The first received pulse corresponds to the LOS component and each of the remaining pulses belong to a definite scatterer. The time delay spread, which is equal to the time delay between the arrival of the LOS component and the last received signal, can lead to significant distortion of the received signal. Another important characteristic of the multipath channel is its time-varying behavior. Because of the motion of the transmitter, the receiver or the scatterers their location is changing over time. The amplitudes, delays and number of

multipath components corresponding to each pulse will vary, if we transmit a number of pulses repetitively [11], [5].

2.2 Small-Scale and Large-Scale Fading

A receiver in a wireless communication system adds up the different Multipath Components (MPC)s, so that they interfere with each other. The interference between them can be constructive or destructive, depending on the phases of the MPCs. The phases depend on the run length of the MPC. In consequence the interference of the MPCs, and thus the amplitude of the total signal, changes with time if either Transmitter (TX), Receiver (RX), or Interacting Object (IO)s are moving. This effect is called *small-scale fading* [11].

The amplitude of each separate MPC changes with time or with location. Obstacles can lead to a shadowing of one or several MPCs. The Mobile Station (MS) has LOS to the Base Station (BS) at the first position. As the MS moves behind a building, the amplitude of the LOS component between BS and MS decreases significantly. The reason for this is that the MS is now in the radio shadow of the building and any wave propagating through or around that building is strongly attenuated. This effect is called *shadowing*. It can occur but for both LOS and NLOS MPC components. There is no sharp border between shadowed zone by obstacles (dark zone) and the light zone (i.e., LOS zone). "The transition from the "light" (i.e., LOS) zone to the "dark" (shadowed) zone is gradual. The MS has to move over large distances (from a few meters, up to several hundreds of meters) from the light to the dark zone"[11]. That is why the effect of shadowing is called *large-scale* fading [11].

2.2.1 Small-Scale Fading Without a LOS Component

Consider a scenario in which N homogeneous plane waves (MPCs) have been generated by reflection/scattering from different IOs. We assume that the IOs and the TX do not move, and the RX moves with a velocity v, furthermore the absolute amplitudes of the MPCs do not change over the region of observation. The sum of the squared amplitudes is [11]

$$\sum_{i=0}^{N} |a_i|^2 = C_p, \tag{2.1}$$

The in-phase and the quadrature-phase components of the received signal are the sum of a large number of random variables, without any dominant component (i.e., $|a_i| \ll C_p$). Based on the central limit theorem bothe the I and Q components of the received signal are Gaussian distributed. Since field strength is the radius $r = \sqrt{(I^2(t) + Q^2(t)}$ of Gaussian distribution, the evnelope of the received signal r, is Rayleigh distributed[11]

$$pdf_{\mathrm{r}}(r) = \begin{cases} \frac{r}{\sigma^2} \exp\left[-\frac{r^2}{2\sigma^2}\right] & \text{for } r \geq 0 \\ 0 & \text{otherwise} \end{cases} \tag{2.2}$$

where σ^2 is the variance of the zero-mean Gaussian random variables I and Q.

2.2.2 Small-Scale Fading With an LOS Component

When a dominant component such as an LOS path is introduced into the Rayleigh fading environment, the fading becomes Rician-distributed. The pdf of the amplitude of Rician fading is

$$pdf_{\mathrm{r}}(r) = \frac{r}{\sigma^2} \exp\left[-\frac{r^2 + A^2}{2\sigma^2}\right] I_0(\frac{rA}{\sigma^2}). \tag{2.3}$$

The ratio of the signal power in the LOS path to the summed signal powers of all other paths is the $RicianKfactor$, $K = \frac{A^2}{2\sigma^2}$ [11].

2.3 Time Variance

The relative motion of transmitter, receiver and scatterers in a radio channel leads to time-variant characteristics. That is the case especially in vehicular communications. In VTV communication the TX , The RX and the scatterers are moving and in Vehicle-to-Infrastructure (V2I) communication the TX or the RX and the scatterers are moving. The time selectivity induces a frequency shift by the received signal called the Doppler shift. The Doppler frequency shift of the received signal by the amount of f_m is defined as [11], [17]

$$f_d = \frac{f_c|\overrightarrow{v}|}{C_0} cos(\alpha), \tag{2.4}$$

where f_c is the carrier center frequency and α denotes the angle between the velocity vector of the vehicle and the direction of the propagating wave. In general, the velocity

$|\overrightarrow{v}|$ is the relative speed between TX and RX. The frequency shift depends on the angle α and its maximum value is $f_m = \frac{f_c|\overrightarrow{v}|}{C_0}$ [11], [17].

2.3.1 Doppler Spectra

In the previous section I have described the physical interpretation of frequency shift caused by movements which is called Doppler effect. By relative motion of the TX , the RX or the scatterrer, the different directions of the MPCs arriving at the receiver cause different frequency shifts. That leads to a widening of the received spectrum. This spectrum is called Doppler spectrum (S_D) and the aim of this section is to derive this spectrum. As mentioned above, the Doppler effect leads to a shift of the received frequency by the amount of f_m, so that the received frequency is [17]

$$f = f_c[1 - \frac{|\overrightarrow{v}|}{C_0}cos(\alpha)] = f_c - f_m, \tag{2.5}$$

where α denotes the angle between the velocity vector of the vehicle and the direction of the propagating wave. The frequency shift depends on the angle α and its maximum value is $f_m = \frac{f_c v}{C_0}$. For the case that there are multiple MPCs, we are interested in the distribution of the received power as a function of α.The total received power is [17]

$$P_r = \int_0^{2\pi} AG(\alpha)p(\alpha)d\alpha, \tag{2.6}$$

where A denotes the average received power, $G(\alpha)$ is the gain of the mobile antenna and $p(\alpha)d\alpha$ denotes the fraction of the total incoming power within $d\alpha$ of the angle α. The received power spectrum as a function of direction α is [17]

$$S(f)|df| = A[p(\alpha)G(\alpha) + p(-\alpha)G(-\alpha)]|d\alpha|, \tag{2.7}$$

$$\frac{d\alpha}{df} = \frac{1}{\frac{df}{d\alpha}} = \frac{1}{f_m\sqrt{1 - \left(\frac{f - f_c}{f_m}\right)^2}}, \tag{2.8}$$

$$S_D(\nu) = \frac{a}{\pi f_m\sqrt{1 - \left(\frac{f - f_c}{f_m}\right)^2}}, \tag{2.9}$$

where S_D is the Doppler spectra function, a is a constant regarding to A and the average received power G and a uniform distribution $p(\alpha) = \frac{1}{2\pi}$ over $[0, 2\pi]$ [17], [19].

2.4 Characterization of Deterministic Linear Time-Variant Systems

[11], [20], [16] A radio channel is described by its impulse response and it can be interpreted as a linear filter. The radio channel is time-invariant , if the TX, the RX and the scatteres are static. Thus its impulse response $h(\tau)$ is not dependent on the absolute time. Many of the wireless channels and specifically the vehicular channels are time-variant with an impulse response $h(t, \tau)$. Where t is the absolute time and τ is the delay. The relation between the input signal $x(t)$ and the output signal $y(t)$ of the channel is defined with the time-variant convolution[11]

$$y(t) = \int_{-\infty}^{\infty} x(t-\tau)h(t,\tau)d\tau. \tag{2.10}$$

We carry out a Fourier transformation of the Impulse Response (IR) with respect to two arguments t, τ or both. That yields four different functions. The radio channel can be described through each of these four equivalent functions.

$H(t, f)$ the time-variant transfer function is the Fourier transform of IR with respect to the variable τ [11]

$$H(t,f) = \int_{-\infty}^{\infty} h(t,\tau)exp(-j2\pi f\tau)d\tau. \tag{2.11}$$

The delay-Doppler function $S(\nu, \tau)$

$$S(\nu,\tau) = \int_{-\infty}^{\infty} h(t,\tau)exp(-j2\pi\nu t)dt. \tag{2.12}$$

The Doppler-variant transfer function $B(\nu, f)$:

$$B(\nu,f) = \int_{-\infty}^{\infty} S(\nu,\tau)exp(-j2\pi f\tau)d\tau. \tag{2.13}$$

2.5 Stochastic System Functions

For the purpose of complete description of radio channels as a stochastic time-variant system, we need the multidimensional pdf of the IR. Since this is too complicated in practice, a second-order description namely the Auto Correlation Function (ACF) is used. If the channel has zero-mean Gaussian distribution, then the second order description contains all the required information about its stochastic behavior [11].

$$R_h = (t, t'; \tau, \tau') = E\{h(t, \tau)h^*(t', \tau')\}, \tag{2.14}$$

$$R_H(t, t'; f, f') = E\{H(t, f)H^*(t', f')\}, \tag{2.15}$$

$$R_s(\nu, \nu'; \tau, \tau') = E\{S(\nu, \tau)S^*(\nu', \tau')\}, \tag{2.16}$$

$$R_B(\nu, \nu'; f, f') = E\{B(\nu, f)B^*(\nu', f')\}. \tag{2.17}$$

2.6 Widesense Stationarity (WSS)

WSS means that the statistical properties of the channel do not change with time, while the channel is not static and the instantaneous amplitude can change. The mathematical definition of wide-sense stationarity is that the second-order statistics do not change with time. That means that the AFC depends only on $t - t'$ and not on the two variables t and t' separately [11]

$$R_h(t, t', \tau, \tau') = R_h(t, t + \Delta t, \tau, \tau') = R_h(\Delta t, \tau, \tau'). \tag{2.18}$$

2.7 Uncorrelated Scatterer (US)

The US implies that the fading coming from different scatterers are not correlated. Since contributions from different scatterers have different delays, we can show the US mathematically as [11]

$$R_h(t, t', \tau, \tau') = P_h(t, t', \tau)\delta(\tau - \tau'), \tag{2.19}$$

$$R_s(\nu, \nu', \tau, \tau') = \tilde{P}_s(\nu, \nu', \tau)\delta(\tau - \tau'). \tag{2.20}$$

If the scatterers are randomly distributed in space -which is the case in most outdoor environments- the phase of an MPC does not contain any information about the phase of another MPC with another delay, then the US assumption is fulfilled [11].

2.8 WSSUS Assumption

Now we can combine the assumptions WSS and US in the WSSUS condition in order to achieve a further simplification. The US implies that R_h depends only on the frequency difference, while WSS implies that R_h depends only on the time difference. The WSSUS assumption changes the ACF equations in the following way[11]

$$R_h = (t, t + \Delta t, \tau, \tau') = \delta(\tau, \tau')P_h(\Delta t, \tau), \tag{2.21}$$

$$R_H = (t, t + \Delta t, f, f + \Delta f) = R_H(\Delta t, \Delta f), \tag{2.22}$$

$$R_s(\nu, \nu', \tau, \tau) = \delta(\nu - \nu')\delta(\tau - \tau')P_s(\nu, \tau), \tag{2.23}$$

$$R_B(\nu, \nu', f, f + \Delta f) = \delta(\nu - \nu')P_B(\nu, \Delta f). \tag{2.24}$$

In practice the WSSUS is not fulfilled for any arbitrary time t. Thus we should define a time interval and also a movement area, over which the WSSUS assumption is fulfilled. That is defined as quasi-WSSUS.

2.9 Tapped Delay Line Models

One approximation of a radio channel is the Tapped Delay Line(TDL) model. The time-variant impulse is

$$h(t, \tau) = \sum_{i=1}^{N} c_i(t)\delta(\tau - \tau_i). \tag{2.25}$$

In this equation the $c_i(t)$ are the time-dependent complex random coefficients for the taps, whose autocorrelation function can be specified through their Doppler spectra. For each tap the Doppler spectrum (e.g. Jakes' spectrum) specifies the variation of the coefficients with time. Different taps can be respesented by different Doppler spectra. τ_i is the delay for the ith tap and N is the number of taps. In most cases the amplitude of the first tap is Rician distributed. A WSSUS channel is adequately modeled as a tapped delay line [11].

2.10 Condensed Parameters

The Root Mean Square (RMS) delay spread is a second-order statistic characterizing the radio channel. In order to define the delay spread we need to define the Power Delay Profile (PDP). The PDP describes how much power arrives at the receiver with a delay between $[\tau, \tau + d\tau]$ regardless of a possible Doppler shift. The PDP is [11]

$$P_{PDP} = \int_{-\infty}^{\infty} |h(t,\tau)|^2 dt. \tag{2.26}$$

In practice the integral extends over the time interval during which the (quasi-)WSS is valid. The mean delay spread is defined as [11]

$$T_m = \frac{\int_{-\infty}^{\infty} P_{PDP}(\tau)\tau d\tau}{\int_{-\infty}^{\infty} P_{PDP}(\tau) d\tau}, \tag{2.27}$$

and the RMS delay spread is defined as [11]

$$\tau_{RMS} = \sqrt{\frac{\int_{-\infty}^{\infty} P_{PDP}(\tau)\tau^2 d\tau}{\int_{-\infty}^{\infty} P_{PDP}(\tau) d\tau} - T_m^2}. \tag{2.28}$$

As we will see later in Ch. 5 the delay spread is a measure if a signal will experience ISI in the radio channel or not. There is also a related parameter to τ_{RMS} in the frequency domain, namely the coherence bandwidth B_c [11]

$$B_c \approx \frac{1}{\tau_{RMS}}. \tag{2.29}$$

The delay dispersion is equivalent to frequency selectivity. If the signal bandwidth $B \gg B_c$, then the channel amplitude varies across the signal bandwidth. The channel is in this case frequency selective. But if $B \ll B_c$ then the channel behaviour is flat fading.

In the case of multipath propagation the RMS Doppler spread ν_{RMS} is a measure for the time selectivity of the radio channel [5],[16].

The RMS Doppler spread is [11]

$$\nu_{RMS} = \sqrt{\frac{\int_{-\infty}^{\infty} P_B(\nu)\nu^2 d\nu}{\int_{-\infty}^{\infty} P_B(\nu) d\nu} - \nu_m^2}, \tag{2.30}$$

where the mean Doppler shift ν_m is [11]

$$\nu_m = \frac{\int_{-\infty}^{\infty} P_B(\nu)\nu d\nu}{\int_{-\infty}^{\infty} P_B(\nu) d\nu}. \tag{2.31}$$

We define the channel coherence time as a time interval during which the second-order channel properties are nearly constant. The time-varying channel decorrelates after T_c seconds [11].

$$T_c \approx \frac{1}{\nu_{RMS}}. \tag{2.32}$$

Chapter 3

Radio Channel Models

A radio channel model is a mathematical representation of the Channel Impulse Response (CIR). A radio channel model is related to a measurement campaign. The Channel Impulse Response (CIR)s for different scenarios can be calculated via feeding the channel parameters collected from measurement campaigns into the channel models. In this thesis I have generated the CIRs of vehicular channels and emulated them on the channel emulator Propsim C2 in order to measure the system performance of a Road Side Unit (RSU) by Kapsch.

There are many channel modeling methods; e.g.,

- **Stored channel impulse responses**: The channel impulse responses $h(t, \tau)$ will be measured and stored via a channel sounder. The advantage of this method is its accuracy. But using stored impulse responses implies difficulty in collection and storing the data. Another disadvantage is that the stored CIRs are related to a certain area and not to the entire propagation environment. Furthermore, the simulations using this approach are reproducible [11].
- **Deterministic channel models**: In this modeling approach, the CIRs are calculated from resolving the Maxwell's equation in a certain area. Determining of the boundary conditions in many scenarios are not feasible due to the large number of involved objects or if applicable it needs a very high computational time. Furthermore, the results could be less accurate regarding to inaccuracy of definition of environmental object, their electromagnetic properties and also the approximate nature of numerical computational methods [11].
- **Stochastic channel models**: The aim of this method is to model the probability density function of the CIRs over a wide area. One example of this approach is the Rayleigh fading model [11].

Stochastic and deterministic methods can be combined. We can obtain the large-scale averaged power from deterministic models and the variations in an averaging area through the stochastic approaches [11].

I have investigated in detail two types of vehicular channel models. The first one is *six time- and frequency- selective empirical channel models for vehicular wireless LANs* [1]. The other one is the proposed *ETSI ITS channel models* [4].

3.1 Six Time- and Frequency-Selective Empirical Channel Models for Vehicular Wireless LANs

The aim of this section is to obtain a better understanding of these vehicular channel models and decide on the implementability of the channel models on the channel emulator Propsim C2. The implementation of the channel models on the channel emulator will be discussed in Ch. 6.

The six time- and frequency selective empirical channel models for vehicular wireless LANs consist of three VTV models and three Roadside-to-Vehicle (RTV) models. Both of them are based on measurements at 5.9 GHz [1].

The type of channel model is a TDL, where each tap is described by a Rician or Rayleigh fading and by a Doppler power spectrum. These channel models are made for the emulation on channel emulators *Spirent 550* [1]. There are some restrictions by parameterization of the models due to fitting the models to the certain channel emulator environment, e.g. it is not possible to create an arbitrary Doppler spectrum in many of the commercial channel emulators.

In order to describe the channel model parameters I have determined primarily the channel impulse response function of the channel models in general. According to Table II in [1]and Appendix Q in [21] the CIR is defined by (3.1) and Table 3.1 (see below):

$$h(t,\tau) = \underbrace{\sum_{p=1}^{P_{\mathrm{LOS}}} c_{\mathrm{LOS},p} \exp\left(j2\pi\nu_{\mathrm{LOS},p}t\right)\delta(\tau-\tau_{\mathrm{LOS},p})}_{\mathrm{LOS}} + \underbrace{\sum_{p=1}^{P} c_p(t)\delta(\tau-\tau_p)}_{\mathrm{NLOS}} \tag{3.1}$$

There are four different Doppler spectral shapes characterizing the Doppler spectra in each tap of the channel models. The Doppler spectra are defined in [21] as

Symbol	Name
P_{LOS}	Number of paths with Rician fading, $P_{\mathrm{LOS}} = 1$ or 2.
$c_{\mathrm{LOS},p}$	channel tap coefficient, complex-valued, time-invariant. $\lvert c_{\mathrm{LOS},p}\rvert / \lvert c_{\mathrm{LOS},1}\rvert = 10^{\frac{g_{\mathrm{LOS},p}}{20}}$ where $g_{\mathrm{LOS},p}$ is the Relative Path Loss in dB with random phase, uniformly distributed on $[-\pi, \pi]$
$\nu_{\mathrm{LOS},p}$	LOS Doppler (Hz), real-valued, time-invariant.
$\tau_{\mathrm{LOS},p}$	Delay value in LOS paths (ns), positive, time-invariant.
P	Number of random fading taps, integer, constant.
$c_p(t)$	complex valued random fading process $c_p(t)$ and $c_q(t)$ are independent for $p \neq q$ (uncorrelated scattering). $E\{c_p(t)\} = 0$ zero-mean WSS random fading process. $E\{c_p(t_1)c_p^*(t_2)\} = r_p(t_1 - t_2)$ definition of fading correlation function $S_p(\nu) = \int -\infty^{\infty} r_p(t) exp(-j2\pi\nu t)\,\mathrm{d}t$ definition of Doppler spectrum $S_p(\nu) = \begin{cases} S_{\mathrm{flat}}(\nu) & \text{Flatshape} \\ S_{\mathrm{rounded}}(\nu) & \text{Roundshape} \\ S_3(\nu) & \text{Classic 3dBshape} \\ S_6(\nu) & \text{Classis 6dBshape} \end{cases}$ with the following spectrum shape and scaling parameters: Fixed Frequency Shift $\nu_{\mathrm{D},p}$ Fading Doppler parameter $\nu_{\mathrm{F},p}$ which is the spectrum half-width Path Power a_p
τ_p	Delay value in NLOS paths (ns), positive, time-invariant.

TABLE 3.1: Used symbols and their definitions

- The Flat Doppler spectrum is defined as

$$S_{\mathrm{flat}}(\nu) = \begin{cases} \frac{a}{2\nu_{\mathrm{F},p}} & \text{for } |\nu - \nu_{\mathrm{D},p}| \leq \nu_{\mathrm{F},p} \\ 0 & \text{otherwise} \end{cases} \tag{3.2}$$

  with the Frequency Shift $\nu_{\mathrm{D},p}$ and the Fading Doppler $\nu_{\mathrm{F},p}$. The factor a is chosen so that the integral of the spectrum is set to the Path Power.

$$\int_{\nu_{\mathrm{D},p}-\nu_{\mathrm{F},p}}^{\nu_{\mathrm{D},p}+\nu_{\mathrm{F},p}} S_{\mathrm{flat}}(\nu)\,\mathrm{d}\nu = a. \tag{3.3}$$

- The Rounded Doppler spectrum is defined as

$$S_{\mathrm{rounded}}(\nu) = \begin{cases} \frac{2a}{\pi\nu_{\mathrm{F},p}} \sqrt{1 - \left(\frac{\nu-\nu_{\mathrm{D},p}}{\nu_{\mathrm{F},p}}\right)^2} & \text{for } |\nu - \nu_{\mathrm{D},p}| \leq \nu_{\mathrm{F},p} \\ 0 & \text{otherwise} \end{cases} \tag{3.4}$$

with the Frequency Shift $\nu_{\mathrm{D},p}$ and the Fading Doppler $\nu_{\mathrm{F},p}$. The factor a is chosen so that the integral of the spectrum is set to the Path Power.

$$\int_{\nu_{\mathrm{D},p}-\nu_{\mathrm{F},p}}^{\nu_{\mathrm{D},p}+\nu_{\mathrm{F},p}} S_{\mathrm{rounded}}(\nu)\,\mathrm{d}\nu = a. \tag{3.5}$$

- The Classic 6dB Doppler spectrum is defined as

$$S_6(\nu) = \begin{cases} \dfrac{a}{\pi\nu_{\mathrm{F},p}\sqrt{1-\left(\frac{\nu-\nu_{\mathrm{D},p}}{\nu_{\mathrm{F},p}}\right)^2}} & \text{for } |\nu-\nu_{\mathrm{D},p}| \le \nu_{\mathrm{F},p} \\ 0 & \text{otherwise} \end{cases} \tag{3.6}$$

with the Frequency Shift $\nu_{\mathrm{D},p}$ and the Fading Doppler $\nu_{\mathrm{F},p}$. The factor a is chosen so that the integral of the spectrum is set to the Path Power.

$$\int_{\nu_{\mathrm{D},p}-\nu_{\mathrm{F},p}}^{\nu_{\mathrm{D},p}+\nu_{\mathrm{F},p}} S_6(\nu)\,\mathrm{d}\nu = a. \tag{3.7}$$

- The Classic 3dB Doppler spectrum is defined as

$$S_3(\nu) = \begin{cases} \dfrac{\frac{a}{\sqrt{\pi}}\Gamma(\frac{5}{4})}{\Gamma(\frac{3}{4})\nu_{\mathrm{F},p}\sqrt[4]{1-\left(\frac{\nu-\nu_{\mathrm{D},p}}{\nu_{\mathrm{F},p}}\right)^2}} & \text{for } |\nu-\nu_{\mathrm{D},p}| \le \nu_{\mathrm{F},p} \\ 0 & \text{otherwise} \end{cases} \tag{3.8}$$

$$\int_{\nu_{\mathrm{D},p}-\nu_{\mathrm{F},p}}^{\nu_{\mathrm{D},p}+\nu_{\mathrm{F},p}} S_3(\nu)\,\mathrm{d}\nu = a. \tag{3.9}$$

For the VTV-Expressway Oncoming scenario, we formulate the channel impulse response explicitly as follows

$$\begin{aligned} h(t,\tau) = \underbrace{c_{\mathrm{LOS},1}\exp(j2\pi\nu_{\mathrm{LOS},1}t)\delta(\tau)}_{\text{Path No. 1 LOS comp.}} &+ c_1(t)\delta(\tau) \\ &+ c_2(t)\delta(\tau-\tau_2) \\ &\vdots \\ &+ \underbrace{c_{12}(t)\delta(\tau-\tau_{12})}_{\text{NLOScomponents}} \end{aligned} \tag{3.10}$$

with the following definitions

$$c_{\mathrm{LOS},1} = \sqrt{\frac{KP}{K+1}}\mathrm{e}^{j\Phi_1} \tag{3.11}$$

$$\nu_{\mathrm{LOS},1} = 1452\,\mathrm{Hz} \tag{3.12}$$

Tap No.	Path No.	Tap Power [dB]	Relative Pathloss [dB]	Delay Value [ns]	Rician K factor[dB]	Frequency Shift [Hz]	Fading Doppler [Hz]	LOS Doppler [Hz]	Modulation	Spectral Shape
1	1	0.0	0.0	0	-1.6	1451	60	1452	Rician	R
1	2	0.0	-24.9	1	n/a	884	858	n/a	Rayleigh	R
1	3	0.0	-25.5	2	n/a	1005	486	n/a	Rayleigh	R
2	4	-6.3	-13.1	100	n/a	761	655	n/a	Rayleigh	C3
2	5	-6.3	-7.5	101	n/a	1445	56	n/a	Rayleigh	R
3	6	-25.1	-28.9	200	n/a	819	823	n/a	Rayleigh	C3
3	7	-25.1	-29.3	201	n/a	1466	75	n/a	Rayleigh	F
3	8	-25.1	-35.6	202	n/a	124	99	n/a	Rayleigh	R
4	9	-22.7	-25.7	300	n/a	1437	110	n/a	Rayleigh	F
4	10	-22.7	-34.4	301	n/a	552	639	n/a	Rayleigh	C3
4	11	-22.7	-27.4	302	n/a	868	858	n/a	Rayleigh	C6
n/a	12	n/a	n/a	n/a	n/a	n/a	n/a	n/a	Rayleigh	n/a

TABLE 3.2: Channel Model Parameters, VTV-Expressway Oncoming. Notes: 1. n/a means not-applicable. 2.Spectral shapes are Flat (F), Round (R), Classic 3 dB (C3), and Classic 6 dB (C6). 3. Modulation is Rician (I) and Rayleigh (Y). [1]

Definition of fading correlation function for WSS Channel

$$E\{c_p(t_1)c_p^*(t_2)\} = r_p(t_1 - t_2) \tag{3.13}$$

The Fourier Transform of the correlation function is the Doppler spectrum

$$S_p(\nu) = \int_{-\infty}^{\infty} r_p(t_1 - t_2) \exp\left(-j2\pi\nu(t_1 - t_2)\right) \mathrm{d}(t_1 - t_2) \tag{3.14}$$

$$\int_{\nu_{\mathrm{D},p}-\nu_{\mathrm{F},p}}^{\nu_{\mathrm{D},p}+\nu_{\mathrm{F},p}} S_p(\nu)\,\mathrm{d}\nu = a. \tag{3.15}$$

The parameters *Frequency Shift*, *Fading Doppler* and *Fading Spectral Shape* in Table II in[1] describe a single Doppler spectrum. In this sequence, these parameters are standing for center frequency, frequency half width of the Doppler spectrum and the shape of the Doppler spectrum in each tap.

It is not foreseen to realize an arbitrary Doppler spectrum in many of the commercial channel emulators. That is why, "off-the-shelf" Doppler spectra, e.g., round, classic, etc. are used, to approximate the measured Doppler. If we look at the delay, we will find that two or three paths have the same delay time (1 ns delay difference is because Spirent channel emulator don't accept more than one having the same time). They will be combined to create the arbitrary Doppler Spectrum in a path in [1].

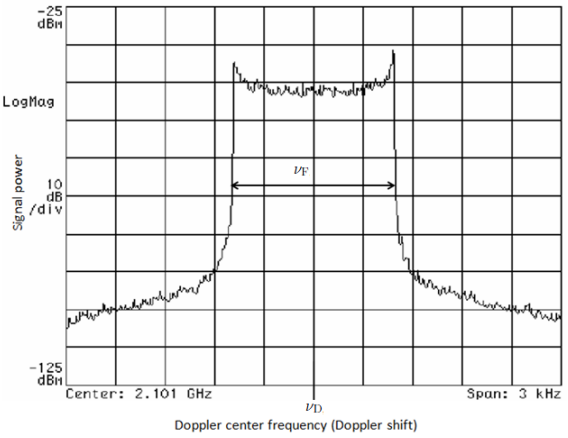

FIGURE 3.1: Doppler spectrum classical Jakes' [3]. ν_F is the Doppler bandwidth and ν_D is the Doppler frequency shift

3.2 ETSI ITS Channel Models

The ETSI ITS channel models are the other channel models I have investigated in my work, in order to implement them on the channel emulator Propsim C2. These models are still under development (at the time of my Master Thesis).

ETSI ITS channel models are very similar to the channel models in Sec. 3.1. However they are presently incomplete. Some channel model parameters are not yet defined or their refinement is still in progress.

As shown in Fig. 3.2, there are presently five ETSI ITS channel models namely Rural LOS, Urban Approaching LOS, Street Crossing NLOS, Highway LOS and Highway NLOS. In each of them, there are known parameters like Power [dB], Delay [ns], Doppler [Hz], Profile (Rician or Rayleigh distributed) and the Rician K factor [dB].

Parameter	Definition	Unit
Power	the average gain of the tap	dB
Delay	time delay of the received signal in the tap	ns
Doppler	Doppler frequency shift	Hz
Profile	Stochatical description of CIRs; Rician or Rayleigh	
K	Rician K factor (Ch. 2)	dB

TABLE 3.3: Channel Model Parameters

A fixed parameter in each model is the relative velocity v of the vehicles. In this section, I describe the five proposed ETSI ITS channel models and the assumptions regarding the parameters which are still under development. One of these parameters is the Doppler

	Tap1	Tap2	Tap3		Units
Power	0	-14	-17		dB
Delay	0	83	183		ns
Doppler	0	492	-295		Hz
Profile	Rice	Rayleigh	Rayleigh		
K	10				dB

Table 5: Rural LOS Parameters

144km/hr max differential

	Tap1	Tap2	Tap3	Tap4	Units
Power	0	-10	-15	-20	dB
Delay	0	100	167	500	ns
Doppler	0	689	-492	886	Hz
Profile	Rice	Rayleigh	Rayleigh	Rayleigh	
K	10				dB

Table 8: Highway LOS Parameters

252 km/hr max differential

	Tap1	Tap2	Tap3	Tap4	Units
Power	0	-8	-10	-15	dB
Delay	0	117	183	333	ns
Doppler	0	236	-157	492	Hz
Profile	Rice	Rayleigh	Rayleigh	Rayleigh	
K	10				dB

Table 6: Urban Approaching LOS Parameters

119km/hr max differential

	Tap1	Tap2	Tap3	Tap4	Units
Power	0	-2	-5	-7	dB
Delay	0	200	433	700	ns
Doppler	0	689	-492	886	Hz
Profile	Rayleigh	Rayleigh	Rayleigh	Rayleigh	
K					dB

Table 9: Highway NLOS Parameters

252 km/hr max differential

	Tap1	Tap2	Tap3	Tap4	Units
Power	0	-3	-5	-10	dB
Delay	0	267	400	533	ns
Doppler	0	295	-98	591	Hz
Profile	Rayleigh	Rayleigh	Rayleigh	Rayleigh	
K					dB

Table 7: Crossing NLOS Parameters

126km/hr max differential

FIGURE 3.2: Chanel parameters Proposed in ETSI ITS WG4 [2], [4]

bandwidth. In order to determine the Doppler bandwidth, I have used the relative speed v in following relations

$$\nu_{\mathrm{D,max}} = \frac{f_c v}{C_0} \tag{3.16}$$

where $\nu_{\mathrm{Doppler,max}}$ is the maximal Doppler frequency shift and the Doppler bandwidth will be calculated as

$$\nu_{\mathrm{F}} = 2.\nu_{\mathrm{Doppler,max}} \tag{3.17}$$

A currently unspecified assumption for the implementation of the models is relating to the Doppler spectral shape. This parameter is assumed as the Classical Jakes' spectrum in all ETSI ITS channel models [2].

Now I will specify the five different scenarios for the ETSI ITS channel models.

- **Rural LOS**: In this scenario as shown in Fig. 3.3, two vehicles are approaching one another. This channel applies in very open environments, where other vehicles, buildings and large fences are absent [2].

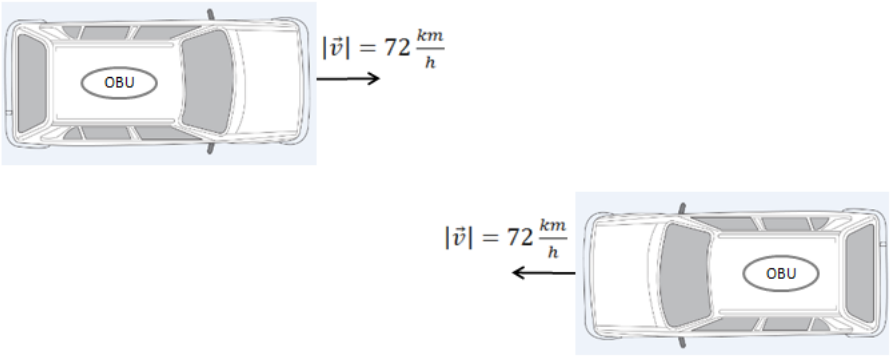

FIGURE 3.3: Scenario description: ETSI ITS Rural LOS [2]

In the Table 3.4, we find all parameters for the implementation of the channel models on the Propsim C2. The relative velocity of the vehicles in this scenario is 144 km/h. So the Doppler bandwidth of all following scenarios is calculated due to the equations from (3.16) and (3.17). The RMS Doppler spread and RMS delay spread are important to understand the behavior of the channel models. To assess these characteristics I have calculated the power delay profile $P_{PDP(\tau)}$ (or delay power spectral density) of the Rural LOS channel model from channel parameters in Table 3.4

$$P_{PDP}(\tau) = \delta(\tau - 0) + 0.0398\delta(\tau - 83) + 0.0199\delta(\tau - 183), \tag{3.18}$$

and in complete analogy to the PDP I have computed the Doppler power spectral density $P_B(\nu)$ and the integrated power

$$P_B(\nu) = \delta(\nu - 0) + 0.0398\delta(\nu - 492) + 0.0199\delta(\nu + 295), \tag{3.19}$$

According to Eq. (2.27) and (2.31), the mean delay spread and the mean Doppler spread are equal to

$$T_m = 6.55 \text{ ns}, \tag{3.20}$$

$$\nu_m = 12.93 \text{ Hz}. \tag{3.21}$$

From the Eq. (2.28) and (2.30) the value of RMS Delay spread and the RMS Doppler spread are calculated as follows

$$\tau_{RMS} = 29.0632 \text{ ns}, \tag{3.22}$$

$$\nu_{RMS} = 102.75 \text{ Hz}. \tag{3.23}$$

Parameter \ Tap	Tap1	Tap2	Tap3	Tap4	Unit
Relative Gain	0	-14	-17	n/a	dB
Delay	0	83	183	n/a	ns
Doppler Shift	0	492	-295	n/a	Hz
Fading Distribution	Rician	Rayleigh	Rayleigh	n/a	
Rician K-factor	10	n/a	n/a	n/a	dB
Doppler bandwidth	1573.4	1573.4	1573.4	n/a	Hz
Doppler spectral shape	Classical Jakes'	Classical Jakes'	Classical Jakes'	n/a	

TABLE 3.4: ETSI ITS Rural LOS channel parameters (RMS Doppler spread=102.75 Hz)(RMS Delay spread=29.06 ns)

- **Urban Approaching LOS**:In this scenario, as depicted in Fig. 3.4, two vehicles approaching each other in an Urban setting with buildings nearby [2].

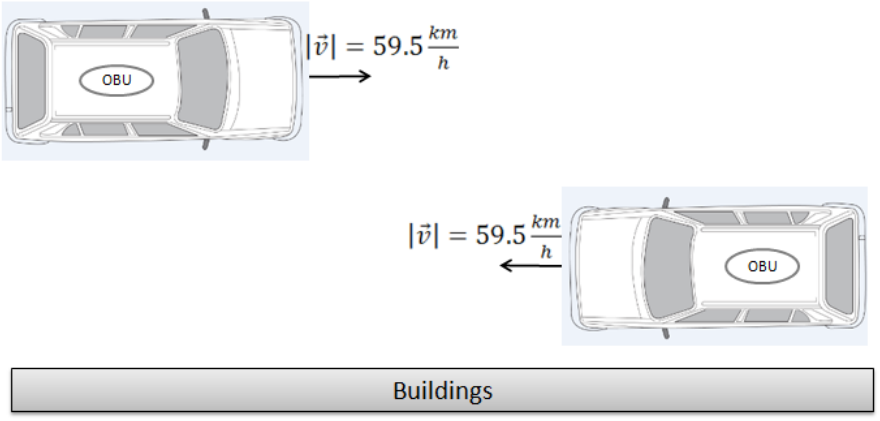

FIGURE 3.4: Scenario description: ETSI ITS Urban Approaching LOS

In the Table 3.5, we can find all needed parameters for the implementation of the channel models on the Propsim C2. The relative velocity of the vehicles in this scenario is 119 km/h. Note that taps 2,3,4 for the Urban Approaching setting are 6-7 dB stronger than in the Rural LOS setting [2].

Parameter \ Tap	Tap1	Tap2	Tap3	Tap4	Unit
Relative Gain	0	-8	-10	-15	dB
Delay	0	117	183	333	ns
Doppler shift	0	236	-157	492	Hz
Fading Distribution	Rician	Rayleigh	Rayleigh	Rayleigh	
Rician K-factor	10	n/a	n/a	n/a	dB
Doppler bandwidth	1300.1	1300.1	1300.1	1300.1	Hz
Doppler spectral shape	Classical Jakes'	Classical Jakes'	Classical Jakes'	Classical Jakes'	

TABLE 3.5: ETSI ITS Urban Approaching LOS channel parameters (RMS Doppler spread=117.67 Hz)(RMS Delay spread=75.13 ns)

- **Street Crossing NLOS**: AS the Fig. 3.5 shows, two vehicles are approaching an urban blind intersection with other traffic present. Buildings and fences are present on all corners [2].

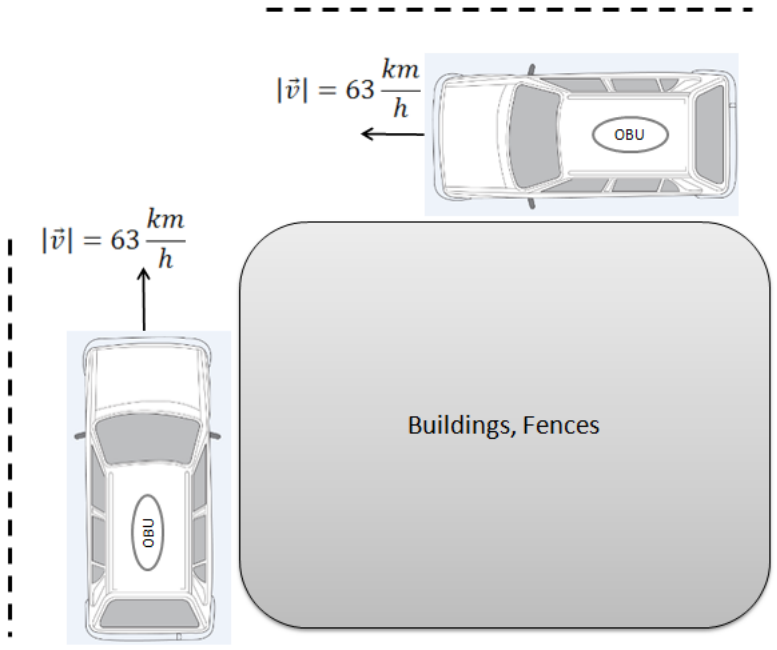

FIGURE 3.5: Scenario description: ETSI ITS Street Crossing NLOS

In the Table 3.6, we can find all needed parameters for the implementation of the channel models on the Propsim C2. The relative velocity of the vehicles in

this scenario is 126 km/h [2]. Note that taps 2,3,4 in Street Crossing are 5-8 dB stronger than in the Urban Approaching setting.

Parameter \ Tap	Tap1	Tap2	Tap3	Tap4	Unit
Relative Gain	0	-3	-5	-10	dB
Delay	0	267	400	533	ns
Doppler Shift	0	295	-98	591	Hz
Fading Distribution	Rayleigh	Rayleigh	Rayleigh	Rayleigh	
Rician K-factor	n/a	n/a	n/a	n/a	dB
Doppler Bandwidth	1376.7	1376.7	1376.7	1376.7	Hz
Doppler Spectral shape	Classical Jakes'	Classical Jakes'	Classical Jakes'	Classical Jakes'	

TABLE 3.6: ETSI ITS Street Crossing NLOS channel parameters (RMS Doppler spread=208.02 Hz)(RMS Delay spread=240.76 ns)

- **Highway LOS**: In this scenario shown in Fig. 3.6, two vehicles are following each other on multilane inter-region roadways such as Autobahns. Signs, overpasses, hill-sides and other traffic are present [2].

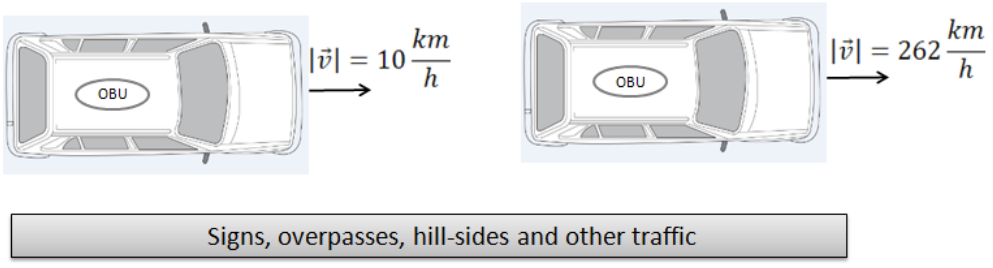

FIGURE 3.6: Scenario description: ETSI ITS Highway LOS

In the Table 3.7, we can find all needed parameters for the implementation of the channel models on the Propsim C2. The relative velocity of the vehicles in this scenario is 252 km/h [2].

Parameter \ Tap	Tap1	Tap2	Tap3	Tap4	Unit
Relative Gain	0	-10	-15	-20	dB
Delay	0	100	167	500	ns
Doppler Shift	0	689	-492	886	Hz
Fading Distribution	Rician	Rayleigh	Rayleigh	Rayleigh	
Rician K-factor	10	n/a	n/a	n/a	dB
Doppler Bandwidth	2753.4	2753.4	2753.4	2753.4	Hz
Doppler Spectral shape	Classical Jakes'	Classical Jakes'	Classical Jakes'	Classical Jakes'	

TABLE 3.7: ETSI ITS Highway LOS channel parameters (RMS Doppler spread=229.58 Hz)(RMS Delay spread=60.04 ns)

- **Highway NLOS**: This scenario, depicted in Fig. 3.7, is similar to the Highway LOS scenario but with occluding trucks present between the vehicles [2].

FIGURE 3.7: Scenario description: ETSI ITS Highway NLOS

In the Table 3.8, we can find all needed parameters for the implementation of the channel models on the Propsim C2. The relative velocity of the vehicles in this scenario is 252 km/h [2].

Parameter\ Tap	Tap1	Tap2	Tap3	Tap4	Unit
Relative Gain	0	-2	-5	-7	dB
Delay	0	200	433	700	ns
Doppler Shift	0	689	-492	886	Hz
Fading Distribution	Rayleigh	Rayleigh	Rayleigh	Rayleigh	
Rician K-factor	n/a	n/a	n/a	n/a	dB
Doppler Bandwidth	2753.4	2573.4	2573.4	2753.4	Hz
Doppler Spectral shape	Classical Jakes'	Classical Jakes'	Classical Jakes'	Classical Jakes'	

TABLE 3.8: ETSI ITS Highway NLOS channel parameters (RMS Doppler spread=450.59 Hz)(RMS Delay spread=222.97 ns)

Channel model \ Characteristics	RMS delay spread [ns]	RMS Doppler spread [Hz]	(RMS delay spread) . (RMS Doppler spread)
Rural LOS	29.06	102.75	2.98 1E -6
Urban Approaching LOS	75.13	117.67	8.84 1E -6
Street Crossing NLOS	240.76	208.02	50.08 1E -6
Highway LOS	60.04	229.58	13.78 1E -6
Highway NLOS	222.97	450.59	100.46 1E -6

TABLE 3.9: Channel models and their channel characteristics

As shown in the Table 3.9 the RMS Doppler spread in Highway NLOS is very high, followed by the Highway LOS, Street Crossing NLOS, Urban Approaching LOS and Rural LOS in descending order. The RMS Delay spread in Street Crossing NLOS is the highest, closely followed by Highway NLOS. The Delay-Doppler product is in Highway NLOS the highest. In second place is Street Crossing NLOS, followed by Highway LOS, Urban Approaching LOS and Rural LOS. The delay-Doppler product in Highway NLOS is the highest, followed by Street Crossing NLOS, Highway LOS, Urban Approaching LOS and Rural LOS.

Chapter 4

Radio Channel Emulator

In general, wireless communication systems include the radio channel plus a number of transceivers as shown in Fig. 4.1. The radio channel propagates electromagnetic waves from the transmitter to the receivers. Multipath propagation(described in Ch. 2) transmitter and receiver antennas, interference, noise and Doppler are the properties of a radio channel. Testing the wireless systems in different phases of the product development process is very important. In a test environment , radio channel emulators replace the real-world radio channel between a radio transmitter and a receiver. The radio channel emulator provides the faded transmitted signal based on mathematical models representing the physical signal transmission medium to the receiver. The adding of disturbing signals (e.g. interference or noise) to the desired signal is quite elementary but modeling of an interference is not. Emulation of multipath fading is more complicated due to fast variations of path delay, amplitudes and phases[3].

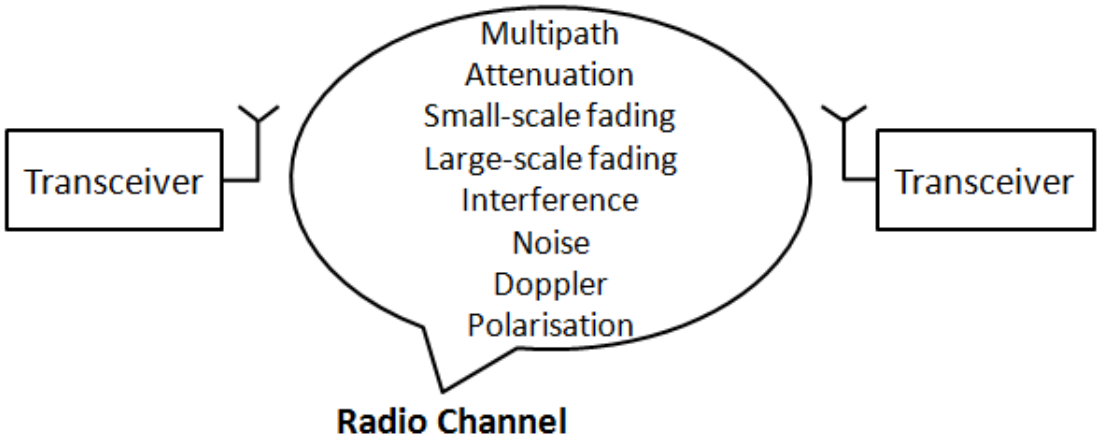

FIGURE 4.1: Physical radio propagation channel

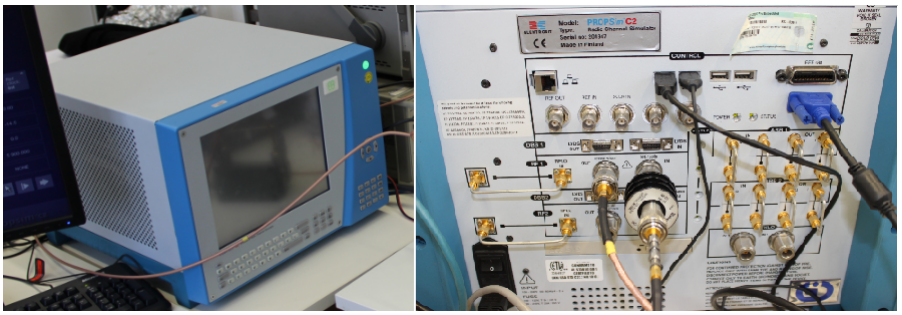

FIGURE 4.2: Propsim C2 front and rear panel

4.1 Radio Channel Emulator Propsim C2

EB Propsim C2 is a wideband channel emulator which emulates the real-time radio channel between a transmitter and a receiver. Multipath propagation and fading is simulated with Propsim C2. Average signal power level is typically attenuated by an external attenuator to the desired power level. Noise, jamming and interference can be generated by an external equipment. Noise and interference can also be generated by a separately available option of internal interference generator. Fig. 4.2 shows the Propsim C2 front panel with integrated keyboard and touch panel and the rear panel [3].

Some key freatures of Propsim C2 are [3]:

- 2 channels
- 30 MHz bandwidth (measured bandwidth at 5.9 GHz is equal to 44 MHz)
- Delay resolution 0.1 ns
- Available interfaces (see section 4.2.1)
- RF to RF interface [Frequencyrange : 350 MHz − 6 GHz]
- Analogue baseband to analogue baseband
- Analogue baseband to RF
- RF to analogue baseband
- Internal local oscillator
- Shadowing emulation
- 2x2 MIMO emulation

- Integrated user interface

"EB Propsim C2 is independent of the incoming signal. Any signal can be connected to Propsim C2 input, as long as RF bandwidth is 30 MHz or less and RF power is 0 dBm at highest. Propsim C2 hardware is independent of channel model. The Channel impulse response matrix is defined by a software and downloaded into the emulator memory." [3]

"Propsim C2 operates like a programmable filter, where the output signal depends on the input signal and the channel model (i.e. channel impulse response). Wideband CIR is typically represented by discrete tapped delay line model" [3] as depicted in Fig.4.3.

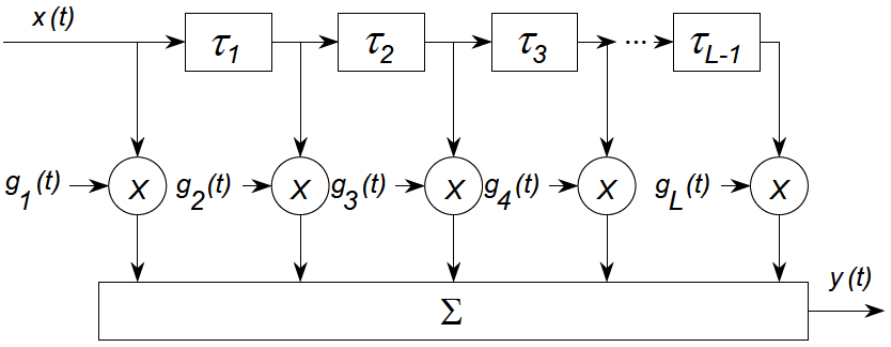

FIGURE 4.3: Tapped delay line model in baseband [3]

The channel impulse response $h(t,\tau)$ is defined as in Eq.(4.1) [3]

$$h(t,\tau) = \sum_{i=1}^{N} \beta_i(t) e^{j\Phi_i(t)} \delta[\tau - \tau_i(t)], \tag{4.1}$$

"where $\beta_i(t)$ and $\Phi_i(t)$ represent the amplitude and phase of the *ith* path arriving at delay τ_i and at time t" [3]. Frequency response is calculated from the impulse response by Fourier Transform as in Eq.(2.10). The received signal $y(t)$ is calculated from the input signal $x(t)$ and the system's impulse response $h(t,\tau)$. The received signal $y(t)$ is a convolution of $x(t)$ and $h(t,\tau)$

$$y(t) = x(t) * h(t,\tau) \tag{4.2}$$

"Propsim C2 modeling means calculation of $h(t,\tau)$ for each channel realisation. $x(t)$ is generated by an external device and $y(t)$ is the Propsim C2 output signal". The $h(t,\tau)$ is calculated beforehand, but $y(t)$ must be calculated in real time [3].

4.2 System Architecture

In this section I describe the Propsim C2 system architecture regarding two major points of view, namely hardware and software. The system is controlled with integrated display, touch panel and keyboard or with Automatic Test Equipment (ATE) interface over General Purpose Interface Bus (GPIB) or Local Area Network (LAN). It is also possible to directly connect some external devices, such as mouse, keyboard or removable storage to the emulator[3].

4.2.1 Emulator Hardware Interfaces

The hardware interfaces of Propsim C2 are Analog Base Band (ABB), Digital Base Band (DBB) and Radio Frequency (RF), as depicted in Fig. 4.4.

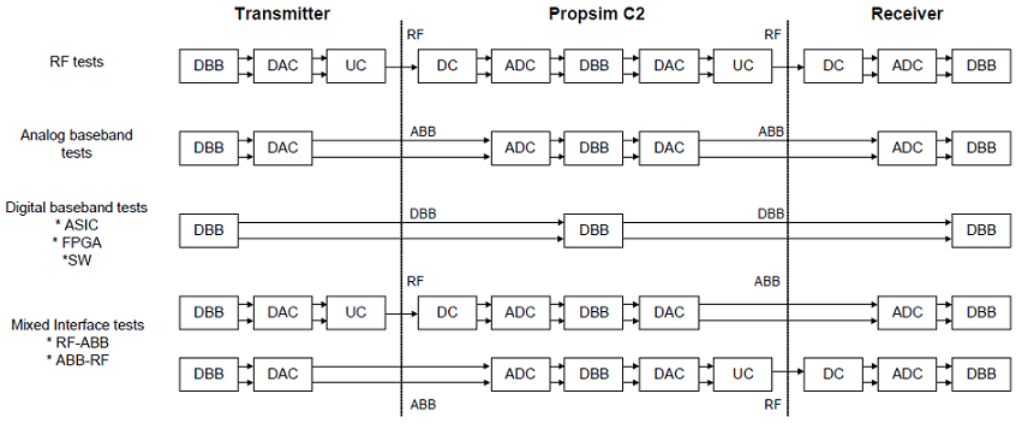

FIGURE 4.4: Signal interface types[3]

A typical transmitter has DBB part, Digital Analog converter (DAC) and Up Converter (UC). A typical receiver has Down Converter , Analog Digital Converter (ADC) and DBB. In-phase / Quadrature (I/Q) modulation and demodulation are also part of up/-down conversion of the signal. RF, ABB and DBB connections are available in Propsim C2. The three different interfaces of Propsim C2 can be used in different phases of the product development process. "DBB interface brings radio channel into very early phase of product development. Fading simulation can be done for Field Programmable Gate Array (FPGA) tests, for example. This would mean significant reduction of development costs due to early detect of possible design flaws. In addition, Propsim C2 offers possibility to use mixed interface modes, where transmitter uses RF interface and receiver ABB interface, or vice versa" [3].

Since the RF interface is the interface which I have used I would like to specify it here. Analog signal path in RF interface of the Propsim C2 can be seen in the Fig. 4.5. The

RF input signal at RF interface input is first down converted to Intermediate Frequency (IF) and then to analog baseband. AD and DA conversions are situated in the BBU unit. The multipath fading emulation and summing of paths is carried out in digital parts utilizing Digital Signal Processing (DSP) technology. After fading, the outcoming signal is up converted to IF and then back to the original RF frequency. "Unless internal Local Oscillator (LO) is used, external RFLO must be connected separately to every active Radio Frequency Unit (RFU). In the RFU, the RFLO signal is divided to the up converter and the down converter. IFLO is generated internally in the RFU" [3].

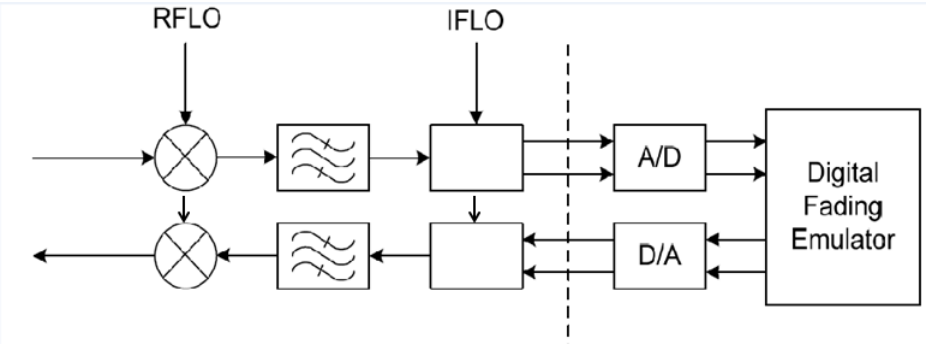

FIGURE 4.5: RF interface[3]

Propsim C2 is equipped with an internal LO option, so the external signal generator is not required for RFLO. The frequency of RFLO is as follows [3]

$f_{rflo} = f_c + 300$ MHz when f_c is below 3 GHz or equal
$f_{rflo} = f_c + 300\,MHz$ MHz when f_c is above 3 GHz.

4.2.2 User Interfaces

The purpose of the user interface is to manage the Propsim C2 Hardware, e.g. running existing simulations, creating new simulations, or editing old ones are done with the user interface. This consists of three screens: *main screen, edit screen and impulse response screen* [3].

4.2.2.1 Main Screen

As Fig. 4.6 shows from the File menu on the main screen the user can load, create or edit simulations. There is also a Directory tool to move simulations from and to external storage devices and networks. With the System menu, the emulator can be set up for LAN or GPIB, which I did not used in my work. Also, the system menu contains log export functionality for troubleshooting purposes. "Another option in System menu is

the self tests for some parts of the emulator, like memory or control bus test, which are automatically executed during emulator start up" [3].

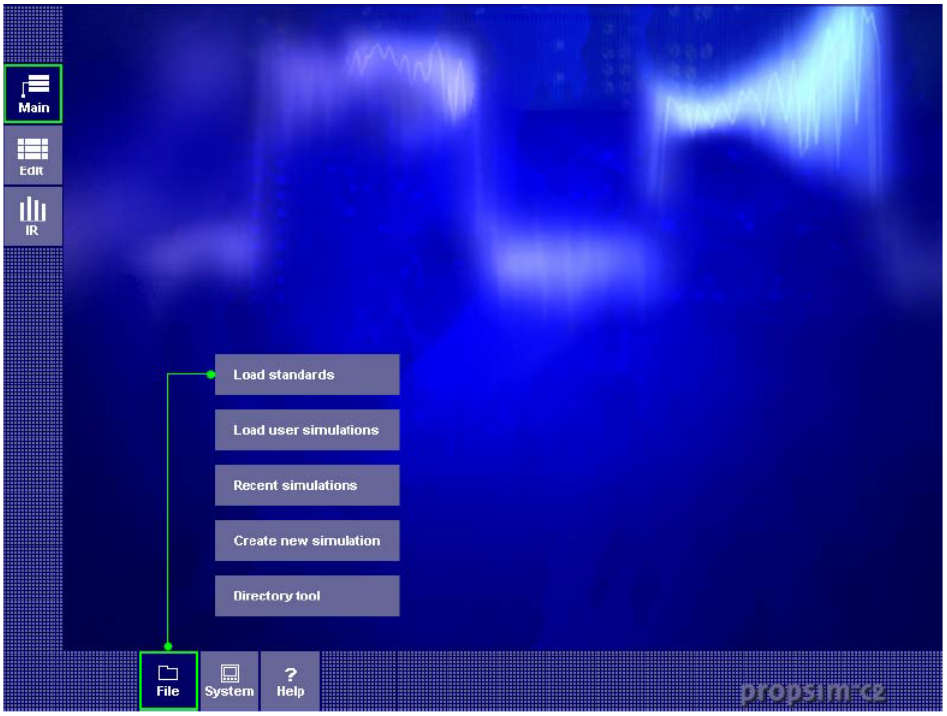

FIGURE 4.6: Main screen [3]

4.2.2.2 Impulse Response Screen

In the Impulse Response Screen (IR Screen), the simulations are configured, run or stopped. Following configuration parameters can be set in IR screen [3]:

- Interface: the interface type like RF, ABB, DBB or the mixed interfaces RF/ABB and ABB/RF can be selected.
- Connection between the channels: using emulator channel, namely Channel 1 (CH1) or Channl 2 (CH2) can be selected. There is a possibility to run both channels simultaneously . They can be run independent or in Multiple Input Multiple Output (MIMO) mode. Also, the second channel can be used as an interference. Therefore there are four options:
  - Isolated channels where both channels are running independently.
  - Inputs connected together
  - Outputs connected together

  - Both inputs and outputs connected together

- RF Local
- Reference Clock
- Mobile speed
- Input level
- Crest factor
- Output gain
- Center frequency
- Interference

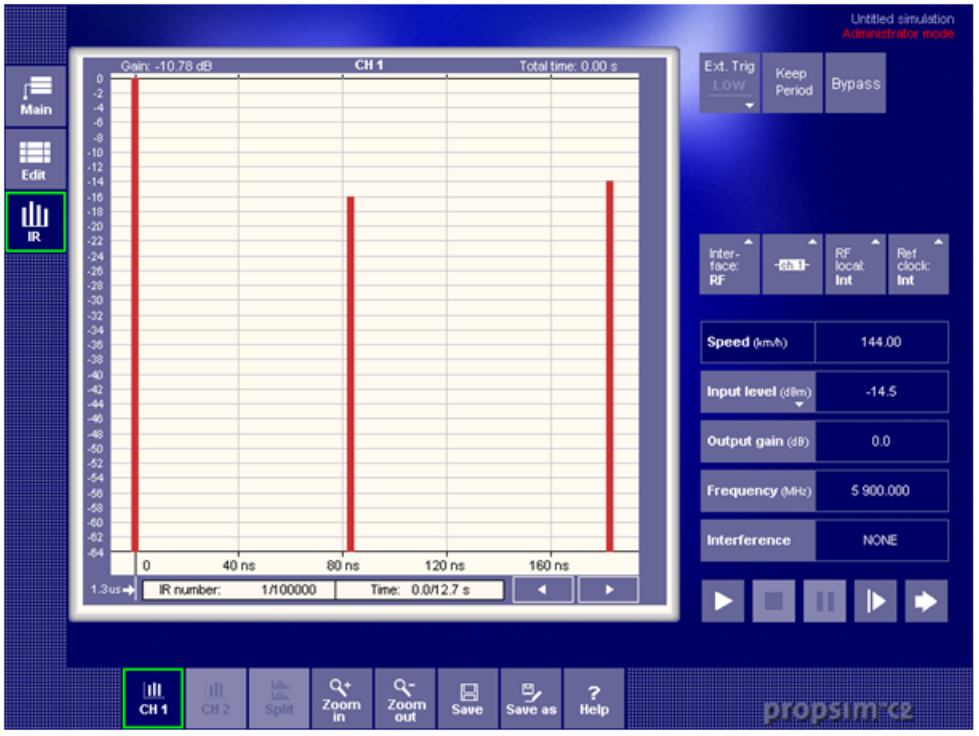

FIGURE 4.7: Impulse response screen [3]

Simulation parameters of the IR screen are shown in Fig. 4.8.

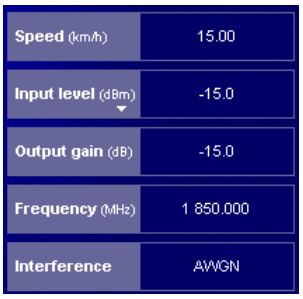

FIGURE 4.8: Simulation parameters[3]

4.2.2.3 Edit Screen

The user can create a new simulation or edit an existing simulation in the Edit screen. As depicted in Fig. 4.9 the signal paths of a simulation can be set in the Edit screen. There are following path parameters in the path list of the Edit screen [3]:

- **Delay**: This parameter indicates the delay of the signal path compared to the LOS path between TX and RX in nanoseconds.
- **Delay function**: Delay function expresses the function according to which the delay behaves. There are following alternatives: Fixed, Hopping, Linear and Sinusoidal. The Delay function in all channel models, implemented in this thesis is fixed. That means that the delay value of the path is constant during the whole simulation period.
- **Delay properties**: For the fixed delay are no properties available.
- **Amplitude**: This parameter specifies the gain of the path in decibels. This can be set between -60 and 0 dB.
- **Amplitude distribution**: It indicates the function for the behaviour of the parameter amplitude. There are following option to select: Constant, Rayleigh, Pure Doppler and Rice. (Where constant means no fading.)
- **Distribution parameters**: This field depends on the selected amplitude distribution. There are following options to set:
  - Constant: Phase shift in degrees.
  - Rayleigh: No parameters
  - Pure Doppler Angle between the mobile motion and the incoming radio wave in degrees.

– Rice: Angle between the mobile speed and the LOS signal in degrees and the Rician K factor.

- **Doppler spectrum**: This parameter indicates the shape of the Doppler spread function and it can be selected between three alternatives: classical Jakes', flat or rounded.

FIGURE 4.9: Edit screen [3]

4.3 Carrier Leakage

"In ideal situation signal processing operations such as mixing and up/down conversions produce only the wanted effect. In the real world mixers leak, amplitude and phase errors arise, cross coupling happens etc. It is well known that these are all natural phenomena and cannot be completely removed from a system. These inevitable effects cause excess signals to appear at the output spectrum of any RF equipment" [13].

"Carrier Leakage (CL) tuner tool is used by Propsim C2 to minimize the carrier signal leakage at emulation center frequency, which can cause mirror images and un-wanted interference in the emulation. The carrier signal leakage is related to emulation center frequency, input and output settings, so for optimal performance the tuning needs to be

done for each emulation separately" [14]. The carrier signal leakage tuning is depicted in figures below:

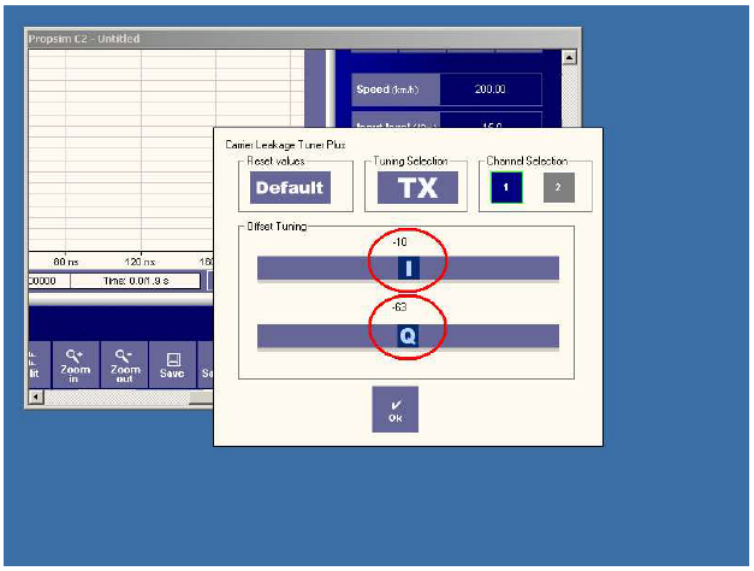

FIGURE 4.10: Carrier Leakage Tuning for Channel-1 TX[14]

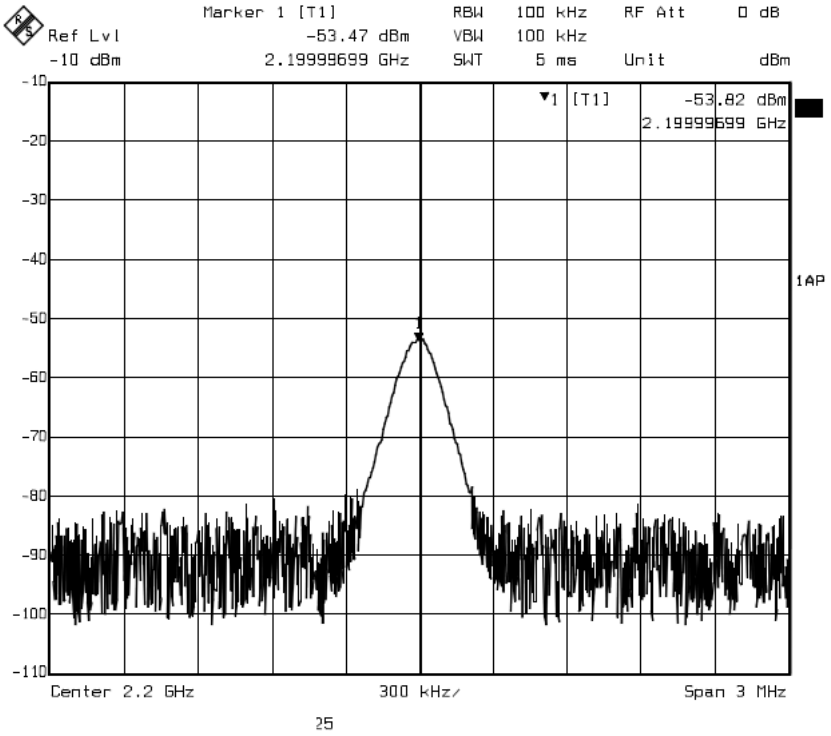

FIGURE 4.11: Carrier leakage signal from channel-1(CH1-TX).[14]

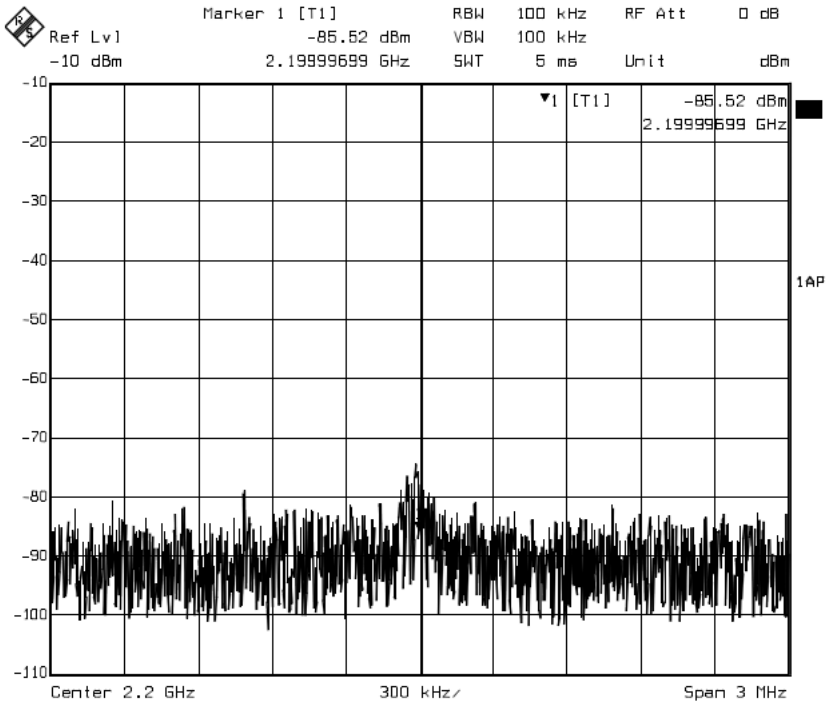

FIGURE 4.12: Suppressed carrier leakage signal from Channel-1(CH1-TX).[14]

4.4 Implementation of Channel Models on Propsim C2

In previous sections, I have described the channel models and the channel emulator Propsim C2. In this section, I describe the implementation of the mentioned channel models on the Propsim C2. There are in general two methods to implement a channel model on the Propsim C2. The first possibility is by using the GUI described in section (4.2.2). The second method is to build the impulse responses in PC , store and run the IR-file in Propsim C2.

4.4.1 Implementation through GUI

As described in section (4.2.2.3), the different parameters for different taps of the channel models can be directly set in the edit screen of the GUI. I would like to start with the six time- and frequency-selective empirical channel models for vehicular wireless LANs. The parameters I need to enter for every single tap for the implementation of these channel models are

- Tap amplitude (tap gain) [dB]

- Tap delay [ns]
- Rician K factor [dB]
- Doppler frequency shift for Rayleigh distributed tap [Hz]
- Doppler bandwidth of each tap [Hz]
- Doppler frequency shift for the LOS path [Hz]
- Amplitude distribution, Rician or Rayleigh
- Doppler spectral shape

If we look at the Fig. 4.9, we notice that the parameters *Doppler bandwidth* along with *Doppler frequency shift* for Rician and Rayleigh distributed taps do not exist. Therefore the question arises how to specify these channel model parameters on Propsim C2.

The Doppler bandwidth can be set through the parameter *mobile speed* described in equations (3.16) and (3.17). The drawback of this method is that all taps of the channel model will have the same Doppler bandwidth and this parameter can not be specified for each tap.

The other question is how to feed the Doppler frequency shift of every Rician or Rayleigh tap into the machine. As seen in previous section, if in the edit screen the path amplitude distribution is selected as Rician, then there is one parameter for the amplitude to set namely the *Phase shift* in degree. So I have set the parameter Doppler frequency shift in Propsim C2. The relation between the Doppler frequency shift and the angle is defined in section (2.3) as bellow

$$\alpha = \arccos\left(\frac{\nu_D C_0}{f_c|\overrightarrow{v}|}\right). \tag{4.3}$$

But in the taps with Rayleigh distribution, there is no parameter to set and therefor it will not be possible to specify the Doppler frequency shift in Rayleigh taps. For this reason the only possibility for an implementation of these channel models on the Propsim C2 via GUI is to approximate the Rayleigh paths through Rician paths, as described in appendix of [22]. I will show an example of an implementation in this way in chapter 6.

According to the central limit theorem, I can approximate one Rayleigh path through at least eight Rician paths. So I can imply the Doppler frequency shift of Rayleigh paths in this way. More details and the measurement results are presented in Appendix B.

4.4.2 Implementation through IR-files

I have described the Implementation of the presented vehicular channel models via GUI on the Propsim C2. As shown, an implementation in this way is only possible through an approximation. Thus, this method is not the most helpful in case of vehicular channel models. The other method of implementation of the channel models on the channel emulator Propsim C2, is to generate the Impulse Responses (IRs) in PC via e.g. a Matlab program. The IR-file will be stored and run on the Propsim C2. To do so, I have used the already existing Matlab code by Anite, which is written for the channel models presented in [1]. I have modified the Matlab code for the ETSI ITS channel models and generated the IRs as shown in Appendix A.

Chapter 5

Standards 802.11p and ETSI ITS-G5

5.1 Orthogonal Frequency Division Multiplexing

The 802.11 p signal is wideband (10 MHz) and OFDM modulated. In this stage I describe the OFDM modulation and the relationship of OFDM and the vehicular radio channels.

5.1.1 Narrowband vs. Wideband

Suppose the rms delay spread τ_{RMS} is small compared to $\frac{1}{B}$, where B is the signal bandwidth. I.e. $\tau_{RMS} \ll \mathrm{B}^{-1}$. This assumption implies that $\mathrm{u}(t-\tau_i) \approx \mathrm{u}(t)$, where $\mathrm{u}(t-\tau_i)$ is the ith channel multipath component with the time delay τ_i. With the aim of clear illustration, I assume the transmit signal as a train of pulses, where each pulse carries information in its amplitude and/or phase. If the multipath rms delay spread τ_{RMS} is smaller than the transmitted pulse duration T, $\tau_{RMS} \ll T$, then the multipath components interfere with each other, as shown in Fig. (5.1). The constructive and destructive interference leads to the narrowband fading of the pulse. Since the time dispersion of the pulse is small, there are small interferences with a subsequently transmitted pulse. On the other hand, if $\tau_{RMS} \gg \mathrm{T}$, then the multipath components interfere strongly. This effect is called ISI. ISI is an important form of linear distortion, which appears in wideband transmitted signals, which should be combated [5].

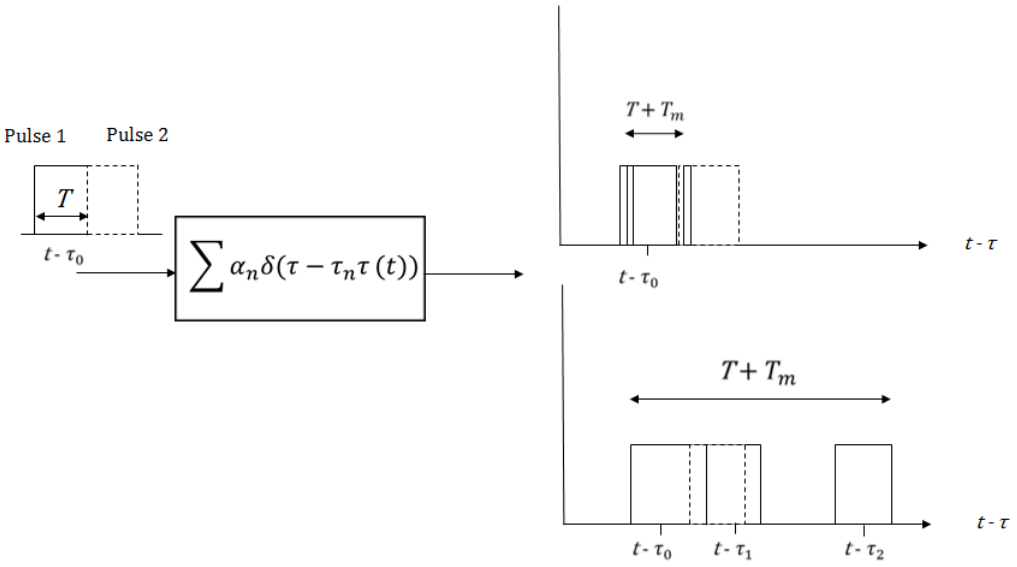

FIGURE 5.1: Multipath resolution [5]

5.1.2 Implementation of OFDM transceivers

Orthogonal Frequency-Division Modulation (OFDM) is a modulation form which converts high-rate (wideband) transmission (datastream) into N low-rate (narrowband) parallel transmissions (datastreams). The N parallel streams are transmitted by modulating N separate carriers, called subcarriers. That leads to an increasing of the symbol duration on each subcarrier by a factor of N. The receiver separates signals carried by different subcarriers. Therefore, the subcarriers have to be orthogonal. Suppose W is the total available bandwidth, then the subcarriers are at the frequencies $f_n = \frac{nW}{N}$ and $W = \frac{N}{T_s}$, where T_s is the symbol duration and $n = 0, 1, ..., N-1$. For Pulse Amplitude Modulation (PAM) with rectangular pulse shape, mutual orthogonality of the subcarriers is seen from the relation [11]

$$\int_{iT_s}^{(i+1)T_s} \exp(j2\pi f_k t) \exp(-j2\pi f_n t) \mathrm{d}t = \delta_{nk}. \tag{5.1}$$

In order to contract a OFDM transceiver, the first step is to split the original data stream into N parallel data streams, where each of them has the bandwidth of $\frac{W}{N}$. For each subcarrier frequency, a local oscillator at the subcarrier frequency $f_n = \frac{nW}{N}$ is needed. Presuming the complex transmit signal at time instant i on the nth subcarrier is $c_{n,i}$. Then the transmit signal can be written as [11]

$$s(t) = \sum_{i=-\infty}^{\infty} s_i(t) = \sum_{i=-\infty}^{\infty} \sum_{n=0}^{N-1} c_{n,i} g_n(t - iT_s), \tag{5.2}$$

where the transmit filter pulse $g_n(t)$ is

$$g_n(t) = \begin{cases} \frac{1}{\sqrt{T_s}} \exp(j2\pi n \frac{t}{T_s}) & \text{for } 0 < t < T_s \\ 0 & \text{otherwise} \end{cases} \tag{5.3}$$

We consider the OFDM symbol for $i = 0$ and sample it at $t_k = \frac{kT_s}{N}$, then

$$s_k = s(t_k) = \frac{1}{\sqrt{T_s}} \sum_{n=0}^{N-1} c_{n,0} \exp(j2\pi n \frac{k}{N}). \tag{5.4}$$

The last equation is interpreted as the Inverse Discrete Fourier Transform (IDFT) of the transmit symbols $c_{n,0}$. This means the transmitter can be realized via an IDFT block, whereby the size of the IDFT block is equal to the number of subcarriers. We replace the IDFT with an Inverse Fast Fourier Transform (IFFT), if the number of subcarriers is a power of 2, which is common. On the receiver side, there is an inverse process. The OFDM signal is shown in Fig. (5.2) [11].

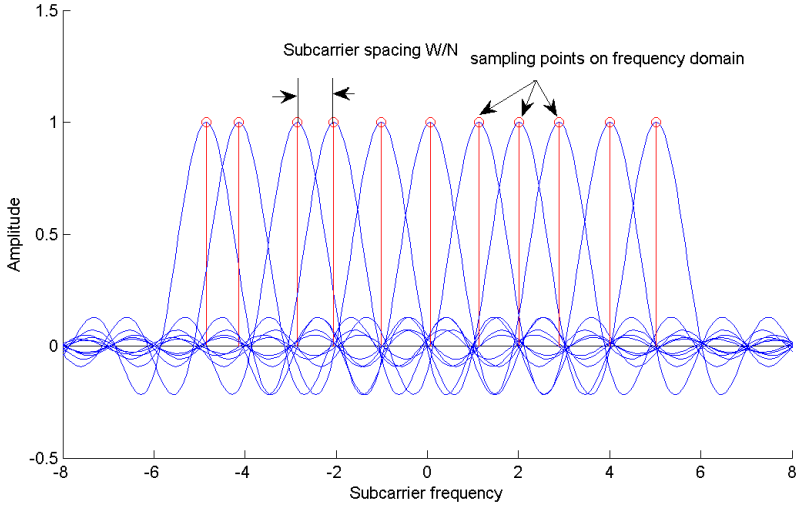

FIGURE 5.2: OFDM signal subcarriers

5.1.3 OFDM in Frequency Selective Channel

As described above if a wideband transmission system operates in a frequency-selective channel, the delay dispersion of the channel will have a large impact on the performance of the transmission system. In an OFDM system, the wideband datastream will be converted into a parallel system of narrowband datastreams. The symbol duration on

each subcarrier of OFDM system is larger than the delay spread of the channel. As shown in chapter 12 of [11], even when the symbol duration is larger than the delay spread, the delay spread can have a negative impact on the transmission performance and lead to significant Bit Error Ratio (BER). Additionally to the ISI, the other negative effect is the Inter Carrier Interference (ICI). The reason for ICI is a loss of the orthogonality between the subcarriers due to the delay dispersion on the radio channel. Both effects can be combated through a guard interval between two subcarriers, called the *Cyclic Prefix (CP)* [11]

$$\overline{g}_n(t) = \begin{cases} g^*(\widehat{T}_s - t) & \text{for } 0 < t < \widehat{T}_s \\ 0 & \text{otherwise} \end{cases} \tag{5.5}$$

$$r_{n,0} = H\left(n\frac{W}{N}\right) c_{n,0} + n_n, \tag{5.6}$$

where $H\left(n\frac{W}{N}\right)$ is the channel transfer function at the frequency kW/N. As the equation 5.6 shows, using the CP in OFDM transmission converts, a frequency-selective channel into a number of parallel flat-fading channels [11].

5.2 Standards IEEE 802.11p and ETSI ITS-G5

The standard 802.11p is an amendment to the WiFi standard IEEE 802.11, which is Ratified in July, 2010 [8], in order to integrate it as Wireless Access in Vehicular Environments (WAVE). The PHY and Media Access Control (MAC) layers of WAVE are implemented by IEEE 802.11p standard, the upper layers by IEEE P1609 [23]. The PHY layer of 802.11p is a variation on 802.11a, whereas the channel bandwidth is scaled to 10 MHz, by halving the clock rate [9]. It utilizes the OFDM modulation technique, consisting of 64 subcarriers in total: 48 data subcarriers, 4 pilot subcarriers and 12 null subcarriers. The reason for the half-rate clock can be explained as followes: By halving the the channel bandwidth, the subcarrier spacing is halved, which enables larger frequency selectivity in wireless vehicular communication. It also increases the length of the CP as a GI, to combat longer delay spreads [10]. The technical Committee on Intelligent Transport Systems (TC ITS) of European Telecommunications Standards Institute (ETSI) has developed a standard for vehicular networks, based on IEEE 802.11p. The major purpose of the ETSI ITS standard is to adapt the 802.11p to the European requirements. In PHY, The OFDM modulation, with 10 MHz bandwidth,is used, as described in IEEE 802.11p. In the following I will shortly explain the major components of the ETSI ITS-G5 standard.

5.2.1 Frequency and Channel allocation

The ETSI ITS G5 covers the following frequency ranges by using the IEEE 802.11p :

ITS-G5A: Operation of ITS-G5 in European ITS frequency bands is dedicated to ITS for safety related applications in the frequency range 5,875 GHz to 5,905 GHz[6]. ITS-G5B: Operation in the european ITS frequency bands, dedicated to ITS non- safety applications, in the frequency range 5,855 GHz to 5,875 GHz [6]. ITS-G5C: Operation of ITS applications in the frequency range 5,470 GHz to 5,725 GHz [6].

The Control Channel dedicated for safety applications, are described in the Table 5.1:

Channel type	Center frequency	IEEE channel number	Channel spacing	Default data rate	TX power limit	TX power density limit
G5CC	5900 MHz	180	10 MHz	6 Mbit/s	33 dBm EIRP	23 dBm/MHz

TABLE 5.1: ETSI channel allocation (from Table 2 in [6])

5.2.2 ETSI ITS Protocol Stack

The most notable distinction between the WAVE and the ETSI ITS is represented by the definition of a facilities layer, as shown in Fig.5.3 as a support for applications. Avoiding the data congestion was the motivation for introducing of a new layer. "The facilities layer provides a collection of functions to support ITS applications. The facilities provide data structures to store, aggregate and maintain data of different types and sources (such as from vehicle sensors and from data received by means of communication)"[24].

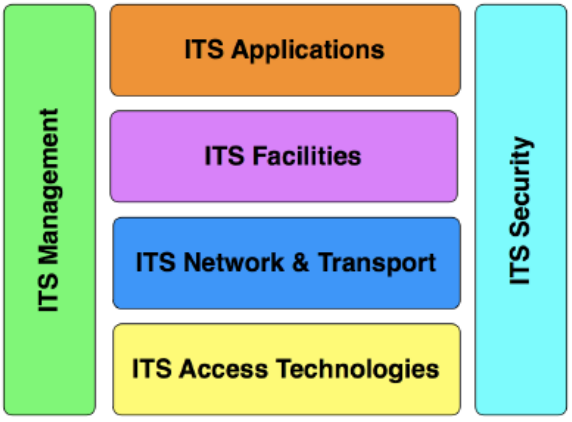

FIGURE 5.3: ETSI ITS protocol stack ([6])

5.2.2.1 ETSI Access technologies Layer

As described in [6] The Access technologies layer of ETSI ITS is similar to the IEEE 802.11p. A major distinction between these is the Decentralized Congestion Control (DCC) [25]. "Decentralized congestion control (DCC) is a mandatory component of ITS-G5 stations operating in ITS-G5A and ITS-G5B frequency bands to maintain network stability, throughput efficiency and fair resource allocation to ITS-G5 stations. DCC requires components on several layers such as the access layer, the networking and transport layer, the facility layer, the management layer of the protocol stack and these components jointly work together to fulfill the following operational requirements:

- Provide fair allocation of resources and fair channel access among all ITS stations in the same communication zone.
- Keep channel load caused by periodic messages below the pre-defined thresholds.
- Reserve communication resources for the dissemination of event driven, high priority messages.
- Provide fast adoption to a changing environment (busy / free radio channel).
- Keep oscillations in the control loops within well-defined limits.
- Comply to specific system requirements, e.g. reliability" [25].

5.2.2.2 ETSI Network and Transport Layer

"The GeoNetworking protocol is a network layer protocol that provides packet routing in an ad hoc network. It makes use of geographical positions for packet transport. GeoNetworking supports the communication among individual ITS stations as well as the distribution of packets in geographical areas" [26].

"The Basic Transport Protocol (BTP) provides an end-to-end, connection-less transport service in the ITS ad hoc network. Its main purpose is the multiplexing of messages from different processes at the ITS Facilities layer, e.g. CAM and DEN services, for the transmission of packets via the GeoNetworking protocol as well as the de-multiplexing at the destination). BTP enables the protocol entities at the ITS Facilities layer to access services of the GeoNetworking protocol and to pass protocol control information between the ITS Facilities layer and the GeoNetworking protocol" [27].

5.2.2.3 ETSI Facilities Layer

the most notable distinction between the WAVE and the ETSI ITS is represented by the definition of a facilities layer as shown in Fig. 5.3 as a support for applications. The introduction of a new layer was motivated due to avoid a data congestion for the safety services. "The facilities layer provides a collection of functions to support ITS applications. The facilities provide data structures to store, aggregate and maintain data of different type and source (such as from vehicle sensors and from data received by means of communication)" [24]. The ETSI facilities layer contains application support, information support and comminication support [28].

One central message type handled in facilities layer is the Cooperative Awareness Message (CAM). CAMs are broadcasted within the ITS-G5 (802.11p) network and provide information of presence, positions as well as basic status ITS stations to neighbouring ITS stations, that are located within a single hop distance. All ITS stations generate, send and receive CAMs, as long as they participate in V2X networks. By receiving CAMs, the ITS station is aware of other stations in its neighbourhood area as well as their positions, movement, basic attributes and basic sensor information. At receiver side, CAMs are evaluated. This allows ITS stations to acquire situational awareness and act accordingly. Information distributed by CAM Management is commonly used by related use cases (e.g. "cooperative driving") and therefore the CAM Management is a mandatory facility. The Approaching Emergency Vehicle and Slow Vehicle Warning are just two use cases which benefit from CAM." The CAMs are typically broadcasted with the frequency of 1-10 Hz and the maximum frame size is 800 Bytes [29]. There are additional messaging types such as, Decentralized Environmental Notification Messages (DENM) which are not in focus of this thesis.

Chapter 6

Packet Error Ratio Measurements

Chapters 3 and 4 give an overview about the definition of the channel models and their implementation on the channel emulator Propsim C2. In this chapter, I describe the performance measurement of Kapsch transceiver MTX-9450 for the ETSI ITS channel models.

6.1 Measurement Description

The aim of this measurement is to calculate the PER diagram over the average received power. The PER is calculated with:

$$PSR = \frac{Number\ of\ correctly\ decoded\ packets}{Number\ of\ transmitted\ packets}. \tag{6.1}$$

$$PER = 1 - PSR \tag{6.2}$$

The number of transmit packets and their length is set at the MTX transmitter. The number of correctly received packets(a packet is identical to a OFDM frame) and also the number of error decoded packets can be calculated and displayed by the Kapsch transceiver at the RX side, as described in Sec. 6.1.2.1.

At the RX I have determined the number of the correctly received packets for different average received power (Sec. 6.1.2.1). Furthermore, I have increased the received power incrementally (step-wise)and measured the average received power. To do so, my first step was to investigate the transceiver's signal in order to measure its power correctly. As seen from the detailed description of the transceiver in Sec.6.1.2.1, the transmit signal

is an OFDM modulated burst-signal as shown in Fig. 6.7. First I have used the power meter *NRP-Z22* by *Rohde und Schwarz* (R&S®) as the power measurement device in the measurement setup. These are three-path diode power sensors that investigate the signal in time-domain and measure the average signal power. The power meter is connected to the PC via a USB-connector. The power meter can be operated through installed software on the PC. The NRP-Z22 in combination with the software *Power Viewer Plus* can measure the signal power in time domain at 5.9 GHz[30]. After some measurement runs I have noticed that this power meter is not suitable for the measurement of this signal. Because the changing of the TX power-against the expectation that the PER curve should be independent of the TX power- had an impact on the PER curve. Again this is because of the output signal spectrum of the channel emulator Propsim C2, relating to which the average power is measured. As mentioned in Ch. 4, there is an LO at a distance of 300 MHz of the useful signal at 5.9 GHz, as shown in Fig. 6.1, where the numbers 2 and 1 are for the LO and the useful signal, respectively. Since the power meter NRP-Z22 measures the power with a large bandwidth, the measured average power is not only the signal power at 5.9 GHz but rather a superimposed average power of signals at 5.6 GHz and 5.9 GHz, namely the useful signal plus the LO. That is why, I have replaced the power meter NRP-Z22 with the signal analyzer FSQ, which can measure the signal power within the definite bandwidth.

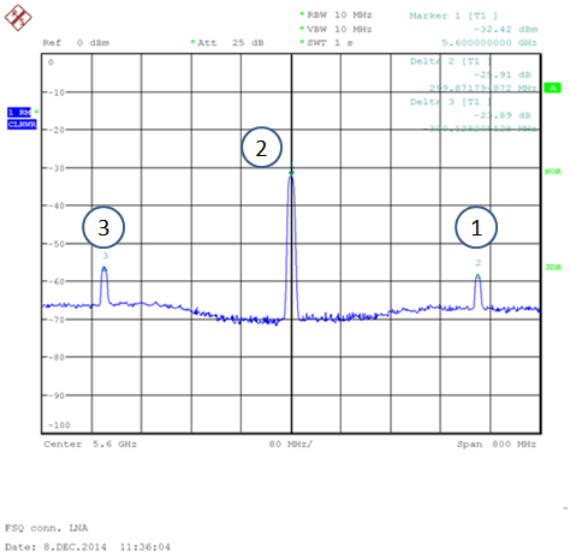

FIGURE 6.1: Propsim C2 output signal

6.1.1 Measurement Setup

This section documents the PER measurement setup more clearly. The transceiver MTX-9450 provides two antenna connectors for the two external omnidirectional antennas. These will normally be used for standard Cooperative ITS (C-ITS) applications requiring radio coverage in all directions. In addition the built-in directional antenna arrays provide radio coverage within an application of a specific communication zone [12]. As the measurement setup in Fig. 6.3 shows, I have used the port 1 (which is a connector N for an external antenna) and connected it to the channel emulator with an RF cable. I have tested the wireless communication between two MTXs and observed, that without a proper shielding TX and RX would communicate via the internal antenna. Therefore in order to ensure that the communication between TX and RX is running only through the channel emulator, I had to shield the internal antenna in the MTX. It has to be mentioned that the internal antenna has been already deactivated through the MTX software. I have covered both transceivers with aluminium foil, as shown in Fig. 6.3 marked as number 5. Some different tests have confirmed that with this shielding, the transmission of packets between TX and RX via internal antenna is completely blocked. That means that the received packets by the transceiver are coming only through the channel emulator.

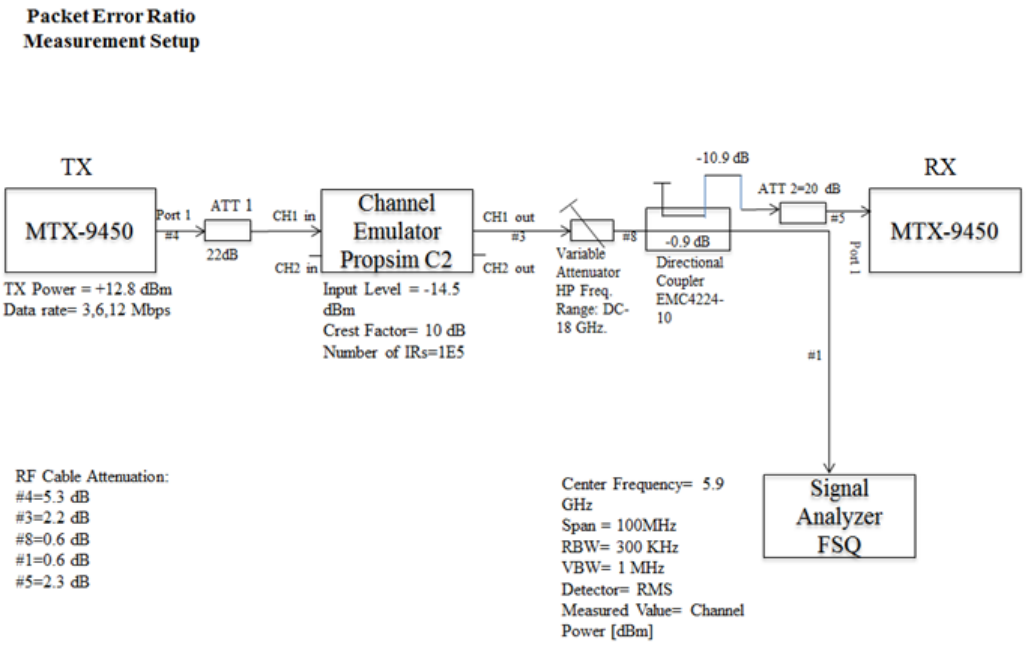

FIGURE 6.2: Measurement setup block diagram

According to Kapsch, the recommended operating power level for the transceiver MTX is 3-6 dB below the maximum power level, which is +28 dBm. Hence I have set the

transmit power level at MTX at TX side by +24 dBm. On the other side, in agreement with the Propsim C2 recommendations, its optimum operation input power level is about -15 dBm[3]. Furthermore, I have used fixed attenuators at the input of Propsim C2, in order to reduce the power level to -14.5 dBm (nearly -15 dBm). The RF cable attenuation is measured as described below. The MTX was connected to the channel 1 (CH1) of Propsim C2 and all measurements are carried out in this RF channel of the Propsim C2. Additional to the channel model parameters used by generating the IR files in Matlab, the following parameters are set in the IR screen of Propsim C2 (see also 4.2.2.2):

- Inputlevel = -14.5dBm
- Crestfactor = 10(dB)
- Outputgain = 0(dB)

At the receiver, I have increased the RX input power level in 1 dB steps, utilizing a variable attenuator . In each measurement run -for each measured RX power- the TX has sent 10000 packets. At the receiver, the number of correctly decoded packets for different received power is calculated. Furthermore, utilizing a Directional Coupler (DC) in the measurement setup (number 3 in Fig. 6.3), provides the possibility to measure the received power online, whereby the received signal will be guided through the transmitted path of the directional coupler to the FSQ. Otherwise, in case of using the couple path of the DC because of the higher attenuation, the signal power level would not be in the measurable area of the FSQ (number 4 in Fig. 6.3). With the help of a RF variable attenuator (number 2 in Fig. 6.3) the RF signal power at the receiver will be increased stepwise.

6.1.2 Measurement Components

The components in my measurement setup, are depicted in Fig. 6.3. In this section I describe the setup components more detailed.

6.1.2.1 MTX-9450

The Kapsch transceiver MTX-9450 was used in the measurement setup as both transmitter and receiver. The device depicted in Fig.6.3 as number 5, shows the MTX receiver with a shielding. There is a power supply board for the MTX with 24/48 V and power

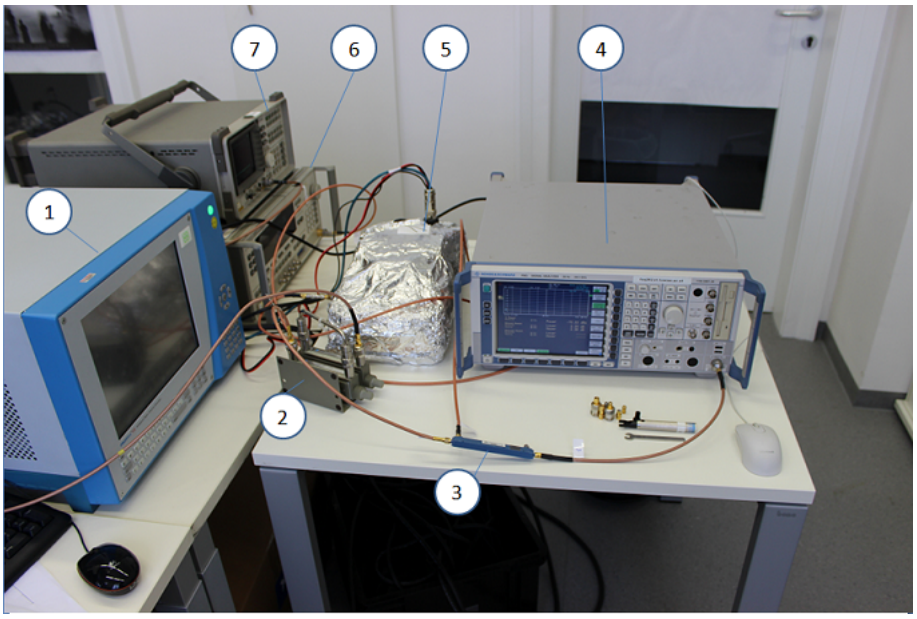

FIGURE 6.3: Measurement Setup

Parameter	Possible Value(s)
Transmit power at connector 1	-10 [dBm] $\leq$ TX power level $\leq$+18 [dBm]
Transmit channel frequency	170,172,174,175,176,178,180,181,182,184
Data rate	3,4.5,6,9,12,18,24,27 [Mb/s]
Payload size	0 - 1100 [Bytes]
Number of packets in one burst	≥ 0
Number of transmit bursts	≥ 0
Delay length between packets	≥ 0 [ms]

TABLE 6.1: MTX Signal parameters

consumption of maximum 24 W, as shown in Fig.6.4. The MTX transmit signal is characterized through parameters mentioned in the Table 6.1.

The parameters in the Table 6.1 should be set by the transmitter. The embedded chip-set *Atheros* in MTX provides the possibility for parameter setting via Secure Shell (SSH) and TelNet. To do that, I have connected both TX and RX via LAN cable to the PC.

The Fig. 6.4 shows the power supply board of both MTX transceivers. In the power supply board besides the power cables, there are two LAN connectors, which are just through-connected, and are independent of the board. The LAN cables on the right side are from the router which is connected to the PC and the two LAN cables on the left side are connected to the two MTX transceivers.

Fig. 6.5 shows the parameter setting like transmit power and the data rate of the transmit signal. Also the number of the frequency channel and the activating or deactivating of the internal antenna can be done here.

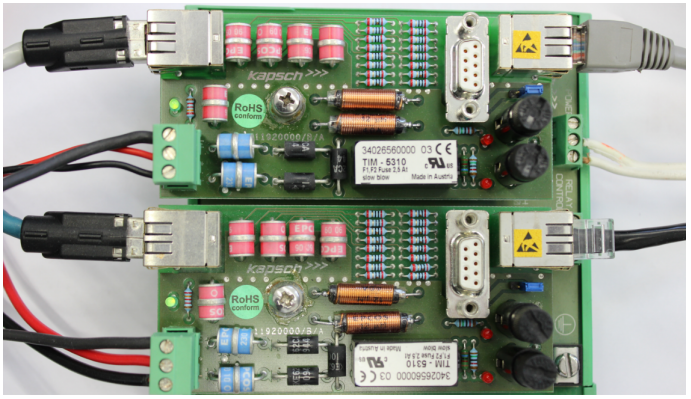

FIGURE 6.4: Power Supply

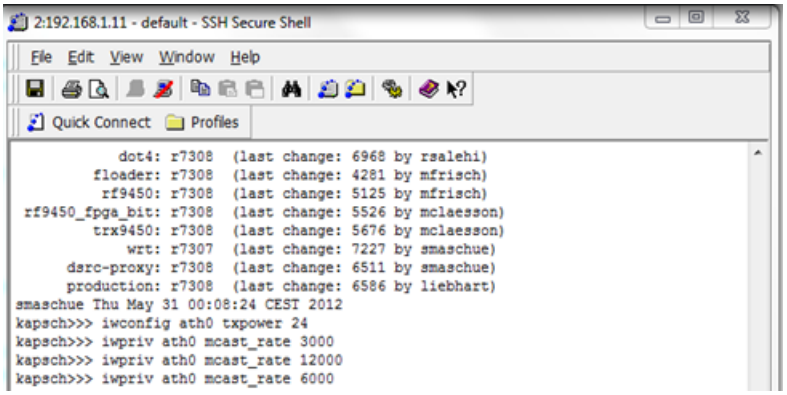

FIGURE 6.5: Secure Shell interface

The parameters such as number of transmit packets in a burst, delay between packets, number of burst and the packet length can be set over TelNet. After the command *traffic_burst* shown in Fig.6.6 four parameters will appear. The first one from left is related to the number of packets (OFDM frames) in each burst. The second parameter is the delay between two consecutive packets. The third parameter indicates the number of bursts in each measurement run. The last parameter is the packet length in Bytes.

FIGURE 6.6: TelNet

As mentioned above, the MTX can display the number of transmit and received packets by the command *athstats* as shown in Fig. 6.8. The number of correctly received packets is calculated through 32 bits Cyclic Redundancy Check (CRC).

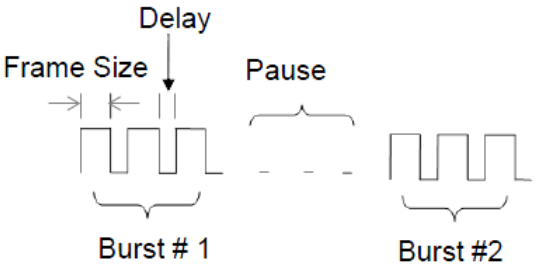

FIGURE 6.7: MTX signal

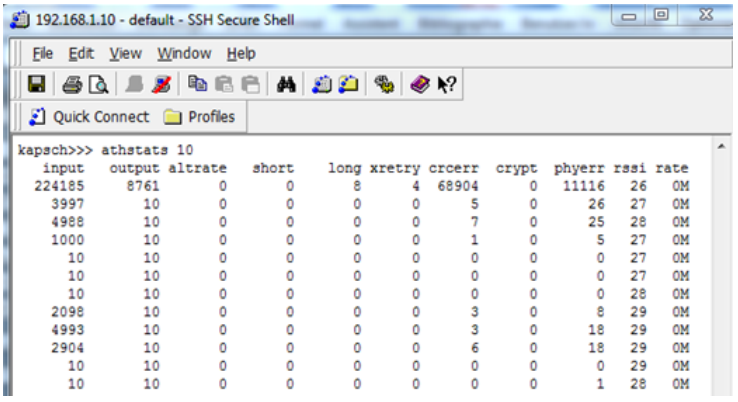

FIGURE 6.8: Signal parameters from "athstats" command

The number in front of the command determines the time period for displaying. For example, *athstats 10* displays every 10 seconds the number of correctly decoded packets and also the number of with error decoded packets, such as CRC error or physical (PHY) error. The aim of the measurement is to calculate the PER. To do so, firstly I have calculated the number of correctly decoded packets and then trough the Eq. from (6.1) and (6.2) the PER.

6.1.2.2 Attenuators

In the measurement setup I have used both fixed and variable attenuators. The fixed attenuator between TX and Propsim C2 was +22 dB (10 dB+6 dB+6 dB). The HP variable attenuator before RX has a wide frequency range, namely from DC to 18 GHz. To protect the MTX receiver, I have also used 20 dB (10 dB+10 dB) attenuation at the MTX RF input. The variable attenuator is depicted (on the left) and two fixed attenuators (attached to the receiver) are both depicted in Fig.6.9.

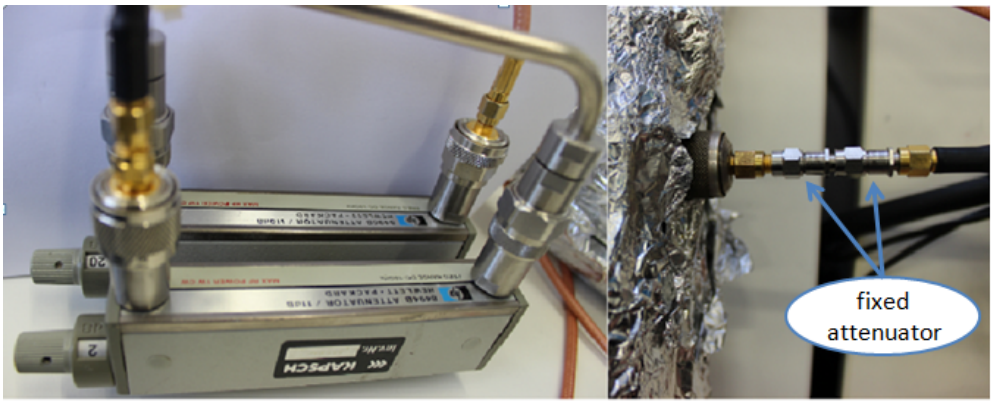

FIGURE 6.9: Variable (left) and fixed RF attenuators (right)

6.1.2.3 Propsim C2

In Ch. 4, I have described the operation of the channel emulator Propsim C2 and the implementation of the channel models on it. Now I would like to shortly mention some parameters of Propsim C2 which were set specifically for the measurement setup.

- Interface: RF interface
- Channel: CH1
- Local Oscillator: Internal LO
- Center Frequency: 5900 MHz
- Speed: Dependent on channel models
- Input Level: -14.5 dBm
- Crest Factor: 10 dB
- Output Gain: 0 dB
- Number of IRs: 10^5
- Warm-up Time: 1 hour.

6.1.3 Calibration Measurement

- **RF Cable:** I have measured the RF attenuation of all available RF cables and numbered them at the beginning for my work. To achieve that, I have connected the signal generator -depicted as number 6 in Fig.6.3- through an RF cable to the

RF power meter. There I have used the Continues Wave (CW) signal at 5.9 GHz from the signal generator and measured the RF power. Next I have added the RF cable, its attenuation I want to measure between the already existing cable and the power meter. The RF power difference is the attenuation of the RF cable. Afterwords I have selected the RF cables according to their length and attenuation.

Table 6.2 shows the RF attenuation of the cables I have used in measurement setup:

Cable number	RF attenuation [dB]
1	5.3
3	2.2
4	0.6
5	0.6
8	2.3

TABLE 6.2: RF cable attenuation

- **RF Attenuators:** I have also measured the RF attenuators at 5.9 GHz through the method mentioned above.

  ATT1=10 dB+6 dB+6 dB=22 dB
  ATT2=10 dB +10 dB=20 dB
  Variable ATT =0 to 40 dB

- **Directional Coupler:** I have measured the directional coupler at the frequency 5.9 GHz for the 10 MHz bandwidth. The attenuation in direct path and in couple path is constant for the entire bandwidth. By every attenuation measurement of DC I have terminated the third port with a 50 Ω terminator. The attenuation in direct path (from # 8 to # 1 in Fig 6.11) is 0.9 dB and in couple path (from # 8 to # 5 in Fig. 6.11) is 10.9 dB.

FIGURE 6.10: Directional Coupler

6.1.3.1 Transmit Signal and Power Measurement

As described in the previous section the MTX RF transmit signal is OFDM modulated. The parameter setting of the transmit signal is as described in Table 6.1.

In order to measure the average received power at 5.9 GHz I have used the channel power function in FSQ with the inherent parameters [31]:

- Center frequency= 5.9 GHz
- Sweep time= 4s (in order to achieve a stable measurement value)
- Resolution bandwidth (RBW) =300 KHz (1-3% of signal bandwidth)
- Video bandwidth (VBW) =1 MHz (three times of RBW)
- Channel bandwidth= 10 MHz

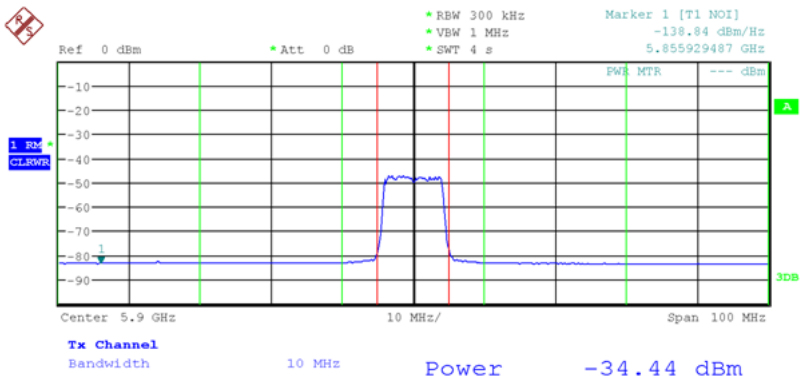

FIGURE 6.11: Channel Power measurement via FSQ

6.1.4 Definition of Measurement Values

The measurement values are presented in the Table 6.3. The values of following parameters are assumed from the ETSI ITS plugtest [4]: Frequency channel, data rate and packet length (payload size).

There are also six different parameters I have set:

- Number of packets: As mentioned above the number of transmit packets in each measurement run should be set. To achieve 10^{-4} for PER value and also for smoothness of the PER curve (statistical aspects) 10^{-4} packets were transmitted in each measurement run.

Measurement parameter	Value
Frequency channel	180 (5.9 GHz)
Data rate	3,6,12 Mb/s
Packet length	1000 Bytes
Number of packets (=frames) in one Burst	10000
Repetitions	1
RX Average Power	-105 to -60 dBm
Power at C2 Input	-14.5 dBm
TX Power	+24 dBm
Propsim C2 Channel	CH1
Crest factor	10 dB

TABLE 6.3: Measurement values

- Delay between packets: In order to have no gaps between the packets, I have set the delay equal to zero.
- Repetitions
- TX power: The transmit power should be 3-6 dB under the maximum possible output power of MTX which +28 dBm is. This is the power level which is set in TelNet. The measured average power at the output connection of the MTX is equal to +12.8 dBm.
- Propsim C2 emulation channel: I have done all of my measurements in channel 1 (CH1) of Propsim C2. The difference of both channels basically is the different carrier leakage as described in Ch. 4.
- power level at propsim C2 input: according to the [3] the optimum operation is achieved with a signal power of about -15 dBm at the input connection of Propsim C2. Therefore this power level is set at about -14.5 dBm.
- RX average power: I have increased the average receive power step wise until the number of received packets was constant, namely the PER curves are in the saturated area.

The main timing and frequency parameters of 802.11p PHY layer are summarized in Tables 6.4 and 6.5. The OFDM symbol duration is $T_{OFDM} = 8\mu s$, which includes a CP with a length of 1.6 μs. Therefore the maximum delay spread should not exceed 1.6 μs. To avoid the ICI in an OFDM system, the OFDM symbol duration should be smaller than the coherence time (as described in Ch. 2).

Data rate [Mb/s]	Baseband modulation	Coding rate (R)
3	BPSK	1/2
6	QPSK	1/2
12	16-QAM	1/2

TABLE 6.4: Data rate-dependent parameters in IEEE 802.11p physical layer (Table 17-13a in [8])

Parameters	Value
Bandwidth	10 MHz
Suncarrier spacing ($\triangle_F$)	156.25 KHz (10 MHz/64)
FFT period (T_{FFT})	6.4 μs ($1/\triangle_F$)
Cyclic Prefix (T_{CP})	1.6 μs ($T_{FFT}/4$)
OFDM symbol duration (T_{OFDM})	8 μs ($T_{FFT} + T_{CP}$)
Preamble	32 μs

TABLE 6.5: Timing-related parameters IEEE 802.11p physical layer (Table 79 in [9], [8])

6.2 Evaluation of Measurements

Firstly, the transmitter and receiver are connected directly. To avoid any damage caused by the received signal power, an 60 dB attenuator is fitted between them. Then a particular number (10000) of packets are sent. Through this test it can be ensured, that the number of packets, which is set via TelNet are really generated, due to the correctly decoding of the same packet number over this AWGN channel. I have started the PER measurement with an AWGN (Additive White Gaussian Noise) channel implemented in Propsim C2. According to the measurement setup in (6.2), I have set in the edit screen of Propsim C2, one constant tap (no fading) in CH1. The transceiver with the IP- address 192.168.1.11 is utilized in all measurements only as a transmitter. A measurement run means sending of 10000 packets from TX to RX through CH1 of Propsim C2 for a particular average received power. The average received power will be increased by decreasing the variable RF attenuator at the RX in 1 dB steps. The needed measurement data for the evaluation process consists of the number of transmitted packets, the number of correctly decoded packets and the average received power. They are taken as a screen shot for each measurement run.

6.2.1 Evaluation of Measurements for NLOS Channel Models

I have observed, that by the PER measurement for channel models without availability of the LOS path, the throughput of the wireless system is equal to zero. In order to proof the impact of the vehicle velocity (vehicle-to-vehicle) on the system performance, I have reduced the velocity in these NLOS scenarios, implemented the NLOS channel models

again on Propsim C2, and repeated the PER measurement. By changing the velocity, the Doppler bandwidth and the Doppler frequency shift should be scaled according to the new velocity. The equations 6.3 and 6.4 describe the parameter scaling for Highway NLOS. This process for the Crossing NLOS is applied analogously. The scaled channel model parameters are presented in tables bellow.

$$\text{Doppler}_{40\text{km/h}} = \text{Doppler} * (40/252), \tag{6.3}$$

$$\text{Bandwidth}_{40\text{km/h}} = \text{DopplerBandwidth} * (40/252) = 437\text{Hz}. \tag{6.4}$$

Parameter \ Tap	Tap1	Tap2	Tap3	Tap4	Units
Relative Gain	0	-3	-5	-10	dB
Delay	0	267	400	533	ns
Doppler Shift	0	93	-31	187	Hz
Fading Distribution	Rayleigh	Rayleigh	Rayleigh	Rayleigh	
Rician K-factor	n/a	n/a	n/a	n/a	dB
Doppler Bandwidth	437	437	437	437	Hz
Doppler Spectral shape	Classical Jakes'	Classical Jakes'	Classical Jakes'	Classical Jakes'	

TABLE 6.6: ETSI ITS Street Crossing NLOS channel parameters modified for relative speed of vehicles=40 km/h

Parameter\ Tap	Tap1	Tap2	Tap3	Tap4	Units
Relative Gain	0	-3	-5	-7	dB
Delay	0	200	433	700	ns
Doppler Shift	0	110	-78	141	Hz
Fading Distribution	Rayleigh	Rayleigh	Rayleigh	Rayleigh	
Rician K-factor	n/a	n/a	n/a	n/a	dB
Doppler Bandwidth	437	437	437	437	Hz
Doppler Spectral shape	Classical Jakes'	Classical Jakes'	Classical Jakes'	Classical Jakes'	

TABLE 6.7: ETSI ITS Highway NLOS channel parameters, relative speed of vehicles=40 km/h

6.2.2 Evaluation Process

A PER measurement for a data rate is completely carried out, if the number of received packets does not increase by increasing the received power. The next step is to calculate the total number of received packets at the transceiver (with the IP- address 192.168.1) for each point of the horizontal axis, namely the average received power. As explained in Sec. 6.1.2.1, the command *athstats 10* in SSH, displays the correctly decoded packets

every 10 seconds. Therefore, for the transmit data rate of 3 Mb/s, the entire transmit packets are displayed in five rows. The MTX transmitter sends a CAM message (as mentioned in Ch. 5) with the frequency of 1 Hz. Thus during a time window of 50 seconds (five display rows), additionally to 10000 payload packets, 50 packets CAMs will be sent, i.e. the total number of transmitted packets for one measurement run is 10050. At the receiver, the sum of these five rows results in the total number of correctly received packets, as shown in Fig. 6.12.

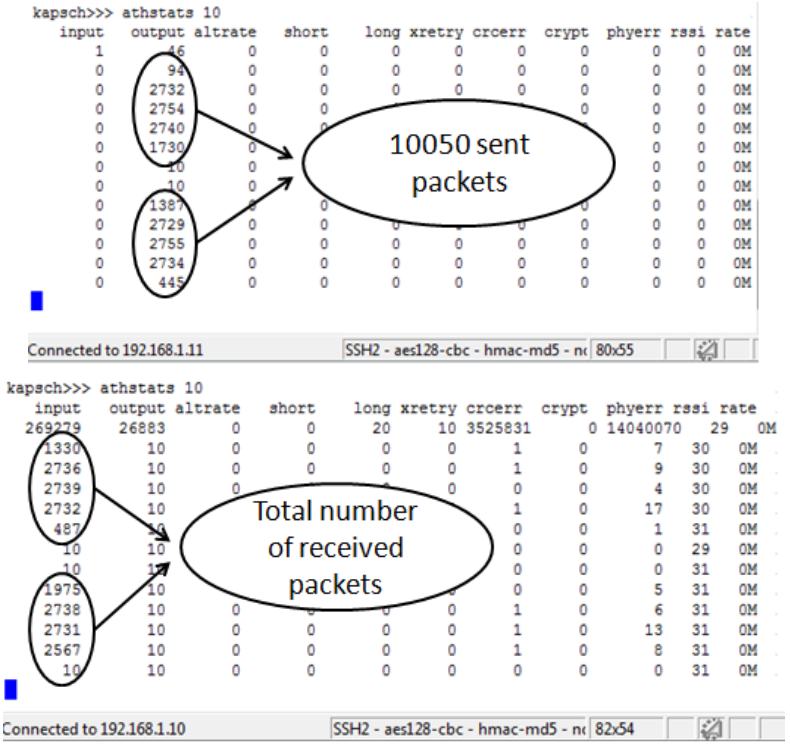

FIGURE 6.12: Number of sent and received Packets

Furthermore, through Eq. (6.1) and (6.2) the PER value, as a point of the PER curve, will be computed. Now two arrays are available: one of them contains the PER value for each measurement run, and the other one, the average received power for every PER value. I have plotted the PER graph in logarithmic scale by Matlab.

6.2.3 Results

The PER for the AWGN channel implemented on Propsim C2:

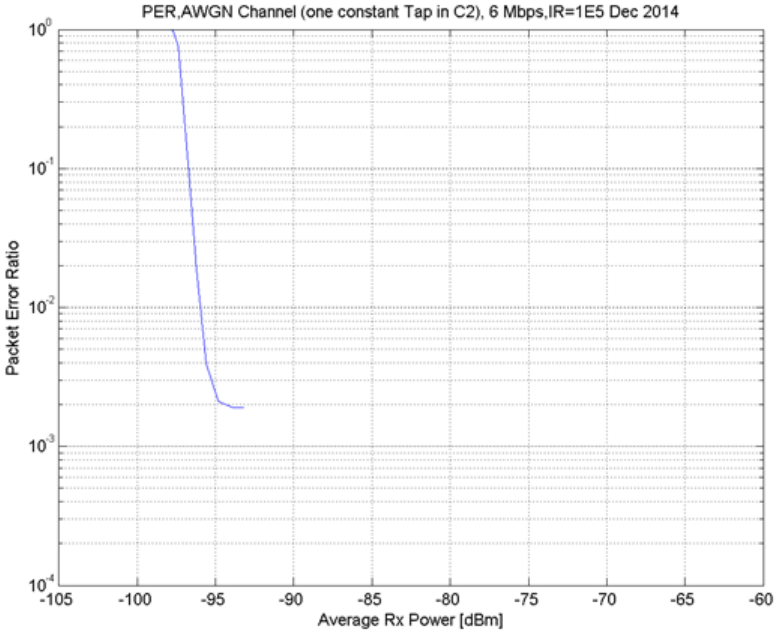

FIGURE 6.13: PER for the AWGN channel implemented on Propsim C2; data rate = 6 Mb/s, number of IRs=10^5

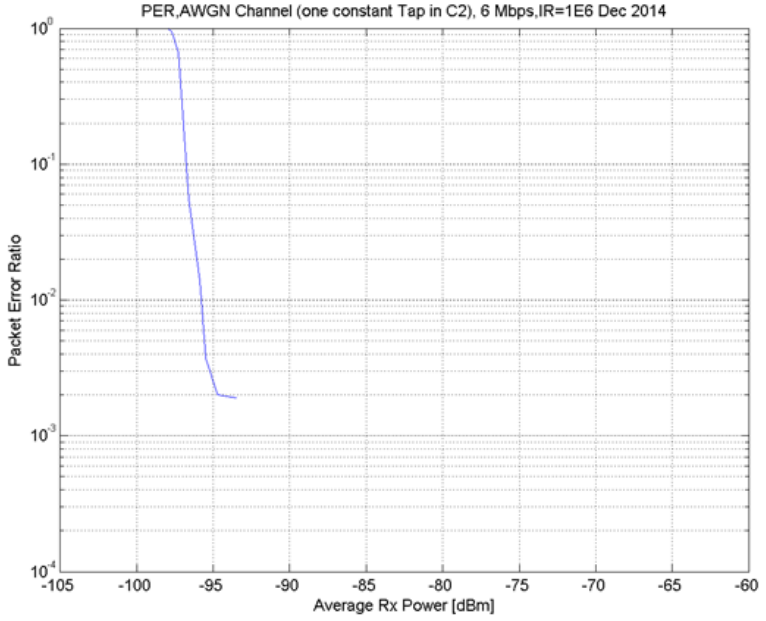

FIGURE 6.14: PER for the AWGN channel implemented on Propsim C2; data rate = 6 Mb/s, number of IRs=10^6

The PER diagrams for the ETSI ITS channel models with LOS path: I have summarised the values for the measurement parameters and the results for the Rural LOS channel model. The Fig. 6.15 shows us the taps on the Propsim C2 GUI. The same applies to the remaining channel models in complete analogy.

ETSI ITS Rural LOS channel models

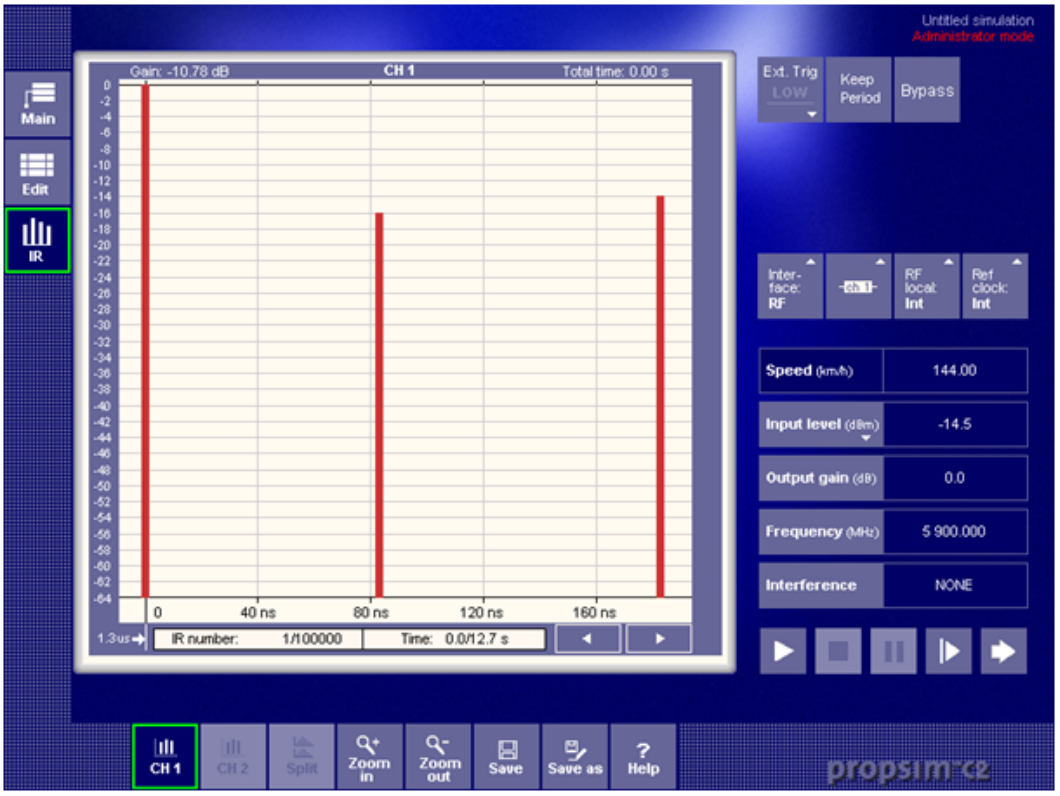

FIGURE 6.15: Channel model ETSI ITS Rural LOS implemented on Propsim C2, Impulse Response Screen

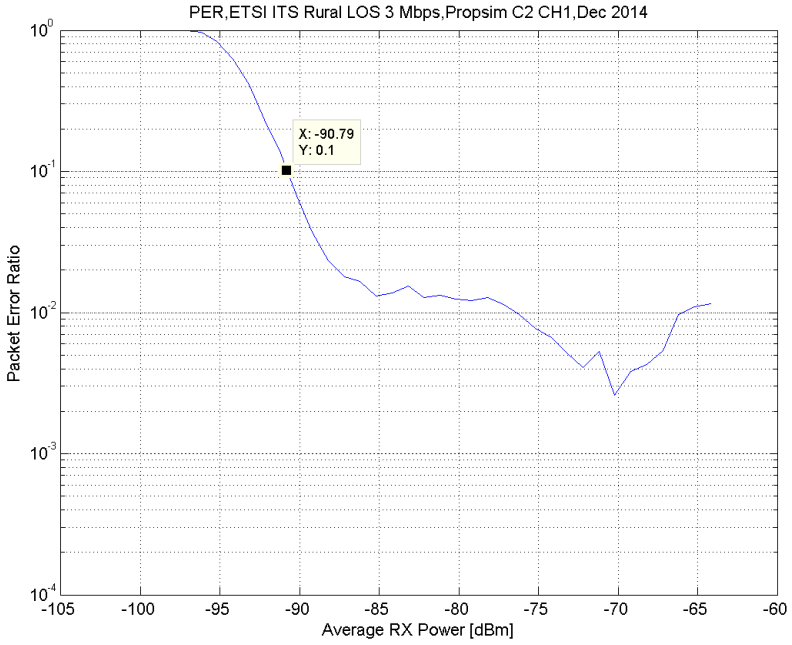

FIGURE 6.16: PER ETSI ITS Rural LOS 3 Mb/s

Data rate	Baseband modulation	Coding rate (R)	Payload	TX power	Measured sensitivity Level,(PER = 10%)
3 Mb/s	BPSK	1/2	1000 Bytes	+12.8 dBm	-90.79 dBm

TABLE 6.8: PER measurement: ETSI ITS Rural LOS 3 Mb/s

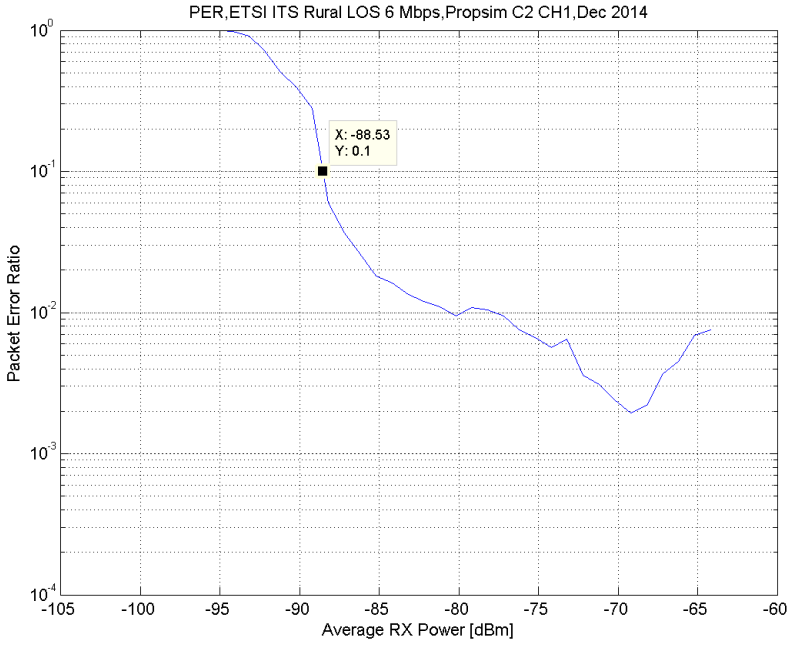

FIGURE 6.17: PER ETSI ITS Rural LOS 6 Mb/s

Data rate	Baseband modulation	Coding rate (R)	Payload	TX power	Measured sensitivity Level,(PER = 10%)
6 Mb/s	QPSK	1/2	1000 Bytes	+12.8 dBm	-88.53 dBm

TABLE 6.9: PER measurement: ETSI ITS Rural LOS 6 Mb/s

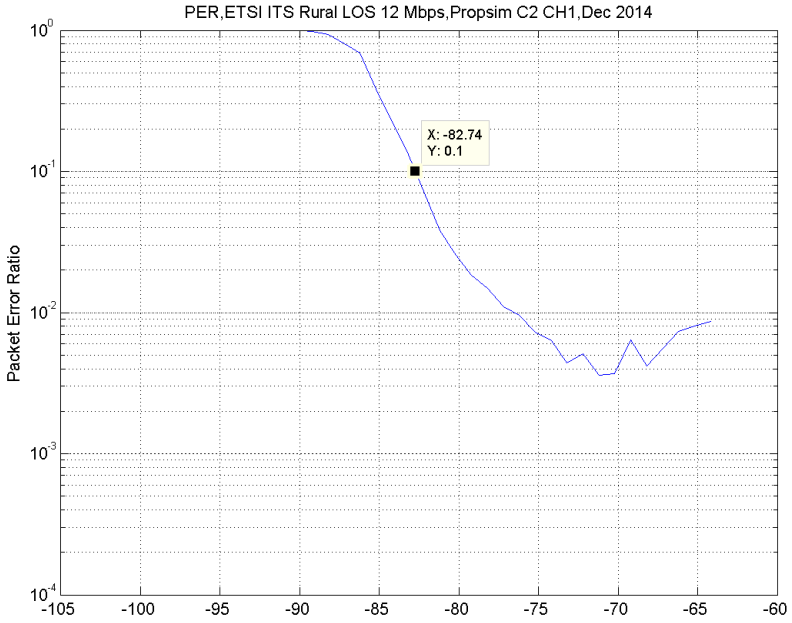

FIGURE 6.18: PER ETSI ITS Rural LOS 12 Mb/s

Data rate	Baseband modulation	Coding rate (R)	Payload	TX power	Measured sensitivity Level,(PER = 10%)
12 Mb/s	16-QAM	1/2	1000 Bytes	+12.8 dBm	-82.74 dBm

TABLE 6.10: PER measurement: ETSI ITS Rural LOS 12 Mb/s

ETSI ITS Urban Approaching LOS channel models

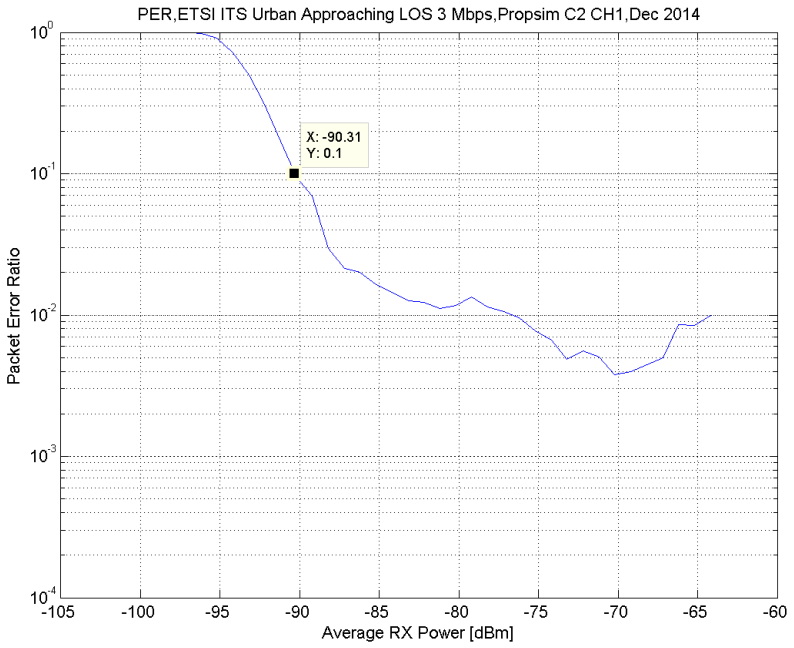

FIGURE 6.19: PER ETSI ITS Urban Approaching LOS 3 Mb/s

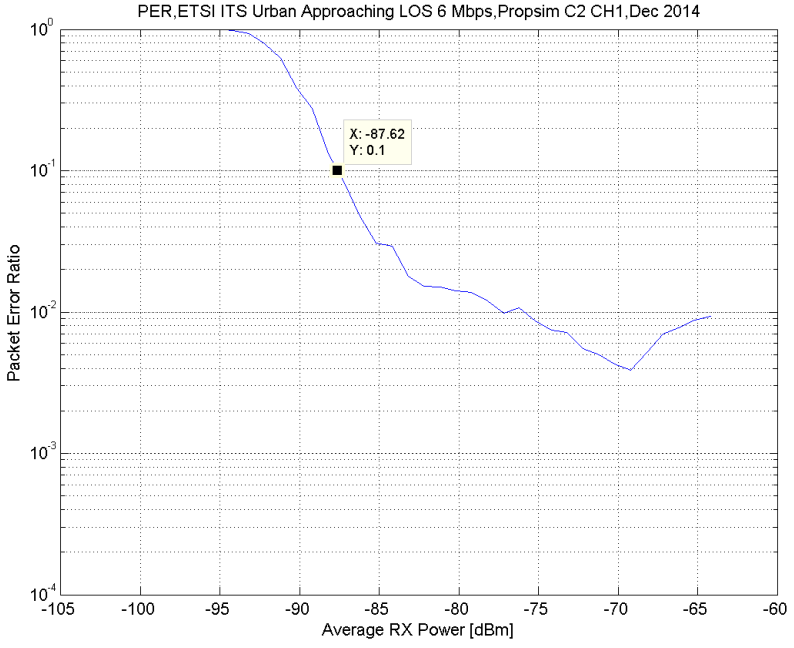

FIGURE 6.20: PER ETSI ITS Urban Approaching LOS 6 Mb/s

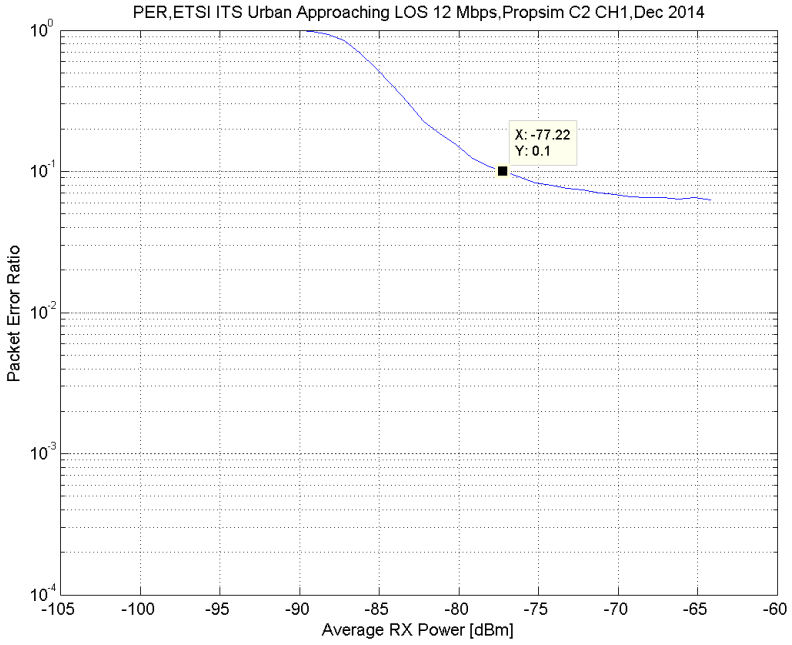

FIGURE 6.21: PER ETSI ITS Urban Approaching LOS 12 Mb/s

ETSI ITS Highway LOS channel models

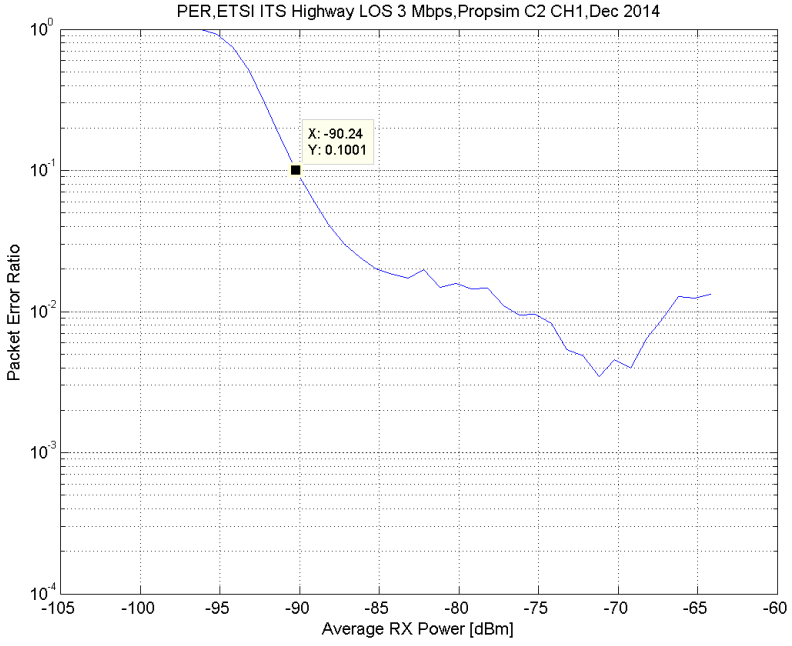

FIGURE 6.22: PER ETSI ITS Highway LOS 3 Mb/s

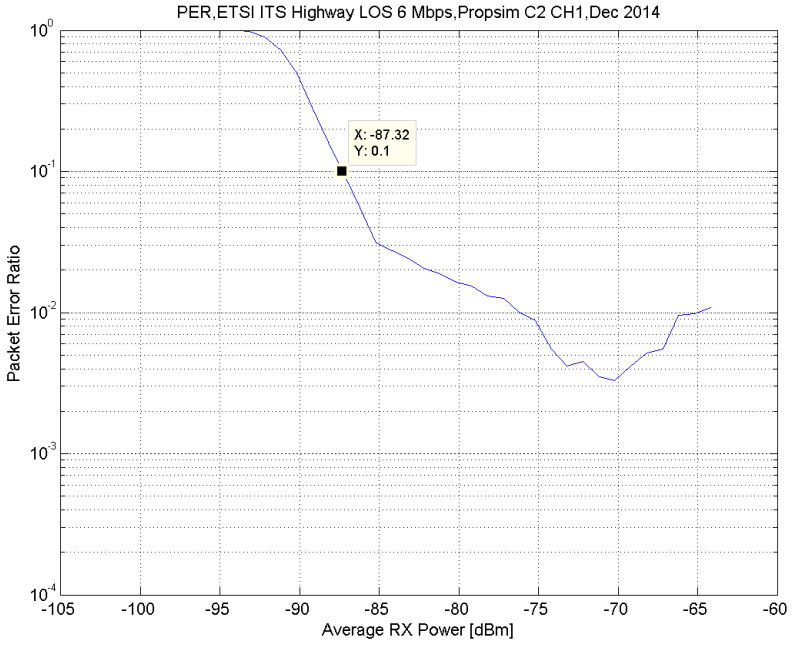

FIGURE 6.23: PER ETSI ITS Highway LOS 6 Mb/s

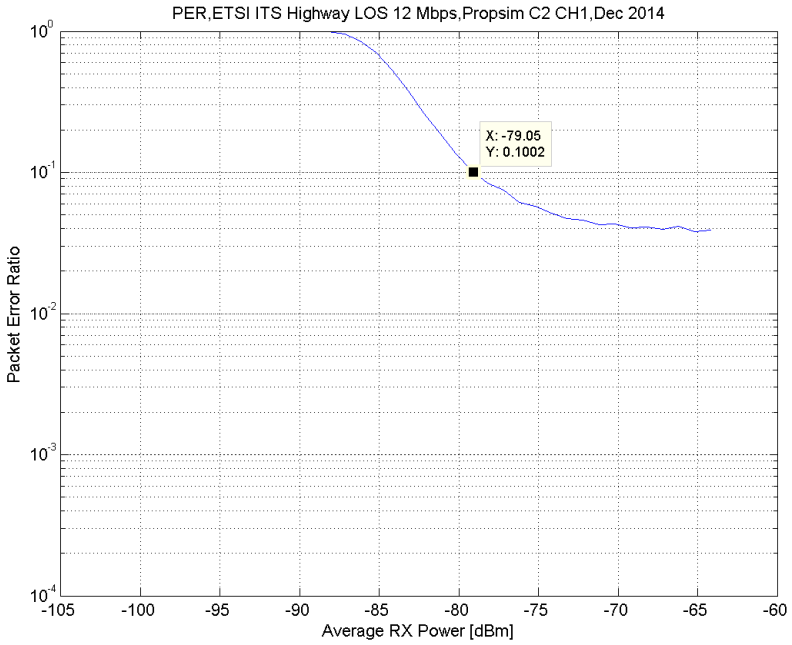

FIGURE 6.24: PER ETSI ITS Highway LOS 12 Mb/s

The PER diagrams for the ETSI ITS channel models without availability of a LOS path: Please note, that the axial scaling on the vertical axis is different from the scaling of previous LOS channel models.

ETSI ITS Highway NLOS channel models

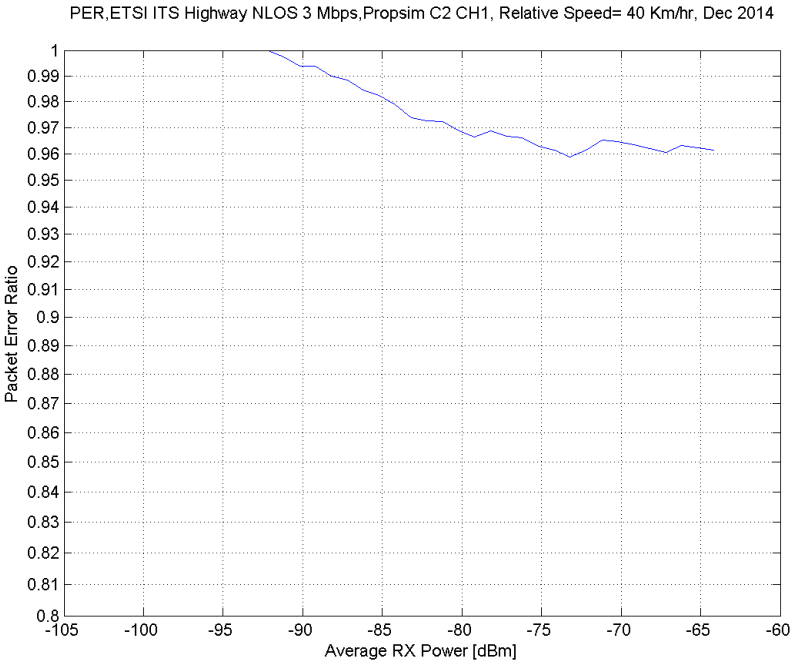

FIGURE 6.25: PER ETSI ITS Highway NLOS 3 Mb/s, relative speed=40 km/h

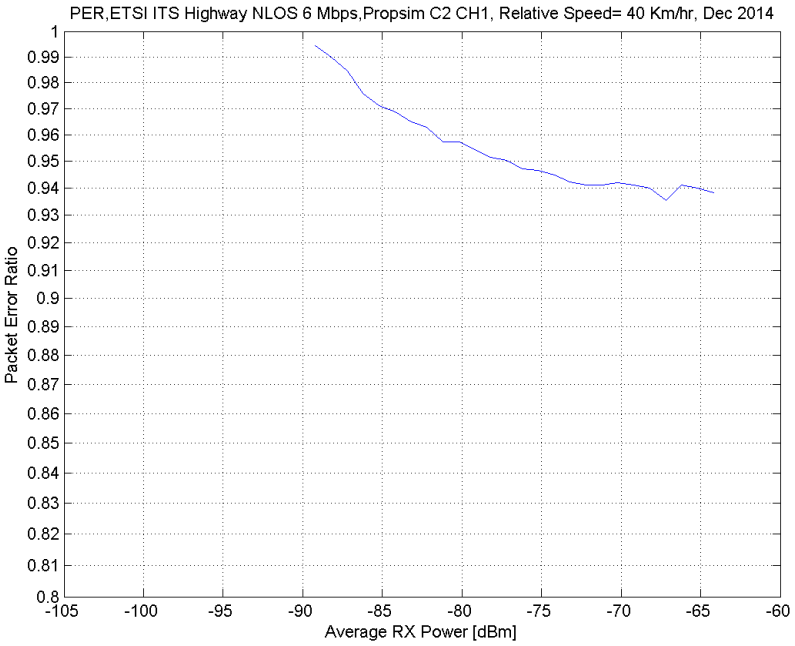

FIGURE 6.26: PER ETSI ITS Highway NLOS 6 Mb/s, relative speed=40 km/h

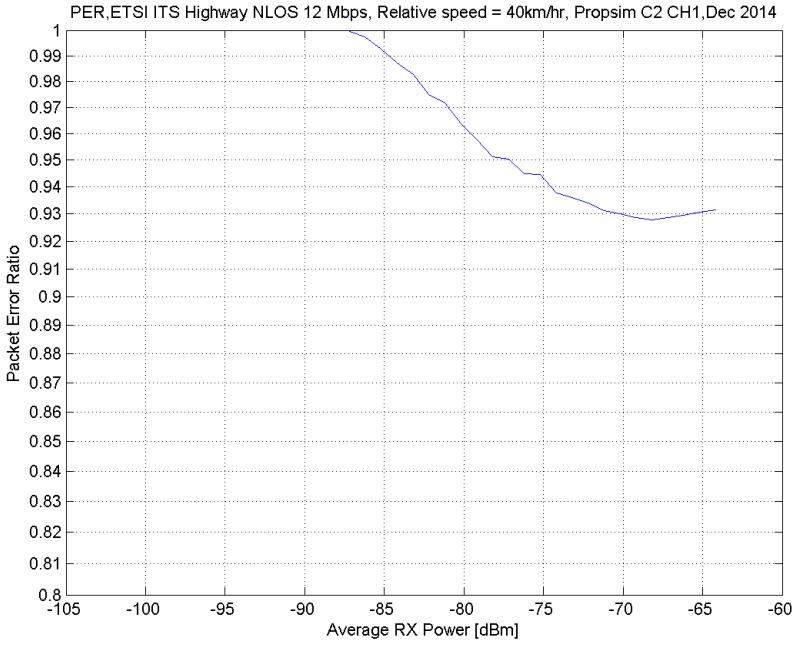

FIGURE 6.27: PER ETSI ITS Highway NLOS 12 Mb/s, relative speed=40 km/h

ETSI ITS Crossing NLOS channel models

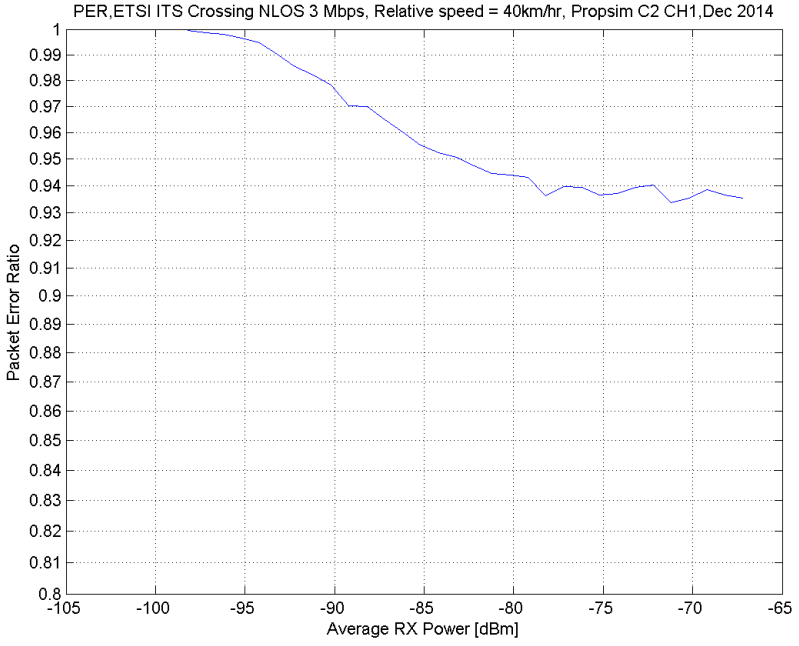

FIGURE 6.28: PER ETSI ITS Crossing NLOS 3 Mb/s, relative speed=40 km/h

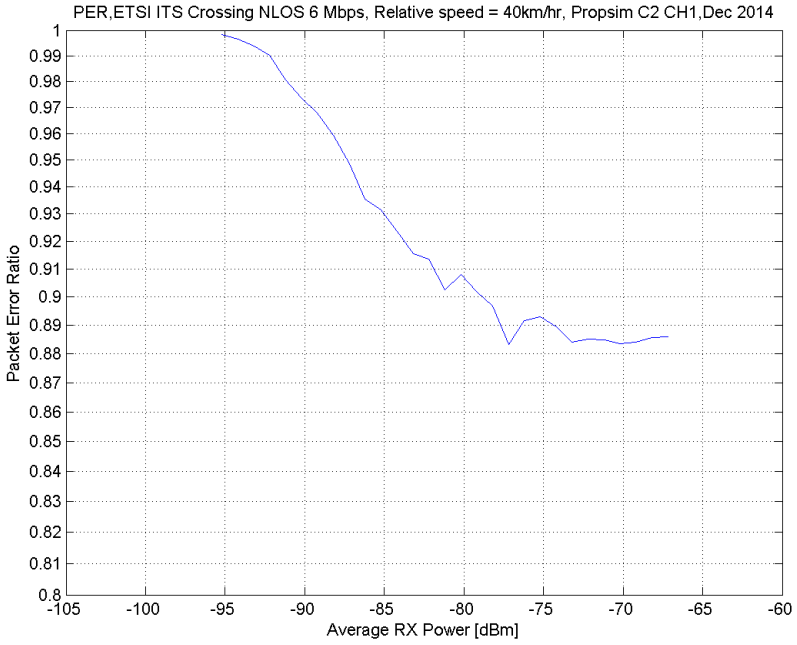

FIGURE 6.29: PER ETSI ITS Crossing NLOS 6 Mb/s, relative speed=40 km/h

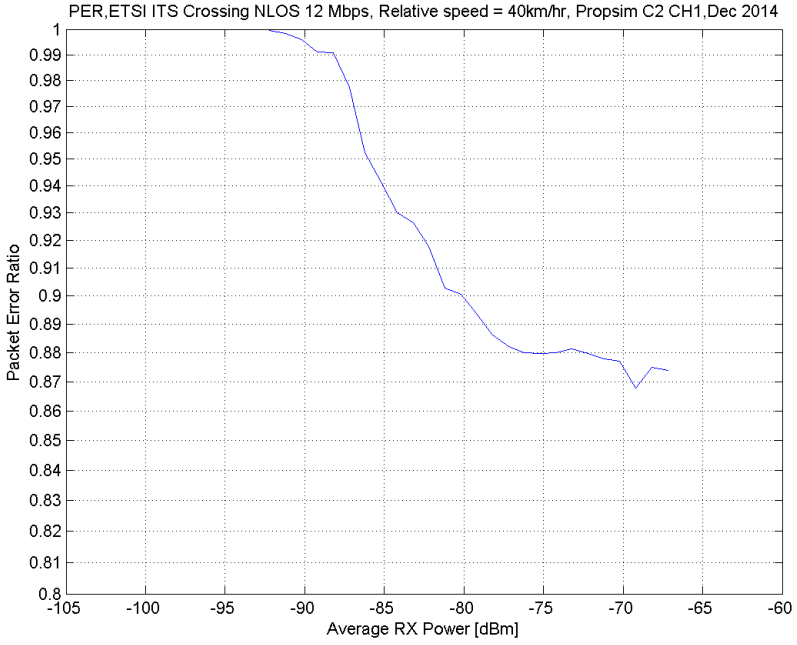

FIGURE 6.30: PER ETSI ITS Crossing NLOS 12 Mb/s, relative speed=40 km/h

Chapter 7

Summary and Conclusion

A description of the wireless channel was presented in Ch. 2. The characteristics of the multipath propagation, such as the delay dispersion or the frequency-selectivity was described. The Rician and Rayleigh distributed paths are mathematically formulated. The time variance and the Doppler spectra of a time-selective channel are described. Next the Linear Time Variant (LTV) communication system was investigated and its second-order channel properties and the stochastic functions are driven. The (quasi–) WSSUS characteristics of an LTV system was specified as a basic assumption for the vehicular channel models. The TDL was presented as a method for modeling the WSSUS channel models. The coherence frequency and the coherence time are defined.

In Ch. 3 the vehicular radio channel models such as the *Six Time- and Frequency-Selective Empirical Channel Models for Vehicular Wireless LANs* and the *ETSI ITS channel models* were investigated. The channel model parameters were clearly defined for the porpuse of their further implementation on the channel emulator Propsim C2. The first goal of my work was to give an answer to the question, whether the *Six Time- and Frequency-Selective Empirical Channel Models for Vehicular Wireless LANs* is implentable on the Propsim C2 or not. After I have clarified that the implementation is feasible, I have started the investigation of the similar channel models namely the *ETSI ITS channel models*. Five different scenarios of the ETSI ITS channel models from [2] have been described. The ETSI ITS channel models are still in refinement and are not completely parameterized. Therefore regarding undefined parameters such as the Doppler spectra and the Doppler bandwidth some assumption have been made, in order to be able to introduce the channel models on the Propsim C2. The Doppler spectra are assumed as classical Jakes' and the Doppler bandwidth is calculated through the relative speed of the two communicating vehicles. The RMS delay spread and the

RMS Doppler spread for each scenario are calculated. These values can be useful for better understanding of the behaviour of different channel models.

In Ch. 4 the radio channel emulator Propsim C2 is investigated. The system architecture of this channel emulator is described. A major problem, which occurred during some measurements, is the Carrier Leakage(CL) including its impairments on the fading emulation. Solutions for combating or mitigating these are discussed in Ch. 4 and 6.

Chapter 5 compares the narrowband with the wideband transmission and highlights the need for a method to combat the frequency-selectivity impacts of the channel in IEEE 802.11p modems. This chapter describes OFDM techniques in relation to the vehicular channels. Furthermore the standards IEEE 802.11p and ETSI ITS-G5 are shortly described.

Chapter 6 contains the methodology of the PER measurement, the measurement setup, components and the values. The evaluation of measurement and the measurement results i.e. the PER curves are presented.

Major conclusions are:

- Approximating Rayleigh-distributed path gain with Doppler shift by a Rician distribution (described in Appendix B) does not yield a good accuracy.
- Vehicular channels as proposed in ETSI ITS G5 are implementable on the EB Propsim C2 through 2 Methods:

  Approximation of Rayleigh-distributed paths by Rician distributed paths as by time-variant CIR.
- For 11p modems the PER improve for vehicular channels with smaller delay-Doppler spread product.
- Lower data rates in 11p are more robust in vehicular channels with higher delay-Doppler spread products.
- The PER performance of a real-world 11p modem for emulated vehicular scenarios without LOS path at relative vehicular speeds larger than 40 km/h is not satisfactory. The 11p packets are lost completely in NLOS channels at relative speeds larger than 60 km/h.

Appendix A

Impulse Response Generating through Matlab

A.1 Matlab Code

```
% Generate IR files for IEEE 802.11p channel model scenarios.
% NOTE! Original (Spirent) Classical 3dB and Classical 6dB Doppler spectra
% are substituted by Jakes (Classical) Doppler spectrum. Later on, if
% necessary, an appropriate IIR filters for 3 and 6dB spectra should be
% created.
%
% Source: "Six Time- and Frequency-Selective Empirical Channel Models for
% Vehicular Wireless LANs"
% Guillermo Acosta-Marum and Mary Ann Ingram
%
% 5.4.2011 Pekka Kyösti (c) Elektrobit
%%%%%%%%%%%%%%%%%%%%%%%%%%%%%%%%%%%%%%%%%%%%%%%%%55


clear

fc = 5.9E9;   % Hz
len = 1E5; % Number of IRs on 16 SD
savepath = 'C:\Users\mashury\Desktop\ETSI ITS\G5\G5 DS\';

for scen=1:5

switch scen
    case 1
% Profile 1: Rural LOS Parameter relative speed 144 km/h
v = 144/3.6;    % 40 m/s Relative speed (differential speed)!!!
Npaths = 3;% number of paths
RelPL = -[0 14 17]; % Tap Power in dB
delay = [0 83 183]; % ns
K = [10 -Inf*ones(1,2)]; % Ricen K-factor [dB], assumed per tap
Fshift = [0 492 -295]; % Frequency shift [Hz] known from channel model
```

```
32 Fdoppl = [786.7 786.7 786.7]; %  Doppler BW [Hz] calculated from BW = 2*(v/c)*fc*
       cos(tehta) if cos(tehta)=1.0 => Doppler BW= 2*Fdoppl.
33 LosDopl = [0 NaN*ones(1,2)]; % LOS Doppler [Hz]
34 RiceanInd = [1 zeros(1,2)]; % Index to Ricean fading paths, the rest are Rayleigh
        , (Achtung Scenario 1 hat nur 11 Paths!)
35 Dspect = [3 3 3]; % Fading spectral shape, 1=Flat, 2=Round, 3=Classic3dB, 4=
       Classic6dB
36 filename = 'Rural LOS';
37 case 2
38 % Profile 2: Urban Approaching LOS Parameter  119 km/h
39 v = 119/3.6;    % 119 km/h  Relative speed (differential speed)
40 Npaths = 4;
41 RelPL = -[0 8 10 15];
42 delay = [0 117 183 333]; % ns
43 K = [10 -Inf*ones(1,3)]; % Ricen K-factor [dB], assumed per tap
44 Fshift = [0 236 -157 492]; % Frequency shift [Hz]
45 Fdoppl = [650.092 650.092 650.092 650.092]; % Doppler BW [Hz]
46 LosDopl = [0 NaN*ones(1,3)]; % LOS Doppler [Hz)
47 RiceanInd = [1 zeros(1,3)]; % Index to Ricean fading paths, the rest are Rayleigh
48 Dspect = [3 3 3 3]; % Fading spectral shape, 1=Flat, 2=Round, 3=Classic3dB, 4=
       Classic6dB
49 filename = 'Urban Approaching LOS';
50 case 3
51 % Profile 3: Crossing NLOS Parameters 126km/h
52 v = 40/3.6;    % 126 km/h for Crossing NLOS reduziert auf 20 Km/h
53 Npaths = 4;
54 RelPL = -[0 3 5 10]; %[dB]
55 delay = [0 267 400 533]; % ns
56 K = [-Inf*ones(1,4)]; % Ricen K-factor [dB], assumed per tap
57 Fshift = [0 295 -98 591]*0.4761; % Frequency shift [Hz] skaliert auf v(relative
       speed)=40 km/h 40/126=0.3174, 20/126=0.1587,60/126=0.4761.
58 Fdoppl = [688.4 688.4 688.4 688.4]*0.4761; %  Doppler BW [HZ]
59 LosDopl = [NaN*ones(1,4)]; % LOS Doppler [Hz)
60 RiceanInd = [zeros(1,4)]; % Index to Ricean fading paths, the rest are Rayleigh
61 Dspect = [3 3 3 3]; % Fading spectral shape, 1=Flat, 2=Round, 3=Classic3dB, 4=
       Classic6dB
62 filename = 'Crossing NLOS';
63 case 4
64 % Profile 4: Highway LOS Parameters 252km/h
65 v = 252/3.6;    % 252 km/h for Highway LOS
66 Npaths = 4;
67 RelPL = -[0 10 15 20]; %[dB]
68 delay = [0 100 167 500]; % ns
69 K = [10 -Inf*ones(1,3)]; % Ricen K-factor [dB], assumed per tap
70 Fshift = [0 689 -492 886]; % Frequency shift [Hz]
71 Fdoppl = [1376.7 1376.7 1376.7 1376.7]; % Doppler BW [Hz]
72 LosDopl = [0 NaN*ones(1,3)]; % LOS Doppler [Hz)
73 RiceanInd = [1 zeros(1,3)]; % Index to Ricean fading paths, the rest are Rayleigh
74 Dspect = [3 3 3 3]; % Fading spectral shape, 1=Flat, 2=Round, 3=Classic3dB, 4=
       Classic6dB
75 filename = 'Highway LOS';
76 case 5
77 % Profile 5: Highway NLOS Parameters 252km/h
78 v = 40/3.6;    % 252 km/h for Highway NLOS relative speed reduziert auf 20 km/h
79 Npaths = 4;
```

```
80  RelPL = -[0 2 5 7];
81  delay = [0 200 433 700]; % ns
82  K = [-Inf*ones(1,4)]; % Ricen K-factor [dB], assumed per tap
83  Fshift = [0 689 -492 886]*0.1984; % Frequency shift [Hz]skaliert auf v(relative
        speed)=40 km/h 40/252=0.1587.20/252=0.07936,60/252=0.23809.50/252=0.1984.
84  Fdoppl = [1376.7 1376.7 1376.7 1376.7]*0.1984; % Doppler BW [Hz]
85  LosDopl = [NaN*ones(1,4)]; % LOS Doppler [Hz)
86  RiceanInd = [zeros(1,4)]; % Index to Ricean fading paths, the rest are Rayleigh
87  Dspect = [3 3 3 3]; % Fading spectral shape, 1=Flat, 2=Round, 3=Classic3dB, 4=
        Classic6dB
88  filename = 'Highway NLOS';
89      otherwise
90  end
91
92  % Doppler spectrum shaping filters
93  load FlatCoef_SD16; ff(1,:)=fforw;fb(1,:)=fback;
94  load RoundCoef_SD16; ff(2,:)=fforw;fb(2,:)=fback;
95  load ClassCoef_SD16; ff(3,:)=fforw;fb(3,:)=fback;
96  load ClassCoef_SD16;ff(4,:)=fforw;fb(4,:)=fback;
97  SDorig = 16;    % SD of IIR filters in mat files,
98  f_cutoff = 0.0605;  % Approximated cut-off frequency for SD=16 IIRs for lp2lp
        conversion,
99  c = 299792458;  % Speed of light [m/s]
100 % F_upd. Theoretical maximum at car2car communications is 4*fmax. In 11p
101 % scenarios 2.5*fmax seem to be enough.
102 fupd = (v/c*fc*2.5*2)*2;  % Sampling frequency fmax*2.5 from car2car *2 from SD
        definition and *2 from Nyquist
103 Ts = 1/fupd;
104
105
106 if len<1000
107     error('At minimum 1000 IR must be generated!')
108 end
109
110 clear h
111 for k=1:Npaths
112     % Create complex Gaussian noise vector
113     noise = complex(randn(1,len),randn(1,len));
114     noise = [noise(1,end-499:end) noise noise(1,1:500)]; % fügt zum noise Vektor
        letzte 500 und erste 500 Elemente zu, (wahrscheinlich wegen der FT)
115     % Adjust Doppler filter to Doppler bandwidth (Fdoppl)
116     %var(noise);
117     SDnew = (fupd/2)/Fdoppl(k); % Filter response width, based on Fdoppl
        parameter % Für ETSI unwichtig weil wir konstante Fdoppl für alle paths haben
        .
118     [fforw,fback] = IIRfilt_lp2lp(ff(Dspect(k),:),fb(Dspect(k),:),SDorig,SDnew,
        f_cutoff);
119     % Perform Doppler spectrum shaping filtering
120     tmp = filter(fforw,fback,noise); %clear noise
121     tmp(1:500)=[];tmp(end-499:end)=[];
122     % Perform Frequency shift & amplitude normalization
123     h(k,:) = tmp.*exp(1j*2*pi*Fshift(k)*[0:Ts:(len-1)*Ts])/sqrt(mean(abs(tmp).^2)
        ); % Freq. Verschiebung und Normierung
124     clear tmp
```

```
125     %figure(1),plot(linspace(-fupd/2,fupd/2,len),fftshift(20*log10(abs(fft(h(k,:)
        )))))%,pause
126     %figure(2),plot(20*log10(abs(h(k,:)))),figure(3),hist(abs(h(k,:)),100)%,pause
127     % Scale to path power Relative path loss (RelPL)
128     h(k,:) = h(k,:)*10^(RelPL(k)/20);
129     % Add LOS path
130     if RiceanInd(k)
131         h(k,:) = h(k,:)+exp(1j*2*pi*Fshift(k)*[0:Ts:(len-1)*Ts])*10^(K(k)/20);
132     end
133 % plot(linspace(-fupd/2,fupd/2,len),fftshift(20*log10(abs(fft(h(k,:))))))
134 
135 %$xlabel('Doppler frequency [Hz]'),ylabel('magnitude [dB]')
136 %title(['ETSI ITS ' filename, k])
137 %print('-dpng',filename)
138 
139 end
140 
141 % Write IRs to disk
142 CIRs = len;                     % Actual CIR count
143 Taps = Npaths;                  % Actual tap (path) count
144 Route_Closed = 1;               % Is route closed; logical 0 or 1 [1]
145 Sample_Density = 2.5*2;         % Samples per half-wave (see fupd definition above
        )
146 Carrier_Frequency = fc;         % Carrier center frequency
147 Tap_Spacing = 12.5;             % 5ns in F8 and 12.5ns in C8. AND ALSO 12.5 ns IN
        C2!
148 CIRUpdateRate = fupd;           % (see fupd definition above)
149 Hardware_Usage = 0;             % Minimize HW usage
150 CIRUpdateRateLocked = 1;        % Lock update rate
151 
152 Coeff = h;                      % Matrix of complex IR coefficients
153 clear h
154 Delay = repmat(delay',1,len);  % Matrix of delays [ns]
155 
156 save([savepath filename '_tmp.mat'],'CIRs','Taps','Coeff','Delay','CIRUpdateRate'
        ,...
157     'Route_Closed','Sample_Density','Carrier_Frequency','Tap_Spacing','
        CIRUpdateRateLocked');
158 
159 savepath2 = 'C:\Users\mashuri\Desktop\ETSI ITS\G5\G5 IR\';
160 mat2ir([savepath filename '_tmp.mat'],[savepath2 filename '.ir'], '11p',
        Tap_Spacing);
161 
162 plot(linspace(-fupd/2,fupd/2,len),fftshift(20*log10(abs(fft(sum(Coeff))))))    %
        fupd ist Geschwindigkeitsabhängig! plot(linspace(-fupd/2,fupd/2,len),fftshift
        (20*log10(abs(fft(sum(Coeff))))))
163 xlabel('Doppler frequency [Hz]'),ylabel('magnitude [dB]')
164 title(['ETSI ITS ' filename])
165 print('-dpng',filename)
166 
167 end
```

```
1  function mat2ir(InputFile, OutputFile, FileDescription, Tap_Spacing)
2  % MAT2IR   Convert .MAT file to PROPSim's .IR file.
3  %   mat2ir
```

```
4  %   mat2ir(inputMatFile, outputIrFile, [description])
5  %
6  % In interactive mode (function is called without parameters), user can
7  % enter input .MAT file, .IR file name and .IR file description.
8  % For batch processing, function also accepts up to three parameters;
9  % input file (must be Matlab .MAT file), output file (.IR file) and
10 % description for .IR file (not required).
11 %
12 % .MAT file must contain following variables;
13 %   CIRs                    : Actual CIR count
14 %   Taps                    : Actual tap (path) count
15 %   Coeff                   : Matrix of complex IR coefficients:
16 %   Delay                   : Matrix of coefficient delays, in nanoseconds:
17 %  Coeff and Delay have CIRs as columns, and taps as rows.
18 %
19 % Following variables are optional; system assumes default values if omitted
20 %   CIRUpdateRate           : Update rate of channel
21 %   Carrier_Frequency       : Carrier center frequency [2,2 GHz]/ 5.9 GHz
22 %   Tap_Spacing             : Tap spacing, in nanoseconds [12,5 ns]
23 %   Route_Closed            : Is route closed; logical 0 or 1 [1]
24 %   Sample_Density          : Samples per half-wave [64]
25 %   Hardware_Usage          : Specify hardware optimization: 0,1,2 [0]
26 %                           : 0 minimizes hardware usage, 2 maximizes delay
27 %                           : accuracy and 1 balances between these two.
28 %   Description             : File description, as char array. Description
29 %                           : given as function parameters (if any)
30 %                           : overrides this variable.
31 %   CIRUpdateRateLocked     : Is CIR update rate locked; logical 0 or 1 [0]
32 %   CarrierFrequencyLocked  : Is carrier frequency locked; logical 0 or 1 [0]
33
34 %  <--- MATLAB'S HELP ENDS HERE -----------------------------------------------
35
36 % NOTE ABOUT COMPILATION:
37 %   Compile to pcode executable with:
38 %   "mcc -B pcode mat2ir.m"
39
40
41 % ===== Load MAT ========================================================
42
43 if nargin<1
44     [matfile, matpath] = uigetfile('*.mat', 'Load .MAT file...');
45
46     if matfile == 0
47         return;
48     else
49         inputfile = [matpath matfile];
50     end
51 else
52     inputfile = InputFile;
53 end
54
55 [CIRs, Taps, Coeff, Delay, Carrier_Frequency, CIRUpdateRate, Tap_Spacing,
       Route_Closed, Sample_Density, ...
56         Interpolation, Description, CIRUpdateRateLocked, CarrierFrequencyLocked]
       = readFile(inputfile);
```

```
57
58 %load (inputfile, 'CIRs', 'Taps', 'Coeff', 'Delay', 'Carrier_Frequency', ...
59 %    'CIRUpdateRate', ...
60 %    'Tap_Spacing', 'Route_Closed', 'Sample_Density', 'Interpolation', ...
61 %    'Description', 'CIRUpdateRateLocked', 'CarrierFrequencyLocked');
62
63 %inputfile = '1.tap';
64 %Carrier_Frequency = 2.2e9;
65 %Coeff = [ -1 -1 -1 -1 ; 1 1 1 1+i ];
66 %Delay = [  0 0 0 0 ; 10 20 30 40 ];
67 %Tap_Spacing = 12.5;
68 %CIRs = 4;
69 %Route_Closed = 1;
70 %Sample_Density = 64;
71 %Taps = 2;
72 %Interpolation = 14;
73
74 %save ('1.mat');
75 %return;
76
77 % ===== Validate data ================================================
78
79 MIN_CIRUPDATERATE = 0.01;
80 MAX_CIRUPDATERATE = 1500000;
81 MIN_CENTERFREQUENCY = 100E6;
82 MAX_CENTERFREQUENCY = 6E9;
83 MIN_SAMPLEDENSITY = 2;
84 MAX_SAMPLEDENSITY = 1024;
85
86 % terminology:
87 %   IRs = CIRs
88 %   Delay_Resolution = Tap_Spacing
89
90 % --- Involuntery parameters; these absolutely must exist
91
92 % check terminology differences
93 if (exist('IRs') ~= 0 & exist('CIRs') == 0)
94     CIRs = IRs;
95 end
96
97 if (exist('Delay_Resolution') ~= 0 & exist('Tap_Spacing') == 0)
98     Tap_Spacing = Delay_Resolution;
99 end
100
101 if exist('CIRs') == 0
102     error('"CIRs" not defined; exiting...');
103     return;
104 end
105
106 if CIRs == 0
107     error ('Data has no CIRs, exiting...');
108     return;
109 end
110
111 if exist('Taps') == 0
```

```
112     error('"Taps" not defined; exiting...');
113     return;
114 end
115 
116 if Taps == 0
117     error ('Data has no taps, exiting...');
118     return;
119 end
120 
121 % check input data matrix sizes;
122 
123 % first, check that data matrices do exist...
124 if exist('Coeff') == 0
125     error('Tap coefficient matrix ("Coeff") not defined');
126     return;
127 end
128 
129 if exist('Delay') == 0
130     error('Delay matrix ("Delay") not defined');
131     return;
132 end
133 
134 % ...then the sizes
135 coeff_size = size(Coeff);
136 delay_size = size(Delay);
137 
138 if coeff_size(1) ~= Taps
139     error ('Coeff matrix has invalid number of taps; exiting...');
140     return
141 end
142 
143 if coeff_size(2) ~= CIRs
144     error ('Coeff matrix has invalid number of CIRs; exiting...');
145     return;
146 end
147 
148 if delay_size(1) ~= Taps
149     error ('Delay matrix has invalid number of taps; exiting...');
150     return
151 end
152 
153 if delay_size(2) ~= CIRs
154     error ('Delay matrix has invalid number of CIRs; exiting...');
155     return;
156 end
157 
158 delay_truncated = 0;
159 for j = 1:delay_size(1)
160     for k = 1:delay_size(2)
161         if (Delay(j,k) > 400000)
162             Delay(j,k) = 400000;
163             delay_truncated = 1;
164         end
165     end
166 end
```

```
167
168 if (delay_truncated == 1)
169     disp ('Too large delay values found; truncating to 400us');
170 end
171
172 % ---- Voluntary parameters check; if these do not exist, default to defaults
173
174 % if isempty(Tap_Spacing)
175 % %     disp('"Tap_Spacing" undefined; defaulting to 12.5');
176 % %    Tap_Spacing = 12.5;
177 %     Tap_Spacing = 5.0;
178 % end
179
180 % validate carrier frequency
181 if isempty(Carrier_Frequency)
182     disp('"Carrier_Frequency" not defined; defaulting to 2.2 GHz');
183     Carrier_Frequency = 5.9e9; % habe die frequenz geändert vorher war diese 2.2
    GHz
184 else
185     if Carrier_Frequency < MIN_CENTERFREQUENCY | Carrier_Frequency >
    MAX_CENTERFREQUENCY
186         error('Invalid carrier frequency specified');
187         return;
188     end
189 end
190
191 % check if route closedness is valid
192 if isempty(Route_Closed)
193     disp('"Route_Closed" not defined; defaulting to closed route');
194     Route_Closed = 1;
195 end
196
197 % validate interpolation
198 if isempty(Interpolation)
199 %     disp('"Hardware_Usage" not defined or invalid; minimizing hardware usage');
200     Interpolation = 0;
201 end
202
203 % validate sample density
204 if isempty(Sample_Density)
205     disp('"Sample_Density" not defined; defaulting to 64');
206     Sample_Density = 64;
207 else
208     if Sample_Density < MIN_SAMPLEDENSITY | Sample_Density > MAX_SAMPLEDENSITY
209         error ('Invalid "Sample_Density" defined; exiting...');
210         return;
211     end
212 end
213
214 % validate CIR update rate
215 if isempty(CIRUpdateRate)
216 %     disp ('"CIRUpdateRate" not defined; defaulting to 10000 Hz');
217     CIRUpdateRate = 10000;
218 else
219     if CIRUpdateRate < MIN_CIRUPDATERATE | CIRUpdateRate > MAX_CIRUPDATERATE
```

```
220         error ('Invalid "CIRUpdateRate" specified; exiting...');
221         return;
222     end
223 end
224
225 if isempty(CIRUpdateRateLocked)
226 %     disp ('"CIRUpdateRateLocked" not defined; defaulting to 0');
227     CIRUpdateRateLocked = 0;
228 end
229
230 if isempty(CarrierFrequencyLocked)
231 %     disp('"CarrierFrequencyLocked" not defined; defaulting to 0');
232     CarrierFrequencyLocked = 0;
233 end
234
235 % ===== Select IR file ================================================
236
237 if nargin < 2
238     [irfile, irpath] = uiputfile({'*.IR', 'Impulse Response files (*.IR)'}, 'Save
        .IR file as...');
239
240     [path,name,ext]=fileparts(irfile);
241     if isempty(ext) || strcmpi(ext,'.ir') == 0
242         irfile = [irfile '.ir'];
243     end
244
245     if irfile == 0
246         return
247     else
248         outputfile = [irpath irfile];
249     end
250 else
251     outputfile = OutputFile;
252 end
253
254 [fid, message] = fopen(outputfile, 'wb');
255 if (fid == -1)
256     error('Error opening output file. Exiting...');
257     return;
258 end
259
260 % description
261
262 if nargin < 3
263     prompt = {'Enter IR file description:'};
264     def = {''};
265     title = 'IR File Description';
266     lineNo = 1;
267     answer = inputdlg ( prompt, title, lineNo, def);
268     FileDescription = answer{1};
269
270     if isempty(FileDescription)
271         FileDescription = 'Mat2Ir generated file';
272     end
273 else
```

```
274     if isempty(Description)
275         FileDescription = 'Mat2Ir generated file';
276     else
277         FileDescription = Description;
278     end
279 end
280 
281 if length(Description) < 1
282     Description = 'Mat2Ir converted file';
283 end
284 
285 tic; % start stopwatch
286 
287 CurrentTime = datestr(now, 0);
288 
289 IndexTable = struct (...
290     'HeaderDataIndex', hex2dec('FFFFFFFF'),...
291     'TapDataIndex',hex2dec('FFFFFFFF'),...
292     'CIRUpdateRateDataIndex',hex2dec('FFFFFFFF'),...
293     'ShadowDataIndex',hex2dec('FFFFFFFF'),...
294     'ReservedDataIndex',hex2dec('FFFFFFFF'),...
295     'EndOfIndexTable',0);
296 
297 IRHeader = struct(...
298     'FileDescription',FileDescription,...
299     'FileCreationTime',CurrentTime,...
300     'SourceDataFilename',inputfile,...
301     'CenterFrequency',Carrier_Frequency,...
302     'SampleDensity',Sample_Density,...
303     'TapSpacing',Tap_Spacing,...
304     'ClosedRoute',Route_Closed,...
305     'Interpolation',Interpolation,...
306     'CIRUpdateRate',CIRUpdateRate,...
307     'UpdateRateLocked',CIRUpdateRateLocked,...
308     'CarrierFrequencyLocked',CarrierFrequencyLocked,...
309     'CreatorProgram','MAT2IR Converter'); % MAT2IR Converter % FIXME
310 
311 % index table has dummy values. will be updated when done...
312 WriteIndexTable(fid, IndexTable);
313 
314 IndexTable.HeaderDataIndex = ftell (fid);
315 WriteHeaderData(fid, IRHeader);
316 IndexTable.TapDataIndex = ftell (fid);
317 
318 % disp ('Processing .MAT file...');
319 
320 WriteIrDataBegin (fid, CIRs, Taps);
321 WriteIrData(fid, Delay, Coeff, Taps, CIRs);
322 
323 % updaterate and shadowing do not exists in IR file anymore; skipped
324 
325 % update index table
326 frewind (fid);
327 WriteIndexTable(fid, IndexTable);
328 
```

```
329 fclose (fid);
330
331 processtime = toc;
332 % disp (' ');
333 % disp ( [inputfile ' converted to ' outputfile ' in ' num2str(processtime) '
        seconds.'] );
334
335 % ========================================================================
336
337 function WriteIndexTable(fid, table)
338 % write IR index table
339 fwrite(fid, table.HeaderDataIndex, 'uint32');
340 fwrite(fid, table.TapDataIndex, 'uint32');
341 fwrite(fid, table.CIRUpdateRateDataIndex, 'uint32');
342 fwrite(fid, table.ShadowDataIndex, 'uint32');
343 fwrite(fid, table.ReservedDataIndex, 'uint32');
344 fwrite(fid, table.EndOfIndexTable, 'uint32');
345
346 % ========================================================================
347
348 function WriteHeaderData(fid, hdr)
349 % Write IR header to file
350 %
351 %
352 % common header params
353
354 FieldsInCommonHeader = 11;
355 fwrite (fid, FieldsInCommonHeader, 'uint16');
356
357 fwrite (fid, length(hdr.FileDescription),'uint16');
358 fprintf (fid, '%s', hdr.FileDescription);
359
360 fwrite (fid, length(hdr.FileCreationTime), 'uint16');
361 fprintf (fid, '%s', hdr.FileCreationTime );
362
363 fwrite (fid, length(hdr.SourceDataFilename), 'uint16');
364 fprintf (fid, '%s', hdr.SourceDataFilename );
365
366 fwrite (fid, 8, 'uint16');
367 fwrite (fid, hdr.CenterFrequency, 'double');
368
369 fwrite (fid, 4, 'uint16');
370 fwrite (fid, hdr.SampleDensity, 'float');
371
372 % fwrite (fid, 2, 'uint16');     % Old, results to integer value e.g. 12.5->13
373 % fwrite (fid, hdr.TapSpacing, 'uint16');   % Old
374 fwrite (fid, 8, 'uint16');      % New, corrected 26.1.2011. Note! Now the...
375 fwrite (fid, hdr.TapSpacing*1E-9, 'double');  %...value is in [s] instead of [ns]
376
377 fwrite (fid, 1, 'uint16');
378 fwrite (fid, hdr.ClosedRoute, 'char');
379
380 fwrite (fid, 1, 'uint16');
381 fwrite (fid, hdr.Interpolation, 'char');
382
```

```
383 fwrite (fid, 8, 'uint16');
384 fwrite (fid, hdr.CIRUpdateRate, 'double');
385
386 fwrite (fid, 1, 'uint16');
387 fwrite (fid, hdr.UpdateRateLocked, 'char');
388
389 fwrite (fid, 1, 'uint16');
390 fwrite (fid, hdr.CarrierFrequencyLocked, 'char');
391
392 % creator-specific fields : just name ...
393 FieldsInCreatorSpecificHeader = 1;
394 fwrite (fid, FieldsInCreatorSpecificHeader, 'uint16');
395
396 fwrite (fid, length(hdr.CreatorProgram), 'uint16');
397 fprintf (fid, '%s', hdr.CreatorProgram );
398
399 % ============================================================================
400
401
402 function WriteIrDataBegin (fid, CIRs, Taps)
403 %
404 fwrite (fid, CIRs, 'uint32');
405 fwrite (fid, Taps, 'uint16'); % if this is 0, each cir has individual tap count.
        SC doesn't like this however...
406
407 % ============================================================================
408
409 function WriteIrData(fid, Delay, Coeff, Taps, CIRs)
410 %
411 % Write actual impulse response data to file.
412 % Changed 13.9.2007 by Pekka
413         de=Delay(:)';
414         re=real(Coeff(:))';
415         im=imag(Coeff(:))';
416         fwrite (fid, [de;re;im], 'float');
417 % for ir = 1:CIRs
418 %     % fwrite (fid, Taps, 'uint16'); % only present if taps in WRiteIrDataBegin
        = 0 (not used now)
419 %     for tap = 1:Taps
420 %         fwrite (fid, Delay(tap,ir), 'float');
421 %         fwrite (fid, real(Coeff(tap,ir)), 'float');
422 %         fwrite (fid, imag(Coeff(tap,ir)), 'float');
423 %     end
424 % end
425
426 % ============================================================================
427
428
429 function [mir__cir,mir__tap,mir__coeff,mir__delay,mir__freq,mir__cirrate,
        mir__spacing,mir__closedroute,mir__sd, ...
430         mir__inter, mir__desc, mir__cirlock, mir__freqlock] = readFile(inputfile)
431 %
432 % Load data from file, setting to proper parameters
433 %
434 CIRs = [];
```

```
435 Taps = [];
436 Coeff = [];
437 Delay = [];
438 Carrier_Frequency = [];
439 CIRUpdateRate = [];
440 Tap_Spacing = [];
441 Route_Closed = [];
442 Sample_Density = [];
443 Interpolation = [];
444 Description = [];
445 CIRUpdateRateLocked = [];
446 CarrierFrequencyLocked = [];
447 Hardware_Usage = [];
448
449 load (inputfile);
450
451 mir__cir = CIRs;
452 mir__tap = Taps;
453 mir__coeff = Coeff;
454 mir__delay = Delay;
455 mir__freq = Carrier_Frequency;
456 mir__cirrate = CIRUpdateRate;
457 mir__spacing = Tap_Spacing;
458 mir__closedroute = Route_Closed;
459 mir__sd = Sample_Density;
460
461 if isempty(Hardware_Usage) == 0
462     if (Hardware_Usage == 0)
463         Interpolation = 0;
464     end
465     if (Hardware_Usage == 1)
466         Interpolation = 4;
467     end
468     if (Hardware_Usage == 2)
469         Interpolation = 14;
470     end
471 end
472
473 mir__inter = Interpolation;
474 mir__desc = Description;
475 mir__cirlock = CIRUpdateRateLocked;
476 mir__freqlock = CarrierFrequencyLocked;
```

```
1  function [Bnew,Anew] = IIRfilt_lp2lp(Borig,Aorig,SDorig,SDnew,f_cutoff)
2  % Converts second order cascade IIR LPF to LPF.
3  % Normalised cutoff frequency theta is transformed
4  %  to cutoff frequency x*theta (theta on range [0,pi]).
5  % Note! To see SOS structure type HELP TF2SOS
6  %
7  % 31.12.2002 PekKy
8  %%%%%%%%%%%%%%%%%%%%%
9
10 %%%%%%%%%%%%%%%%%%
11 % Original IIR %%%
12 [oSOS,G] = tf2sos(Borig,Aorig);
```

```
13
14 %%%%%%%%%%%%%%%%%%%%%%
15 % LPF -> LPF conversion
16 x = SDorig/SDnew;       % Desired ratio x = f_cutoff_old / f_cutoff_new
17 theta = f_cutoff;   % Cutoff frequency of original IIR, (SD=55.25) pi ????
18 alfa=sin((1-x)*theta/2)/sin((1+x)*theta/2);
19 SOS(:,1) = oSOS(:,1)-oSOS(:,2)*alfa+oSOS(:,3)*alfa^2;
20 SOS(:,4) = oSOS(:,4)-oSOS(:,5)*alfa+oSOS(:,6)*alfa^2;
21 SOS(:,2) = -2*oSOS(:,1)*alfa+oSOS(:,2)*(1+alfa^2)-2*oSOS(:,3)*alfa;
22 SOS(:,5) = -2*oSOS(:,4)*alfa+oSOS(:,5)*(1+alfa^2)-2*oSOS(:,6)*alfa;
23 SOS(:,3) = oSOS(:,1)*alfa^2-oSOS(:,2)*alfa+oSOS(:,3);
24 SOS(:,6) = oSOS(:,4)*alfa^2-oSOS(:,5)*alfa+oSOS(:,6);
25 tmp = [repmat(SOS(:,1),1,3) repmat(SOS(:,4),1,3)];
26 SOS = SOS./tmp;       % Transformed IIR on 2nd order sections
27
28 %%% Responce plots %%%
29  %[Borig,Aorig] = sos2tf(oSOS);
30  %figure(1),freqz(Borig,Aorig)
31 [Bnew,Anew] = sos2tf(SOS);
32 % figure(2),freqz(Bnew,Anew)
```

Appendix B

Implementation of Channel Models on Propsim C2 through GUI

As described in Ch. 4 (4.4.1), one of the implementation methods of the channel models on the Propsim C2 is through the GUI. Since in the GUI of the Propsim C2 the Rician paths have the parameter angle as defined in Eq.(2.4) I have approximated the Rayleigh distributed paths through Rician distributed paths. Therefore it is feasible to feed the Doppler frequency shift of each path on the Propsim C2 through the angle α.

As mentioned in [22] at least 8 Rician paths are needed in the approximation. Hence the power of each Rayleigh distributed path has been divided by 8.

In the Rural LOS channel model the Doppler frequency shift of the tap 2 is equal to 492 Hz, therefore the $\alpha_1 = 51.28$ and analogue for the tap 3 the Doppler frequency shift is equal to -295 Hz and $\alpha_2 = 112.02$, both of the angles have the unit degree. The corresponding power (tap gain) for the approximation of the tap 2 is equal to -23,07 dB and for the tap 2 is equal to -26.03 dB. This means that the tap 2 is replaced with 8 Rician distributed paths each with the angle $\alpha_1 = 51.28$ and power -23.07 dB. Analogue instead of the tap 3 there are 8 paths in the approximation method with the angle $\alpha_2 = 112.202$ and the power -26.03 dB. The delay distance between paths is 1 ns, due to the delay resolution of the Propsim C2. The Rician K factor is equal to 2 dB. (The approximation has been carried out also with some other values for the Rician K factor, and the results did not change significantly.)

The PER for one scenario of the proposed ETSI ITS channel models is depicted in the Fig. below.

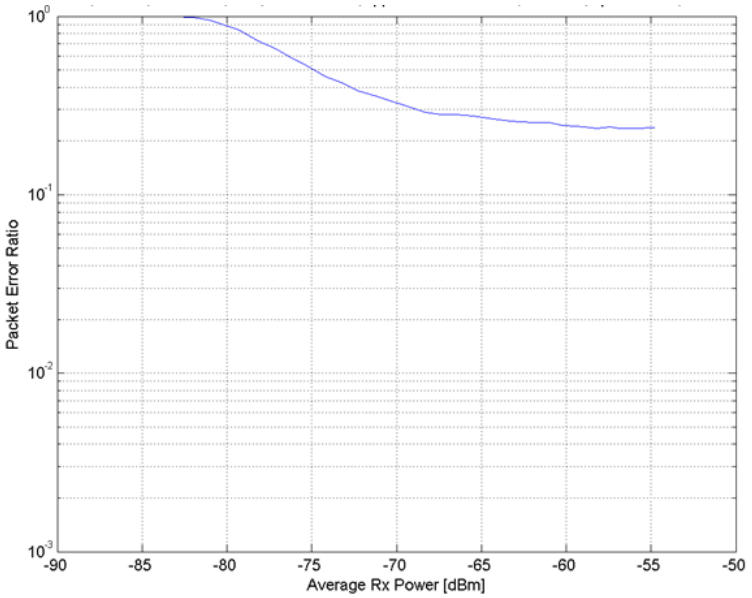

FIGURE B.1: PER ETSI ITS Rural LOS 3 Mbps, Implemented through approximation on Propsim C2

Appendix C

Software Defined Radio

As the continuation of my thesis, I worked on a research project to design and to implement a vehicular channel emulator on Software Defined Radio (SDR). SDR is a radio communication system in which usually is composed of one or more configurable RF front ends and an FPGA board on which the baseband processing could be programmed by means of a relevant software. This would provide the flexibility required for real-time emulation of non-stationary models for vehicular scenarios.

The chosen platform is NI USRP-Rio 2953R [32] which operates at frequencies up to 6GHZ with 40 MHz bandwidth. It features two MIMO RF chains which can be configured as 2x2. It is equipped with a Xilinx Kintex-7 FPGA which is programmable with the NI LabVIEW FPGA Modul.

We also used LabVIEW Communications 802.11 Application Framework by NI which provided a modifiable PHY and MAC layer suitable for 802.11 families.

My role in this project has included the testbed set up and test and measurement of the system for benchmarking of Kapsch modems MTX-9450 using the real-time channel emulator implemented on the NI USRP Rio as the communication link. I also worked on modifying the 802.11 framework to facilitate 802.11p transmission and reception. This was achieved e.g. by changing the time characteristics i.e. symbol time form 20 ms required by 802.11 to 10 ms specified in 802.11p, and modifying different parameters in the code to ensure the broadcast mode rather than original point to point communication mode. I designed a module to calculate the PER and embedded the module in the LabVIEW Communications 802.11 Application Framework code.

We performed tests to exhibit the conformance of the modified 802.11 framework as 802.11p transceiver with sending and receiving data to and from the Kapsch modem MTX-9450.

For the emulator, we used the parameters of the ETSI ITS channel models described in Ch. 3, as well as the parameters of the non-stationary models presented in [33] and benchmarked the Kaspch modems MTX-9450. The results of the last one were published in [7].

The demonstrated tests in NI RF Roundtable workshop held in TU Wien on November 2015 were as follows:

- Transmission between two USRPs via antenna, as depicted in Fig. C.1.

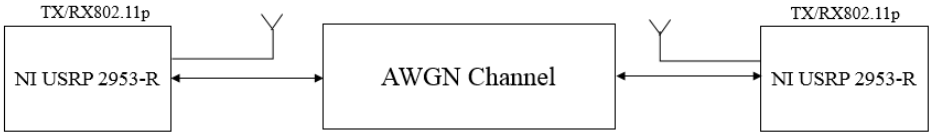

FIGURE C.1: Transmission over the air between USRPs, used LabVIEW Communications 802.11 Application Framework

- Transmission between two USRPs and also between one USRP and one MTX-9450 via antenna as depicted in Fig. C.2.

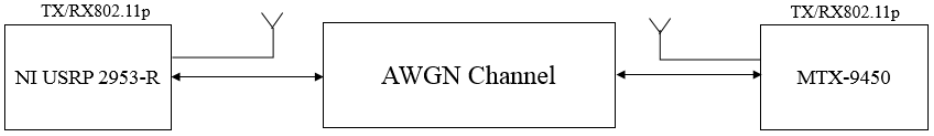

FIGURE C.2: Transmission over the air between USRP and MTX-9450, used LabVIEW Communications 802.11 Application Framework

- Transmission of 11p packets through the channel emulator NI USRP-Rio 2953R, depicted in Fig. C.3 and Fig. C.4. The architecture of the channel emulator is described in [7].

C.1 Radio Channel Emulator Implementation on SDR

A radio channel emulator is designed and implemented on the NI USRP RIO [32] as a SDR platform. The architecture of the channel emulator is described in [7]. We have implemented the non-stationary channel models as shown in [33] and also the proposed VTV ETSI ITS channel models (an discussed in Ch. 3) on the channel emulator. We have benchmarked the Kapsch MTX-9450 with the setup presented in Ch. 6. The PER

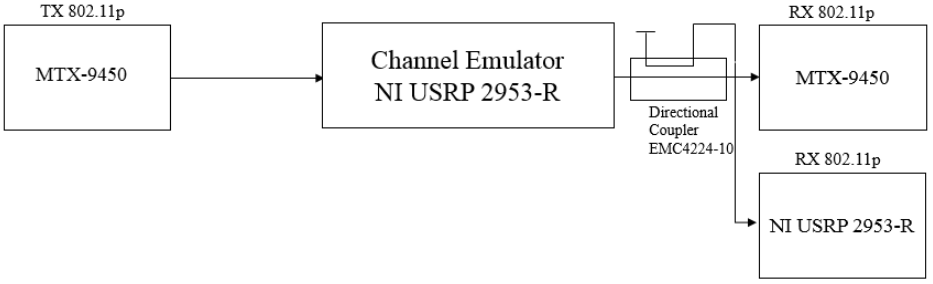

FIGURE C.3: Radio channel emulator implemented on the NI USRP-Rio 2953R

for the proposed ETSI ITS channel models for the data rate 6 Mbps is depicted in Fig. C.5 and C.6

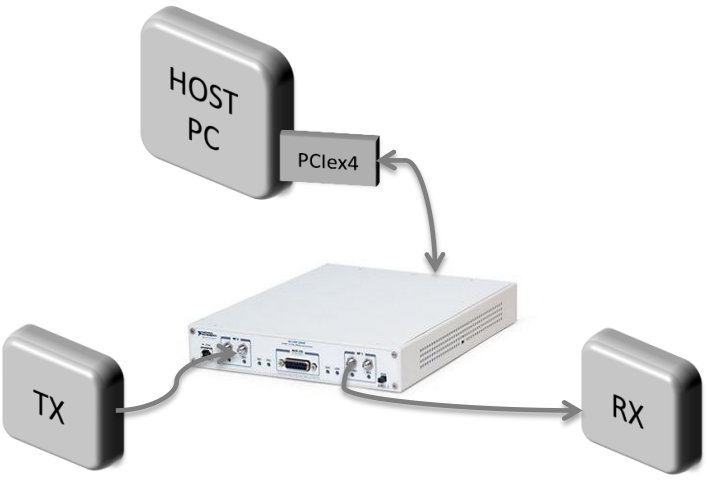

FIGURE C.4: USRP Channel Emulator

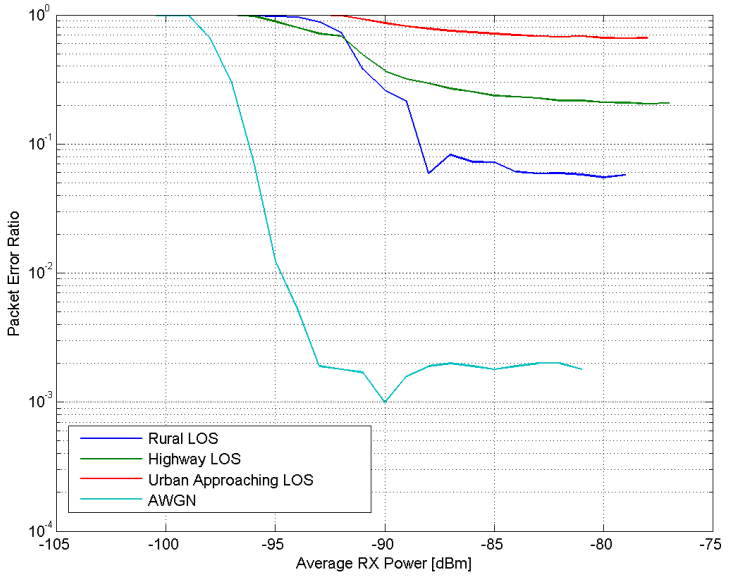

FIGURE C.5: PER ETSI ITS LOS channel models, for the SDR channel emulator

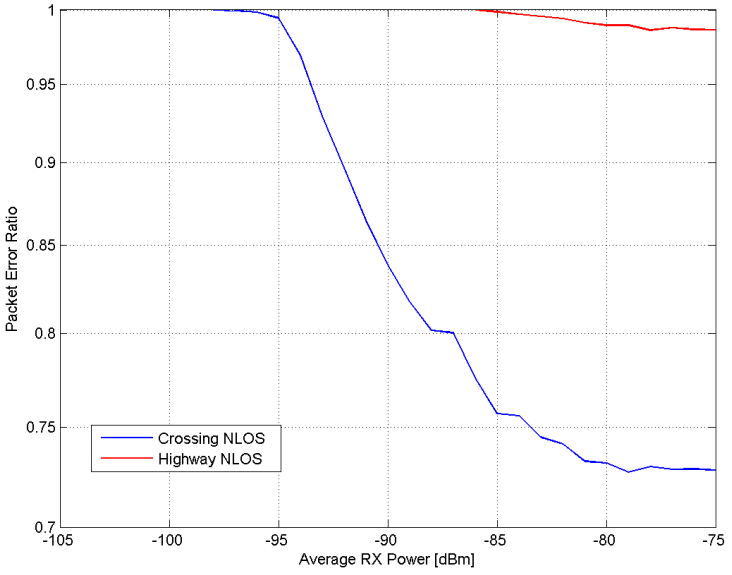

FIGURE C.6: PER ETSI ITS NLOS channel models, for the SDR channel emulator

Bibliography

[1] G. Acosta-Marum and M. A. Ingram, "Six time- and frequency-selective empirical channel models for vehicular wireless lans," *Vehicular Technology Magazine, IEEE*, 2007.

[2] P. Alexander, "G5 radio channel models," Cohda Wireless, Tech. Rep., 17 Sept 2013, car2Car Com/Arch meeting Daimler, Ulm.

[3] *Widebad Radio Channel Emulator EB Propsim C2 User Manual.*

[4] *3rd ETSI ITS plugtest 25-29 November 2013, Essen, Germany*, ETSI Std., 2013.

[5] A. Goldsmith, *Wireless Communications.* Cambridge University, 2005.

[6] *ETSI ES 202 663 V1.1.0 Intelligent Transport Systems (ITS); European profile standard for the physical and medium access control layer of Intelligent Transport Systems operating in the 5 GHz frequency band*, ETSI Std.

[7] G. Ghiaasi, M. Ashury, D. Vlastaras, M. Hofer, Z. Xu, and T. Zemen, "Real-time vehicular channel emulator for future conformance tests of wireless its modems," *EuCAP 2016*, 2016.

[8] *The Institute of Electrical and Electronics Engineers IEEE Standard for Information Technology Telecommunications and Information Exchange Between Systems - Local and Metropolitan Area Networks - Specific Requirements. Part 11: Wireless LAN Medium Access Control (MAC) and Physical Layer (PHY) Specifications - Amendment 6: Wireless Access in Vehicular Environments, July 2010*, IEEE Std.

[9] *802.11-1999 IEEE Standard for Information Technology Telecommunications and Information Exchange Between Systems Local and Metropolitan Area Networks-Specific Requirements- Part 11: Wireless LAN Medium Access Control (MAC) and Physical Layer (PHY) Specifications*, IEEE Std.

[10] D. H. Paul Alexander and A. Grant, "Cooperative intelligent transport systems: 5.9-ghz fields trials," *IEEE*, 2011.

[11] A. Molisch, *Wireless Communication*, third edition ed., J. Wiley and Sons, Eds. John Wiley and Sons, 2006.

[12] *Kapsch MTX*. [Online]. Available: http://www.kapsch.net/ktc/downloads/datasheets/v2x/Kapsch-KTC-DS-MTX-9450-Wave_Transceiver?lang=en-US

[13] *EB Propsim C-series output spectrum.*

[14] *EB Propsim C2 DCTuner operation guide.*

[15] G. M. Franz Hlawatsch, Ed., *Wireless Communications Over Rapidly Time-Varying Channels*. Academic Press.

[16] A. Paier, "The vehicular radio channel in the 5 ghz band," Ph.D. dissertation, Technische Universität Wien, 2010.

[17] T. S. Rappaport, Ed., *Wireless Communications Principles and practice*. Prentice Hall PTR.

[18] C. F. Mecklenbräuker, A. F. Molisch, J. Karedal, F. Tufvesson, A. Paier, L. Bernado, T. Zemen, O. Klemp, and N. Czink, "Vehicular channel characterization for wireless system designe and performance," *IEEE*, vol. 99, no. 7, 2011.

[19] R. H. Clarke, "A statistical theory of mobile-radio reception," *Bell Systems Technical Journal*, vol. 47, pp. 957–1000, 1968.

[20] P. Bello, "Characterization of randomly time-variant linear channels," *IEEE Transactions Communications*, pp. 360–393, 1963.

[21] *Draft specification IEEE 802.11p, Version 0.26, Appendix Q.*, IEEE Std.

[22] T. Zemen and C. F. Mecklenbräuker, "Time-variant channel estimation using discrete prolate spheroidal sequences," *IEEE TRANSACTIONS ON SIGNAL PROCESSING, VOL. 53, NO. 9,*, 2005.

[23] G. Uzcategui, R.Acosta-Marum, "Wave: A tutorial," *Communications Magazine, IEEE*, vol. 47, no. 5, pp. 126 – 133, May 2009.

[24] *ETSI TS 102 636-3 V1.1.1 Intelligent Transport Systems (ITS); Vehicular Communications; GeoNetworking; Part 3: Network architecture*, ETSI Std.

[25] *ETSI TS 102 687 V1.1.1 Intelligent Transport Systems (ITS); Decentralized Congestion Control Mechanisms for Intelligent Transport Systems operating in the 5 GHz range; Access layer part*, ETSI Std.

[26] *ETSI TS 102 636-4-1 V1.1.1 GeoNetworking;Part 4*, ETSI Std.

[27] *ETSI TS 102 636-5-1 V1.1.1 Intelligent Transport Systems (ITS); Vehicular Communications; GeoNetworking; Part 5: Transport Protocols; Sub- part 1: Basic Transport Protocol*, ETSI TS Std.

[28] *ETSI EN 302 665 V1.1.1 Intelligent Transport Systems (ITS); Communications Architecture*, ETSI Std., 9 2010.

[29] *ETSI TS 102 637-2 V1.2.1 Intelligent Transport Systems (ITS); Vehicular Communications; Basic Set of Applications; Part 2: Specification of Cooperative Awareness Basic Service*, ETSI Std., 3 2011.

[30] *Leistungsmesskopf (AVG) R&S®NRP-Z22 1137.7506.02 , R&S®NRP-Z23 1137.8002.02 R&S®NRP-Z24 1137.8502.02.*

[31] [Online]. Available: http://cdn.rohde-schwarz.com/pws/dl_downloads/dl_common_library/dl_manuals/gb_1/f/fsq_1/FSQ_OpMa_de_gl.pdf

[32] *USRP RIO*. [Online]. Available: http://www.ni.com/datasheet/pdf/en/ds-538

[33] M. G. Z. Xu and T. Zemen, "Cluster-based non-stationary vehicular channel model," *EuCAP*, 2016.